

**PHYTOCHEMICAL AND ANTIOXIDANT STUDIES OF
THE STEM BARK OF *GARCINIA PARVIFOLIA***

By

LEE LE WENG

A project report submitted to the Department of Chemical Science

Faculty of Science

Universiti Tunku Abdul Rahman

in partial fulfillment of the requirements for the degree of

Bachelor of Science (Hons) Chemistry

May 2016

ABSTRACT

PHYTOCHEMICAL AND ANTIOXIDANT STUDIES OF THE STEM BARK OF *GARCINIA PARVIFOLIA*

Lee Le Weng

Garcinia species belonging to family Clusiaceae have been long known to contain a wide array of chemical constituents, such as xanthenes, depsidones, phloroglucinols, flavonoids and benzoquinones, which are structurally intriguing and biologically active. Meanwhile, *Garcinia parvifolia* was also reported to exhibit these bioactive chemical constituents, which are distributed over various parts of this plant. Hence, the stem bark of *G. parvifolia* was phytochemically and biologically studied in this project. The dichloromethane and ethyl acetate extracts of the stem bark yielded three xanthenes, one tetraprenyltoluquinone and one sterol, namely α -mangostin [53], rubraxanthone [54], 1,3,7-trihydroxy-2,4-bis(3-methylbut-2-enyl)xanthone [55], [2*E*,6*E*,10*E*]-(+)-4 β -hydroxy-3-methyl-5 β -(3,7,11,15-tetramethyl-2,6,10,14-hexadecatetraenyl)-2-cyclohexen-1-one [52] and stigmasterol [56]. The structure of these isolated compounds was successfully elucidated using spectroscopic methods, including NMR, IR, UV/Vis and mass spectrometry. Subsequently, the antioxidant activity of the crude extracts and isolated compounds was examined using DPPH assay. In comparison with the positive controls, ascorbic acid and kaempferol, the dichloromethane and ethyl acetate extracts exhibited moderate antioxidant activity with IC₅₀ values of 41 and 45

$\mu\text{g mL}^{-1}$, respectively. Among the isolated compounds, only compound **54** and **55** were found to be active towards DPPH radicals, with IC_{50} values of 195 and $189 \mu\text{g mL}^{-1}$, respectively.

ABSTRAK

Spesies *Garcinia* milik keluarga Clusiaceae telah lama diketahui kerana ia mengandungi pelbagai sebatian semula jadi yang unik dan bioaktif, seperti xanthones, depsidones, phloroglucinols, flavonoid dan benzoquinones. Sementara itu, pelbagai bahagian of *Garcinia parvifolia* juga dilaporkan mengandungi sebatian-sebatian tersebut. Oleh sebab itu, kajian kimia dan aktiviti biologi tentang kulit batang *G. parvifolia* telah dijalankan dalam projek ini. Ekstrak diklorometana dan etil asetat kulit batang telah menghasilkan tiga xanthones, satu tetraprenyltoluquinone dan satu sterol, iaitu α -mangostin [53], rubraxanthone [54], 1,3,7-trihydroxy-2,4-bis(3-methylbut-2-enyl)xanthone [55], [2*E*,6*E*,10*E*]-(+)-4 β -hydroxy-3-methyl-5 β -(3,7,11,15-tetramethyl-2,6,10,14-hexadecatetraenyl)-2-cyclohexen-1-one [52] and stigmasterol [56]. Struktur sebatian-sebatian ini telah berjaya ditentukan dengan kaedah spektroskopi, termasuk NMR, IR, UV/Vis dan spektrometri jisim. Selepas itu, aktiviti antioksidan ekstrak mentah dan sebatian-sebatian yang diasingkan telah diperiksa dengan DPPH assay. Sebagai perbandingan dengan kawalan positif, asid askorbik dan kaempferol, diklorometana dan etil asetat ekstrak menunjukkan aktiviti antioksidan sederhana dengan memberikan nilai IC₅₀, iaitu 41 dan 45 $\mu\text{g mL}^{-1}$ masing-masing. Antara sebatian-sebatian yang telah diasingkan, hanya kompaun 54 dan 55 didapati aktif terhadap radikal DPPH dengan menunjukkan nilai IC₅₀ 195 dan 189 $\mu\text{g mL}^{-1}$ masing-masing.

ACKNOWLEDGEMENTS

First and foremost, I would like to express my heartfelt gratitude towards my supervisor, Dr. Lim Chan Kiang, for the guidance, knowledge and patience given throughout the final year project. Besides that, I can never be thankful enough towards my supervisor for his selflessness and times sacrificed in running NMR samples, checking the fractions, amending my thesis draft and others.

Next, I am most grateful to my postgraduate senior, Hemaroopini a/p Subramaniam, for her assistances and knowledge in handling the instruments and in conducting DPPH assay. Moreover, I would like to express my appreciations towards the laboratory staffs of Department of Chemical Science for their helps and kindness in running my samples for mass spectrometric analysis. I would also like to take this opportunity to thank my FYP partner, Chia Lun Chang, and other laboratory mates who had ever helped me out when encountered some problems in the laboratory.

Last but not least, a thousand thanks towards my family and friends who provided me support, motivations and solicitudes along the way in order to make this project a success.

DECLARATION

I hereby declare that the project report is based on my original work except for quotations and citations which have been duly acknowledged. I also declare that it has not been previously or concurrently submitted for any other degree at UTAR or other institutions.

(LEE LE WENG)

APPROVAL SHEET

The project report entitled **“PHYTOCHEMICAL AND ANTIOXIDANT STUDIES OF THE STEM BARK OF *GARCINIA PARVIFOLIA*”** was prepared by LEE LE WENG and submitted as partial fulfillment of the requirements for the degree of Bachelor of Science (Hons) Chemistry at Universiti Tunku Abdul Rahman.

Approved by:

Date: _____

(Dr. Lim Chan Kiang)

Supervisor

Department of Chemical Science

Faculty of Science

Universiti Tunku Abdul Rahman

FACULTY OF SCIENCE

UNIVERSITI TUNKU ABDUL RAHMAN

Date: _____

PERMISSION SHEET

It is hereby certified that **LEE LE WENG** (ID No: **12ADB04514**) has completed this final year project entitled “**PHYTOCHEMICAL AND ANTIOXIDANT STUDIES OF THE STEM BARK OF *GARCINIA PARVIFOLIA***” under supervision of Dr. Lim Chan Kiang from the Department of Chemical Science, Faculty of Science.

I hereby give permission to the University to upload the softcopy of my final year project in pdf format into the UTAR Institutional Repository, which may be made accessible to the UTAR community and public.

Yours truly,

(LEE LE WENG)

TABLE OF CONTENTS

	Page
ABSTRACT	ii
ABSTRAK	iv
ACKNOWLEDGEMENTS	v
DECLARATION	vi
APPROVAL SHEET	vii
PERMISSION SHEET	viii
TABLE OF CONTENTS	ix
LIST OF FIGURES	xii
LIST OF TABLES	xv
LIST OF ABBREVIATIONS	xvi
CHAPTER	
1 INTRODUCTION	1
1.1 General Introduction	1
1.2 Botany of Plant Studied – <i>Garcinia parvifolia</i>	6
1.2.1 Taxonomy	6
1.2.2 Morphology	6
1.2.3 Habitat, Geographic Distribution and Vernacular Name	8
1.2.4 Ethnomedicinal Uses and Biological Properties	8
1.3 Problem Statement	9
1.4 Objectives of Study	10
2 LITERATURE REVIEW	11
2.1 Phytochemical Studies	11
2.1.1 Xanthones	12
2.1.2 Phloroglucinols	13
2.1.3 Flavonoids	15
2.2 Phytochemical and Biological Studies of <i>Garcinia parvifolia</i>	16

2.3	Phytochemical and Biological Studies of Other <i>Garcinia</i> Species	19
2.3.1	<i>Garcinia cowa</i>	19
2.3.2	<i>Garcinia hombroniana</i>	22
2.3.3	<i>Garcinia mangostana</i>	24
2.3.4	Summary of the Literature Reviews on the <i>Garcinia</i> Species	27
3	MATERIALS AND METHODS	31
3.1	Plant Materials	31
3.2	Materials and Solvents	31
3.3	Extraction, Isolation and Purification of Phytochemicals from <i>G. parvifolia</i>	34
3.4	Chromatography	35
3.4.1	Column Chromatography (CC)	35
3.4.2	Gel Permeation Chromatography (GPC)	37
3.4.3	Thin Layer Chromatography (TLC)	37
3.5	TLC Visualization Methods	38
3.5.1	Ultraviolet (UV) Light	38
3.5.2	Iodine Vapor Stain	39
3.5.3	Ferric Chloride Reagent	39
3.6	Instruments	40
3.6.1	Nuclear Magnetic Resonance (NMR) Spectroscopy	40
3.6.2	Infrared (IR) Spectroscopy	40
3.6.3	Ultraviolet-Visible (UV-Vis) Spectroscopy	41
3.6.4	Liquid Chromatography-Mass Spectrometry (LC-MS)	41
3.6.5	Melting Point Apparatus	42
3.6.6	Polarimeter	42
3.7	Antioxidant Assay	43
4	RESULTS AND DISCUSSION	45
4.1	Isolation of Compounds from the Dichloromethane Stem Bark Extract of <i>G. parvifolia</i>	45
4.1.1	Characterization and Structural Elucidation of [2 <i>E</i> ,6 <i>E</i> ,10 <i>E</i>]-(+)-4 β -hydroxy-3-methyl-5 β -(3,7,11,15-tetramethyl-2,6,10,14-hexadecatetraenyl)-2-cyclohexen-1-one [52]	47

4.2	Isolation of Compounds from the Ethyl Acetate Stem Bark Extract of <i>G. parvifolia</i>	60
4.2.1	Characterization and Structural Elucidation of α -Mangostin [53]	63
4.2.2	Characterization and Structural Elucidation of Rubraxanthone [54]	73
4.2.3	Characterization and Structural Elucidation of 1,3,7-Trihydroxy-2,4- bis(3-methylbut-2-enyl) xanthone [55]	84
4.2.4	Characterization and Structural Elucidation of Stigmasterol [56]	93
4.3	Antioxidant Assay	99
5	CONCLUSIONS	103
5.1	Conclusion	103
5.2	Future Studies	104
	REFERENCES	105

LIST OF TABLES

Table		Page
1.1	Taxonomic hierarchy of <i>Garcinia parvifolia</i>	6
2.1	Biological activities of various parts of <i>Garcinia parvifolia</i>	17
2.2	Summary of the literature reviews on the <i>Garcinia</i> species	27
3.1	List of materials and industrial grade solvents used for extraction, isolation and purification of phytochemicals from <i>G. parvifolia</i>	31
3.2	List of materials and industrial grade solvents used for extraction, isolation and purification of phytochemicals from <i>G. parvifolia</i> (continued)	32
3.3	List of materials and analytical grade solvents used for TLC analysis	32
3.4	Material and analytical grade chemical used for UV/Vis analysis	32
3.5	Material used for IR analysis	32
3.6	List of material and deuterated solvents used for NMR analysis	33
3.7	Material and HPLC grade solvents used for LC- and GC-MS analysis	33
3.8	List of material and reagents used in antioxidant assay	33
4.1	Summary of NMR assignment of [2 <i>E</i> ,6 <i>E</i> ,10 <i>E</i>]- (+)-4 β hydroxy -3-methyl-5 β -(3,7,11,15-tetramethyl-2,6,10,14-hexadeca-tetraenyl-2-cyclohexen-1-one [52] in comparison with the literature data	51
4.2	Summary of NMR assignment of α -mangostin [53]	67
4.3	Summary of NMR assignment of rubraxanthone [54]	77
4.4	Summary of NMR assignment of 1,3,7-trihydroxy-2,4-bis(3-methylbut-2-enyl)xanthone [55]	87
4.5	Summary of NMR assignment of stigmasterol [56] in comparison with the literature data	95
4.6	Inhibitory concentration (IC ₅₀) of positive controls, crude extracts and isolated compounds in DPPH assay	99

LIST OF FIGURES

Figure		Page
1.1	Tree, leaves, flowers and fruits of <i>Garcinia parvifolia</i>	7
2.1	Common molecular structure of xanthones	12
2.2	Basic molecular structure of phloroglucinols	13
2.3	Examples of phloroglucinols	14
2.4	Common molecular structure of flavonoids	15
2.5	Structures of secondary metabolites isolated from <i>G. parvifolia</i>	18
2.6	Structures of secondary metabolites isolated from <i>G. parvifolia</i> (continued)	19
2.7	Structures of secondary metabolites isolated from <i>G. cowa</i>	21
2.8	Structures of secondary metabolites isolated from <i>G. hombroniana</i>	23
2.9	Structures of secondary metabolites isolated from <i>G. hombroniana</i> (continued)	24
2.10	Structures of secondary metabolites isolated from <i>G. mangostana</i>	25
2.11	Structures of secondary metabolites isolated from <i>G. mangostana</i> (continued)	26
3.1	Overall set up of column chromatography	36
3.2	Developed TLC plate	38
3.3	96-well plate used in DPPH assay	44
4.1	Isolation pathway of [2 <i>E</i> ,6 <i>E</i> ,10 <i>E</i>]-(+)-4 β -hydroxy-3-methyl-5 β - (3,7,11,15-tetramethyl-2,6,10,14-hexadecatetraenyl)-2-cyclohexen -1-one [52]	46
4.2	Structure of [2 <i>E</i> ,6 <i>E</i> ,10 <i>E</i>]-(+)-4 β -hydroxy-3-methyl-5 β -(3,7,11,15- tetramethyl-2,6,10,14-hexadecatetraenyl)-2-cyclohexen -1-one [52]	47
4.3	An equilibrium mixture of keto and enol forms of compound 52	48

4.4	HRESI Mass spectrum of compound 52	48
4.5	¹ H NMR spectrum of compound 52 (400 MHz, CDCl ₃)	53
4.6	Expanded ¹ H NMR spectrum of compound 52 (400 MHz, CDCl ₃)	54
4.7	¹³ C NMR spectrum of compound 52 (100 MHz, CDCl ₃)	55
4.8	DEPT spectrum of compound 52 (100 MHz, CDCl ₃)	56
4.9	HMQC spectrum of compound 52	57
4.10	HMBC spectrum of compound 52	58
4.11	UV/Vis spectrum of compound 52	59
4.12	FT-IR spectrum of compound 52	59
4.13	Isolation pathway of α -mangostin [53], rubraxanthone[54], 1,3,7-trihydroxy-2,4- <i>bis</i> (3-methylbut-2-enyl)xanthone [55] and stigmasterol [56]	62
4.14	Structure of α -mangostin [53]	63
4.15	HRESI mass spectrum of compound 53	64
4.16	¹ H NMR spectrum of compound 53 (400 MHz, CDCl ₃)	68
4.17	¹³ C NMR spectrum of compound 53 (100 MHz, CDCl ₃)	69
4.18	HMQC spectrum of compound 53	70
4.19	HMBC spectrum of compound 53	71
4.20	UV/Vis spectrum of compound 53	72
4.21	FT-IR spectrum of compound 53	72
4.22	Chemical structure of rubraxanthone [54]	73
4.23	HRESI mass spectrum of compound 54	74
4.24	¹ H NMR spectrum of compound 54 (400 MHz, acetone-d ₆)	78
4.25	¹³ C NMR spectrum of compound 54 (100 MHz, acetone-d ₆)	79
4.26	DEPT spectrum of compound 54 (100 MHz, acetone-d ₆)	80
4.27	HMQC spectrum of compound 54	81

4.28	HMBC spectrum of compound 54	82
4.29	UV/Vis spectrum of compound 54	83
4.30	FT-IR spectrum of compound 54	83
4.31	Chemical structure of 1,3,7-trihydroxy-2,4- <i>bis</i> (3-methylbut-2-enyl)xanthone [55]	84
4.32	HRESI mass spectrum of compound 55	85
4.33	¹ H NMR spectrum of compound 55 (400 MHz, acetone-d ₆)	88
4.34	¹³ C NMR spectrum of compound 55 (100 MHz, acetone-d ₆)	89
4.35	HMQC spectrum of compound 55	90
4.36	HMBC spectrum of compound 55	91
4.37	UV/Vis spectrum of compound 55	92
4.38	FT-IR spectrum of compound 55	92
4.39	Chemical structure of stigmasterol [56]	93
4.40	¹ H NMR spectrum of compound 56 (400 MHz, CDCl ₃)	96
4.41	Expanded ¹ H NMR spectrum of compound 56 (400 MHz, CDCl ₃)	96
4.42	¹³ C NMR spectrum of compound 56 (100 MHz, CDCl ₃)	97
4.43	UV/Vis spectrum of compound 56	98
4.44	FT-IR spectrum of compound 56	98
4.45	Resonance-stabilized of free radicals formed in compound 54	101
4.46	Resonance-stabilized of free radicals formed in compound 55	101
4.47	Graph of inhibition rate against concentration of crude extracts and positive controls	102
4.48	Graph of inhibition rate against concentration of isolated compounds	102

LIST OF ABBREVIATIONS

A_1	Absorbance of the test sample
A_0	Absorbance of the blank (negative control)
AGEs	Advanced glycation end-product
B.C.	Before Christ (used in timeline)
β	Beta
^{13}C	Carbon-13
C=C	Carbon=Carbon
C-H	Carbon-Hydrogen
C-O	Carbon-Oxygen (or Carbinol)
C=O	Carbon=Oxygen (or Carbonyl)
cm	Centimeter
δ	Chemical shift
δ_{C}	Chemical shift of carbon
δ_{H}	Chemical shift of proton
c	Concentration of sample in g/mL
J	Coupling constant in Hertz
$^{\circ}\text{C}$	Degree in Celsius
Acetone- d_6	Deuterated acetone
CDCl_3	Deuterated chloroform
d	Doublet
dd	Doublet of doublet
DCM	Dichloromethane
EtOAc	Ethyl acetate
FTIR	Fourier-Transform Infrared Spectroscopy
GC-MS	Gas Chromatography-Mass Spectrometry
g	Gram
IC_{50}	Half maximal inhibitory concentration
J_{CH}	Heteronuclear coupling between carbon and proton

HMBC	Heteronuclear Multiple Bond Coherence
HMQC	Heteronuclear Multiple Quantum Coherence
Hz	Hertz
HRESIMS	High Resolution Electrospray Ionization Mass
HPLC	High Performance Liquid Chromatography
IR	Infrared
kg	Kilogram
LC-MS	Liquid Chromatography-Mass Spectrometry
m/z	Mass-to-charge ratio
λ_{\max}	Maximum wavelength
MeOH	Methanol
μg	Microgram
μL	Microliter
μmol	Micromole
mg	Miligram
mL	Mililiter
mm	Milimeter
mM	Milimoles
mol	Mole
m	Multiplet
nm	Nanometer
NMR	Nuclear Magnetic Resonance
1D-NMR	One Dimension Nuclear Magnetic Resonance
O-H	Oxygen-Hydrogen (or Hydroxyl)
ppm	Part per million
KBr	Potassium bromide
^1H	Proton
R_f	Retention factor
s	Singlet
TMS	Tetramethylsilane
TLC	Thin Layer Chromatograph

t	Triplet
TE	Trolox Equivalent
2D-NMR	Two Dimension Nuclear Magnetic Resonance
UV-Vis	Ultraviolet-Visible
DPPH	1,1-diphenyl-2-picrylhydrazyl
BPX5	5% phenyl/ 95% methyl polysilphenylene/ siloxane phase

CHAPTER 1

INTROUDCTION

1.1 General Introduction

Natural product is generally defined as any substance that derived from living organisms such as animals, plants and microorganisms, and also can be referred to as secondary metabolite. According to Cooper and Nicola (2014), metabolites are the small molecules that can be found during natural metabolic processes before the final product is produced. It is split into two groups – primary and secondary metabolites. Primary metabolites, such as vitamins, lipids, polysaccharides and acetic acid, are the metabolites that synthesized by the cells and indispensable for growth, development, respiration and reproduction. On the other hand, secondary metabolites are not found in these processes above but they are primarily involved in immune system, serve as attractor and allelopathic substances (Crozier, et al., 2006).

About four millennia ago, natural products had been widely used for health care and disease prevention in China, India and even North Africa. For example, mandrake and garlic were used to relieve pain and treat circulatory diseases, respectively. Meanwhile roots of the endive plants were normally collected for the patients who suffer from gall bladder disorder. Following the continuous

development of extraction techniques, various types of active compounds had been successfully isolated from plants. Between 1803 and 1806, morphine had been isolated by Friedrich Sertürner from *Papaver somniferum* and it is used as an analgesic drug starting from 1830 (Tesso, 2005). Other active components include atropine from *Atropa belladonna*, quinine from stem bark of *Cinchona succirubra* and Taxol® from the bark of the Pacific yew tree.

Cragg and Newman (2013) stated that, from 2600 BCE, the source of natural products has been regarded as an invaluable source for discovering and developing new drugs until today. It is known that these natural products can be extracted from several sources such as plants, animals and microorganisms. Among these sources, plant materials have shown the most significant impact in the development of traditional medicine for millennia. Dating from 2600 BCE, around 1000 substances of plant origin had been documented in Mesopotamia, and most of them are still prescribed for inflammation, parasitic infections, cough and other infirmities. In addition, “Ebers Papyrus” was one of the best records that included approximately 700 medicines which were all derived from plant materials since 1500 BCE (Dias, et al., 2012).

The exploration of source of marine organisms as a potential source for drug discovery has shown an increase in interest in the mid-1970s. Approximately 2500 novel substances were effectively extracted from various marine organisms

from 1977 to 1987, and 840 of these substances had been structurally elucidated in 1998. In 2010, a total of 1003 new compounds were reported from a number of studies. These statistical data had shown that marine organisms are able to give a substantial impact to drug discovery in the future, and some of the bioactive compounds are specifically available in marine organisms.

The microorganism is another source that is rich of bioactive compounds and has been extensively explored after the discovery of penicillin from *Penicillium notatum* by Fleming in 1929. For instance, cephalosporins, which exhibit strong antibacterial activities, can be obtained from *Cephalosporium acremonium*. Rapamycin is a metabolite derived from *Streptomyces* species which is used for lowering cholesterol level.

It had been long known that most of the natural products offer a variety of distinctive pharmacological effects including anticancer, antibacterial, anti-inflammatory, antioxidant and other therapeutic effects. According to Butler (2004), the natural products serve as a potential and even indispensable source of drug leads in drug discovery and development, especially for anticancer and antihypertensive drugs. In his context, several studies showed that natural product-derived drugs had taken a significant lead in total drug launches since 1981. Salicin is an anti-inflammatory drug and analgesics which can be extracted from the bark of willow and *Populus* species. Owing to side effects and

limitations of salicin use, aspirin which is pharmacologically similar to salicin has been developed. Other examples of natural product-derived drugs include pilocarpine, digitoxin, morphine, quinine and others. In addition, Kourkoutas, et al. (2014) stated that natural products are widely involved in the process of producing flavouring agents, dyes, fibres, glues, perfumes, fragrances and cosmetic additives. Furthermore, the natural occurring products are also relatively crucial in food production due to their antimicrobial activities.

During the drug discovery, development and improvement, the structure and biological activities of these natural products must be studied and determined so as to give rise to the modified and more effective new drugs. Nevertheless, this process is often tedious and time-consuming (Ngo, et al., 2013). Recently, development of 'OMICS' technology can easily overcome the issue mentioned by characterizing the molecules of the metabolites in term of their roles, activities and interaction. Besides that, this astonishing technology also covers studies of many biological fields such as genomics, proteomics, metabonomics and others. The changes within certain group of molecules can also be observed and monitored while manipulating the environmental and pathogenic factors. Through the study of the molecular changes, the mode and action of the natural drugs can be precisely determined. As a result, determination and evaluation of natural products would no longer be an obstacle during the drug discovery and development.

It is no doubt that the interest of many pharmaceutical companies towards natural products study had been steadily reduced due to the introduction of high throughput screening and combinatorial chemistry when advancing into the 21st century (Lemke and Williams, 2013). Despite that, numerous 'boitech' companies are still remained active in drug discovery and development using source of natural products. It can be predicted that many natural product-derived drugs will be developed in the future and even used to cure the ailments including HIV/AIDS, tuberculosis, cancer, cardiovascular disease, hepatitis C and others. Although the source of natural products has been explored for almost 200 years, Lemke and Williams (2013) stated that this source is still prolific to provide improved and new drugs for the treatments of various ailments.

According to Hussain, et al. (2012), marine derived products can also be an extremely important source for providing new anticancer drugs in the years ahead. There are several advantages associated with the use of marine natural products as anticancer drugs. For example, these compounds were found to demonstrate very promising anticancer activity even in nanogram dose. Besides that, due to the complex structure of these marine derived product, a more specific and distinctive mechanism of action can be predicted. Ziconotide or Prialt® is one of the approved marine-derived drugs and has been used to allay the chronic pain.

1.2 Botany of Plant Studied – *Garcinia parvifolia*

1.2.1 Taxonomy

In this study, *Garcinia parvifolia* which belongs to Cluciaceae family was selected. The taxonomic information of *Garcinia parvifolia* is shown in Table 1.1.

Table 1.1: Taxonomic hierarchy of *Garcinia parvifolia*

Kingdom	:	Plantae
Divison	:	Magnoliophyta
Class	:	Magnoliopsida
Order	:	Malpighiales
Family	:	Cluciaceae/Guttiferae
Genus	:	<i>Garcinia</i>
Species	:	<i>Garcinia parvifolia</i>

1.2.2 Morphology

Garcinia parvifolia is an evergreen tree up to 33 m and 23 cm in height and in diameter at breast height, respectively (Tan, et al., 2013). Averagely, its trunk can grow no less than 23 cm in diameter, and yellow sap will be oozed while making a cut on the tree bark (Lim, 2012). The leaves of this plant are opposite, penniveined and stalked. Besides that, the leaves are 3.5-17 by 2-7 cm and possess gnarled leaf blades which are dark green. Many resin ducts can be found on the abaxial surface of the leaves but partially visible. Next, the flowers of *Garcinia parvifolia* are monoecious – male and female flowers are present

together in the plant but in different physical appearance. The male flowers are yellowish white in color whereas the female flowers are yellow colored. Moreover, the male flowers are generally wider than the female flowers by approximately 4 mm. According to Siong (2003), the underripe fruits produced are green colored and as they ripen, the fruits will appear yellow-orange color. Meanwhile, the fruits can be up to 17 mm in width. Hassan, et al. (2013) stated that its white pulp is sour and sweet with white seeds inside and a fruity aroma. The overall physical appearance of *Garcinia parvifolia* is displayed in Figure 1.1.



Figure 1.1: Tree, leaves, flowers and fruits of *Garcinia parvifolia*

1.2.3 Habitat, Geographic Distribution and Vernacular Names

Hassan, et al. (2013) revealed that *Garcinia parvifolia* requires a humid tropical habitat for sturdy growth and development. Hence it is indigenous to the peat swamp, lowland primary and secondary, and damp submontane forests (Lim, 2012). Other than that, this plant also grows well in the hills and along the rivers.

Garcinia parvifolia is widespread over some of the tropical Asia countries such as Thailand, Peninsular Malaysia, Borneo, Indonesia and New Guinea. According to Rukachaisirikul, et al. (2006), other than Asia, this plant also naturally occurs in Africa, New Caledonia as well as Polynesia.

There are several common vernacular names which have been used in different geographical areas. For example, in Sabah, *Garcinia parvifolia* is locally known as “asam kandis” or “takob akob.” This plant is also referred to as “asam aur-aur” among the people in Brunei or “asam kundong” among Sarawakian.

1.2.4 Ethnomedicinal Uses and Biological Properties

Garcinia parvifolia is reported to serve as traditional medicine for treatment of various ailments, and to remedy fever in the endemic areas in Indonesia (Kardono, et al., 2006). Syamsudin, et al. (2007a) stated that this plant is often used by Indonesian to cure malaria. In addition, some illnesses such as cough, sore throat

and swelling can be treated using this medicinal plant (Gerten, et al., 2015). The extract from the plant is also used for post-natal treatment in several countries.

Syamsudin, et al. (2007b) revealed that a variety of bioactive metabolites, especially isoprenylated xanthenes, benzophenones and biflavonoids, can be isolated from the plant species of *Garcinia*. These prenylated xanthenes have been found to show a wide spectrum of pharmacological potentials such as antibacterial, cytotoxicity, antioxidant, antiplasmodial, anti-inflammatory, antifungal and anti-HIV activities (Kardono, et al., 2006).

1.3 Problem Statement

The global commercial demand for antioxidants is expected to increase substantially in the coming few decades due to a strong demand by food and beverage, cosmetic and pharmaceutical industries. They are commonly used as supplements, medicines and food additives in fat and oil products. Antioxidants are defined as the substances that minimize or inhibit the production of free radicals by oxidation reactions (Sindhi, et al., 2013). They can be obtained from natural sources, especially plants, and also from synthetic approaches. Nevertheless, natural antioxidants are always found to be more favorable than synthetic ones because the synthetic antioxidants are found to be relatively more carcinogenic, unstable under high temperature, and less adaptability to human metabolisms. Due to these reasons, a continuous search for new natural

antioxidants with both improved efficacy and low toxicity is necessary as alternative to the use of synthetic antioxidant. In line with this, *Garcinia parvifolia* which is rich in phenolic compounds was selected in this study with the aim to isolate new natural antioxidants from this plant species.

1.4 Objectives of Study

The three main objectives of conducting this research are shown as following:

- i. To extract and isolate chemical constituents from the stem bark of *Garcinia parvifolia*.
- ii. To elucidate and identify the structures of isolated compounds using modern spectroscopic methods such as UV/Vis spectroscopy, infrared spectroscopy (IR), nuclear magnetic resonance (NMR) and mass spectrometry (MS).
- iii. To investigate the antioxidant activity of crude extracts and isolated compounds via DPPH assay.

CHAPTER 2

LITERATURE REVIEW

2.1 Phytochemical Studies

Although the secondary metabolites do not play a crucial role during life processes, they have been extensively used as traditional medicines for treatment of various diseases, such as intestinal worms, sore throat, skin and kidney problems and others, since time immemorial. Most of these secondary metabolites exhibit a broad range of pronounced pharmacological activities including antitumor, antimicrobial, antioxidant, antiplasmodial and other effects (Saxena, et al., 2013). Hence, these secondary metabolites have been a valuable source of bioactive compounds for drug research and development over decades (Dhawale, 2013). Their roles can range from drug precursors to prototypes and pharmacological probes during drug discovery (Salim, et al., 2008). The genus *Garcinia* is known to be rich in several classes of secondary metabolites such as xanthones, phloroglucinols and flavonoids.

2.1.1 Xanthenes

Xanthenes, which mostly occur as yellow pigment, are also known as 9*H*-xanthen-9-one or dibenzo- γ -pyrone (Pinto, et al., 2005). It has a common molecular formula of C₁₃H₈O₂. This class of metabolites can be widely found in several plant families such as Clusiaceae, Gentianaceae, Moraceae and Polygalaceae, fungi and lichens (Velišek, et al., 2008). The type of xanthenes ranges from oxygenated to prenylated and glycosylated xanthenes. Besides that, the type and position of the chemical substituents appeared in the scaffold also exerts a broad range of biological activities such as antitumor, antioxidant, antibacterial, antifungal and others (Yoswathana and Eshtiaghi, 2015). As a result, there is an increasing interest from many scientists to extensively explore, isolate and study the xanthone derivatives (Luo, et al., 2013). For example, xanthenes which consist of prenyl and pyrano groups exhibit both antibacterial and antimalarial activities. Meanwhile, glycosylated and tetrahydroxy xanthenes were reported to exhibit antiretroviral activity (Pinto, et al., 2005). The common molecular structure of xanthenes is shown in Figure 2.1.

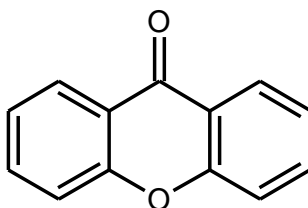


Figure 2.1: Common molecular structure of xanthenes

2.1.2 Phloroglucinols

Other major chemical constituents which can be isolated from the family of Clusiaceae are phloroglucinols or 1,3,5-benzotriol derivatives showing a basic molecular formula of $C_6H_6O_3$. This class of secondary metabolite is also abundantly found in other plant families such as Myrtaceae, Crassulaceae, Fagaceae, Euphorbiaceae and Rosaceae (Singh and Bharate, 2008). Other than plant kingdom, some marine and microorganism are also found to produce phloroglucinols. The phloroglucinols have been grouped into monomeric, dimeric, trimeric, tetrameric or higher, or phlorotannins, according to the number of phloroglucinol unit exists. The basic molecular structure of phloroglucinols is shown in Figure 2.2.

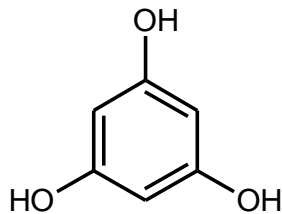
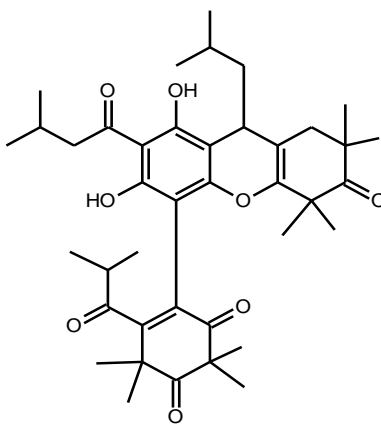


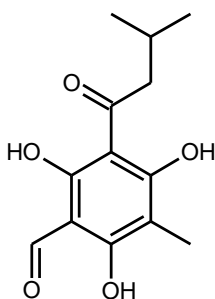
Figure 2.2: Basic molecular structure of phloroglucinols

Natural phloroglucinol derivatives are of great importance in the pharmaceutical industry as a result of their diverse biological activities including antioxidant, cytoprotective, anti-inflammatory as well as tyrosinase inhibitory activities (Lee, et al., 2013). Eucalyptone G [**1**] from *Eucalyptus globulus* Labill was reported to demonstrate a strong antibacterial activity (Mohamed and Ibrahim, 2007). Grandinol [**2**] and homograndinol [**3**], which are monomeric phloroglucinols, had

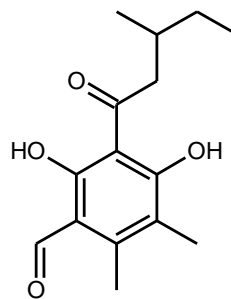
been determined to exert antiviral, germination and photosynthetic electron transport inhibitory activities. Furthermore, robustaol A [4], a dimeric phloroglucinol derivative from *Eucalyptus robusta*, had shown to be a strong antiplasmodial agent (Singh and Bharate, 2008).



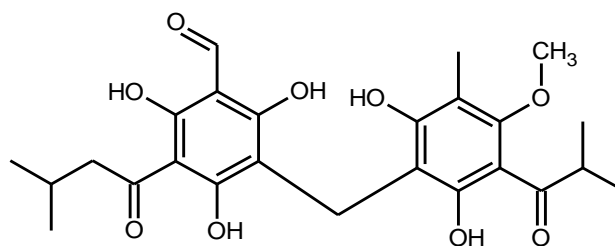
[1]



[2]



[3]



[4]

Figure 2.3: Examples of phloroglucinols

2.1.3 Flavonoids

Undeniably, the isolation and study of flavonoid compounds have shown an upsurge in interest in the nineteenth century because this group of secondary metabolites exhibits an extensive array of pharmacological activities (Halbwirth, 2010). Basically, flavonoids or bioflavonoids have a basic C₆-C₃-C₆ carbon skeleton or flavan structure. This structure is composed of two benzene units, labeled as rings A and B, joined through a heterocyclic pyran ring C (Kumar and Pandey, 2013). The flavonoids are widely distributed in higher plants, some green algae, fungal species and marine coral (Mohammed, 2009). They can be found in several forms, such as aglycones, glycoside or methylated, in the plants. Besides that, the variation in the degree of oxidation, position and type of substituents in the ring C permits the flavonoids to be grouped into several classes which include flavones, flavonols, flavanones, flavanonols, isoflavones, flavanols, flavandiols and anthocyanidin. The common molecular structure of flavonoids is shown in Figure 2.4.

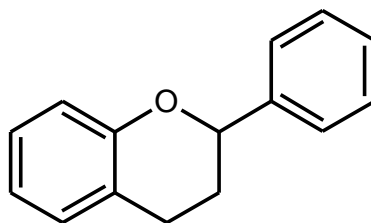


Figure 2.4: Common molecular structure of flavonoids

Mohammed (2009) revealed that flavonoids play manifold and crucial roles in the plants, such as being free radical scavenger, ultraviolet (UV) light absorber, coloring components, visual attractor and enzyme inhibitors. They have also been reported to be responsible for several major plant processes such as growth, respiration, protection against pathogen and photosynthesis. The biological activities of certain flavonoids are usually a function of type of substituents, configuration and number of hydroxyl groups. Reportedly, there is a wide range of pharmacological actions that flavonoids can provide, such as antioxidant, hepatoprotective, antibacterial, anti-inflammatory, anti-tumor and antiviral activities.

2.2 Phytochemical and Biological Studies of *Garcinia parvifolia*

Garcinia parvifolia has received increased attention and interest from many phytochemists due to its interesting pharmacological activities. It was reported that various parts of the plant was found to give different classes of compounds exhibiting a varying biological activities. For instance, the leaf extracts led to isolation of four prenylated depsidones which exhibited significant anticancer activity (Xu, et al., 2000). According to Pattalung, et al. (1988), the xanthone constituents, especially rubraxanthone, from the latex of *Garcinia parvifolia* had been found to demonstrate strong antimicrobial activity. The biological activities of crude extracts from different parts of *Garcinia parvifolia* are concluded in Table 2.1.

Table 2.1 Biological activities of various parts of *Garcinia parvifolia*

Plant parts	Biological activities	References
Leaves	Antioxidant, anticancer, antiplasmodial , antibacterial	Rukachaisirikul, et al., 2008 Syamsudin, et al., 2007
Fruits	Antioxidant, anti-Alzheimer, acetylcholinesterase inhibition, anticancer, antimicrobial, antiplasmodial	Xu, et al., 2000 Syamsudin, et al., 2007a Hassan, et al., 2013
Stem bark	Antioxidant, anticancer, antiplasmodial, antimicrobial, antiplatelet	Syamsudin, et al., 2007a; 2007b Lathifah, et al., 2009
Twig	Antioxidant, antibacterial	Rukachaisirikul, et al., 2006
Roots	Antioxidant, anticancer, Antimicrobial, antiplasmodial	Kardono, et al., 2006 Syamsudin, et al., 2007a
Latex	Antimicrobial, antiplatelet	Pattalung, et al., 1988 Jantan, et al., 2002

Besides that, *Garcinia parvifolia* were also found to possess many pharmacologically active and structurally intriguing xanthone derivatives and biflavonoids. In 1996, Iiluma, et al. had successfully isolated four xanthenes , named rubraxanthone [5], 1,3,6-trihydroxy-8-(7-hydroxy-3,7-dimethyl-2,5-octadienyl)-7-methoxyxanthone [6], 1,3,6- trihydroxy-8-(6,7-epoxy-3,7-dimethyl-2-octenyl)-7-xanthone [7] and 1,3,7-trihydroxy-2,4-diisoprenylxanthone [8], from the stem bark of *G. parvifolia*.

Later, Rukachaisirikul, et al. (2008) reported that the leaf extract yielded the first benzoquinone, parvifoliquinone [9], along with six other metabolites: parvifoliol B [10], C [11], E [12], garcidepsidone B [13], nigrolineaisoflavone A [14] and mangostinone [15]. The antibacterial assay against methicillin-resistant

Staphylococcus aureus (MRSA) showed that compounds [10], [13] and [14] displayed significant antibacterial activity with minimum inhibitory concentration (MIC) values of 32, 128 and 64 $\mu\text{g/mL}$, respectively.

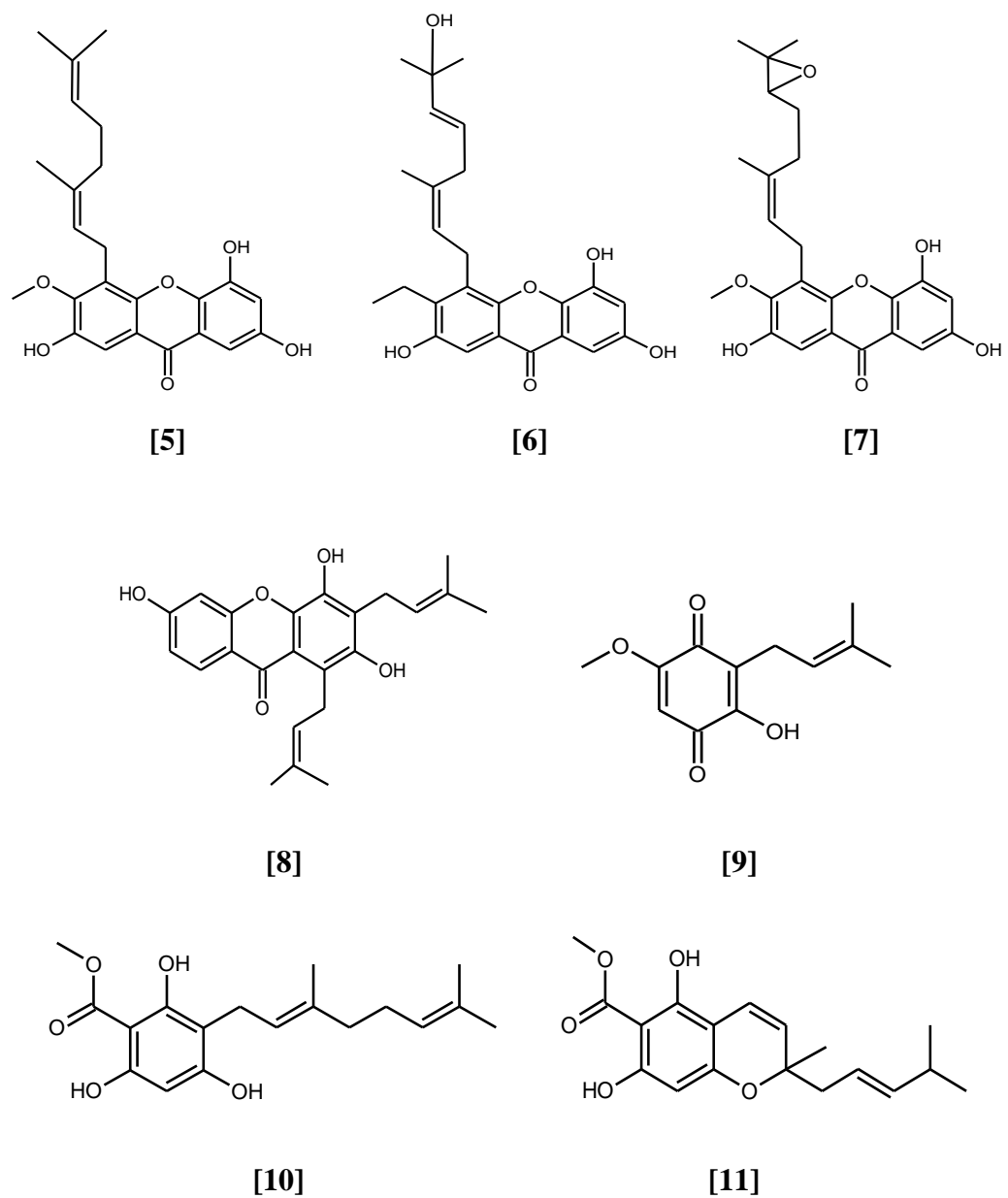


Figure 2.5: Structures of secondary metabolites isolated from *G. parvifolia*

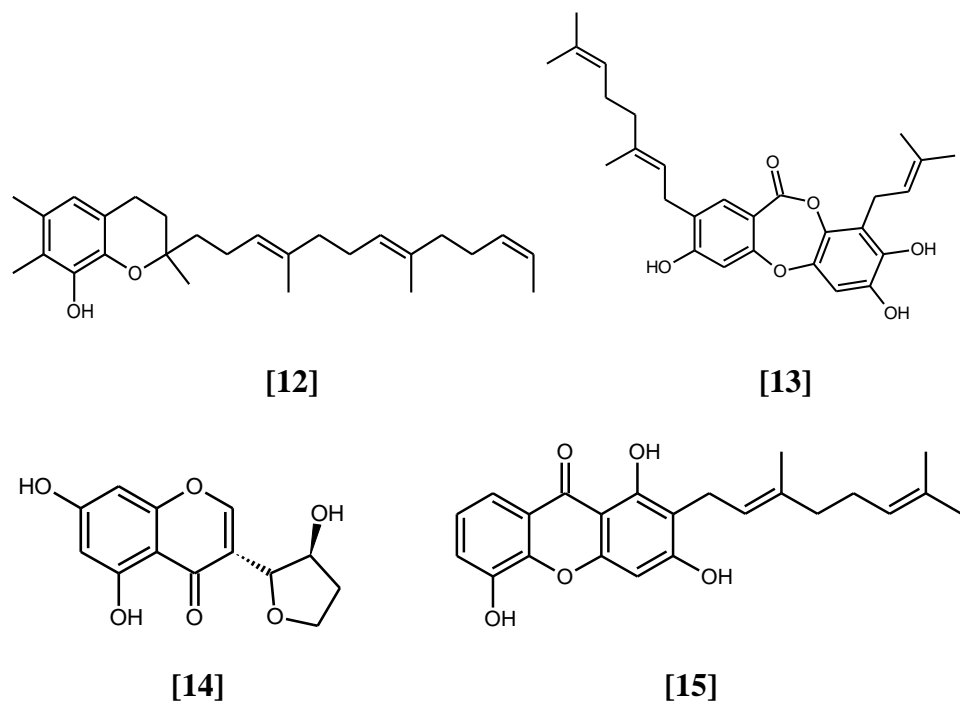


Figure 2.6: Structures of secondary metabolites isolated from *G. parvifolia* (continued)

2.3 Phytochemical and Biological Studies of Other *Garcinia* Species

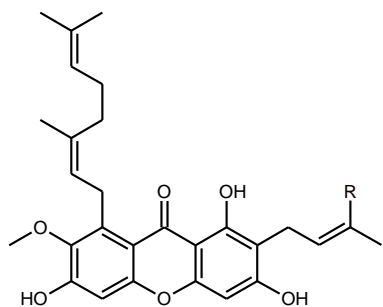
Currently, there are approximately 300 *Garcinia* species which had been recorded but, so far, only a few of them, such as *G. cambogia*, *G. cowa*, *G. hombroniana*, *G. mangostana*, *G. nitida*, *G. speciosa* and others, were extensively studied.

2.3.1 *Garcinia cowa*

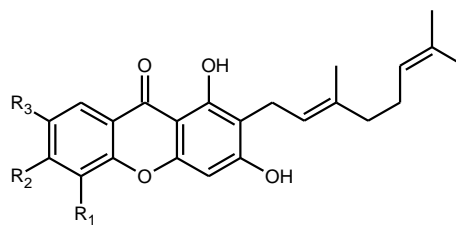
Garcinia cowa, usually called the “cha muang”, is one of the prominent *Garcinia* species which is indigenous to Malaysia, Thailand, Burma as well as Myanmar

(Auranwiwat, et al., 2014; Kaennakam, et al., 2015). It has been an important part of the folklore medicine in Thailand. For example, some parts of this species, such as leaves and fruits, are often used to treat cough, dyspepsia and fever. Other than that, it can serve as supplement and laxative (Siridechakorn, et al., 2012).

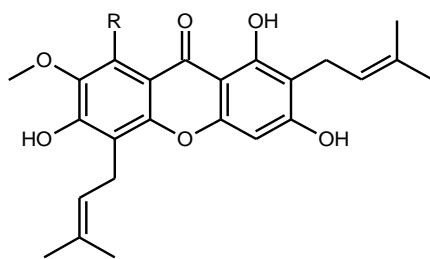
Besides that, Auranwiwat, et al. (2014) revealed that a total of 76 compounds, which are both structurally interesting and biologically remarkable, had been reported from the previous researches on this plant. 46 out of these compounds were xanthone derivatives and the others were phloroglucinols, biflavonoids and terpenoids. In year 2005, Mahabusarakam, et al. reported that the latex extract of *G. cowa* afforded cowaxanthone [16], cowanin [17], cowanol [18] and 1,3,6-trihydroxy-7-methoxy-2,5-bis(3-methyl-2-butenyl)xanthone [19], together with seven minor chemical constituents: mangostinone [20], fucaxanthone A [21], cowagarcinone A [22], B [23], C [24] and D [25]. Later, compounds 16, 17, 18, 19, 21 and 22 were subjected to DPPH assay but none of these showed promising radical scavenging activities, with IC₅₀ of more than 200 µg/mL.



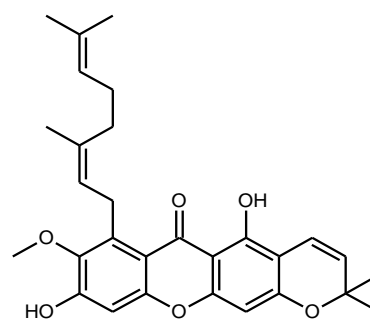
[17] R= CH₃
 [18] R= CH₂OH



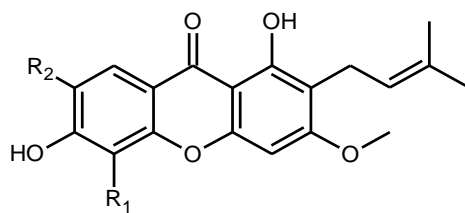
[16] R₁= H; R₂= OH; R₃= OCH₃
 [20] R₁= OH; R₂= H; R₃= H



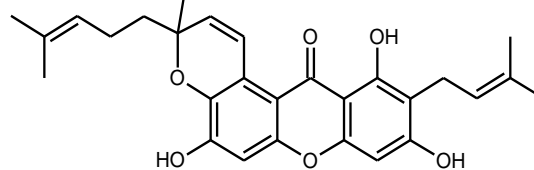
[19] R= H
 [22] R= geranyl



[21]



[23] R₁= H; R₂= OCH₃
 [24] R₁= OCH₃; R₂= H



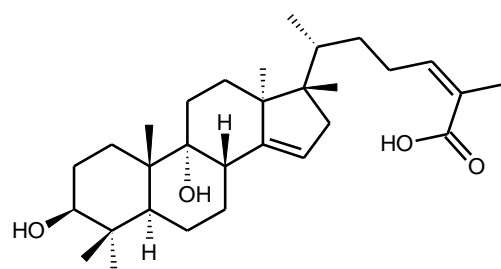
[25]

Figure 2.7: Structures of secondary metabolites isolated from *G. cowa*

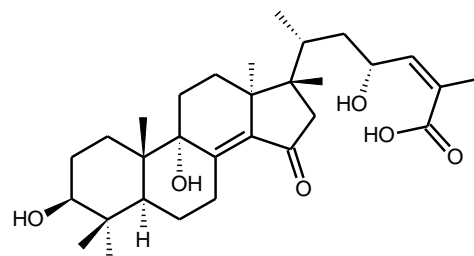
2.3.2 *Garcinia hombroniana*

Garcinia hombroniana, usually known as ‘Waa’ in Thailand, serves as a traditional medicine for preventing infections after accouchement and also treatment of itching (Jamila, et al., 2014). Phytochemical studies on various parts of this plant showed that *G. hombroniana* is rich in xanthonenes, flavonoids as well as triterpenes. These isolated chemical constituents were also found to be a good antioxidant, antiplasmodial and even anticancer agents (Dyary, et al., 2015).

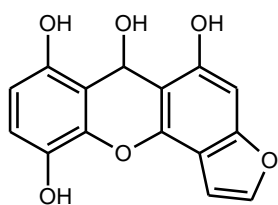
In year 2012, Klaiklay, et al. revealed that extensive separation of the twig extract of *G. hombroniana* led to isolation of six new compounds such as garcihombronanes K [26] and L [27], garcihombronones A [28], B [29], C [30] and D [31], along with four known chemical constituents including (22*Z*,24*E*)-3β,9α-dihydroxy-17,14-friedolanosta-14,22,24-trien-26-oic acid [32], garcihombronane B [33], cheffouxanthone [34] and bangangxanthone A [35]. Among these isolated compounds, compounds 34 and 35 displayed a good antibacterial activity against methicillin-resistant *S. aureus* at MIC values of 64 and 32 µg/mL, respectively. Compound 34 was also found to be active against *S. aureus* at MIC value of 16 µg/mL. The remaining compounds showed no antibacterial potential with MIC values beyond 200 µg/mL.



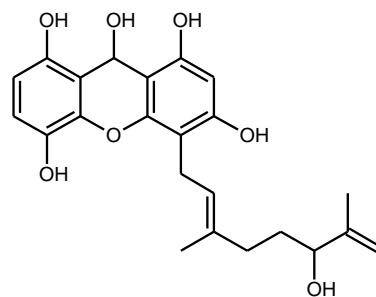
[26]



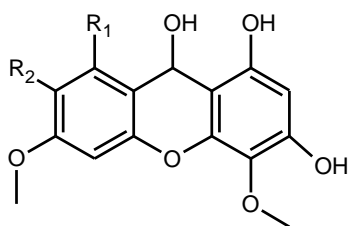
[27]



[28]

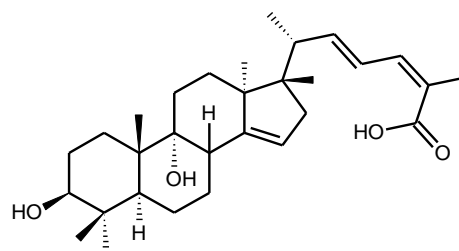


[29]

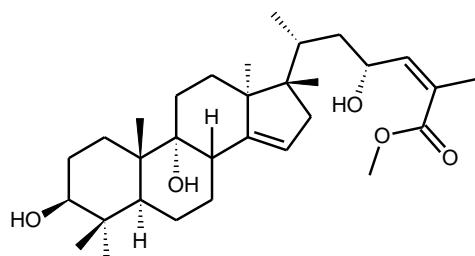


[30] R₁ = OH, R₂ = H

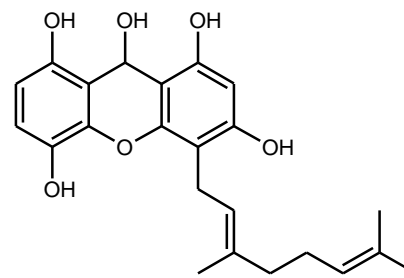
[31] R₁ = H, R₂ = OH



[32]

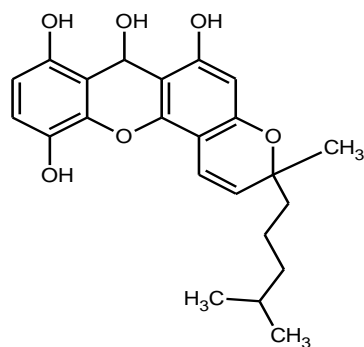


[33]



[34]

Figure 2.8: Structures of secondary metabolites isolated from *G. hombroniana*



[35]

Figure 2.9: Structures of secondary metabolites isolated from *G. hombroniana* (continued)

2.3.3 *Garcinia mangostana*

Garcinia mangostana or mangosteen is one of the indigenous plants of Southeast Asia including Malaysia, India, Thailand, Vietnam, Philippines and others (Ibrahim, et al., 2014; Thong, et al., 2015). The utilization of its fruit hulls as traditional medicines for treatment of a variety of infirmities including dysentery, fever, infections, trauma and wounds, has been predominant in the endemic areas of these countries (Wittenauer, et al., 2012). Although *G. mangostana* has been widely subjected to the phytochemical and biological studies for past few decades, this species was reported to provide many novel secondary metabolites, especially prenylated and oxygenated xanthone derivatives. At the same time, some isolated compounds from this species have also been evaluated for other rare pharmacological activities such as anthelmintic, anti-Alzheimer, anti-obesity, antihyperglycemic and neuraminidase inhibitory activity (Ryu, et al., 2011; Ibrahim, et al., 2014).

In 2011, Ryu, et al. reported the isolation of 16 xanthone derivatives, namely 9-hydroxycalabaxanthone [36], β -mangostin [37], α -mangostin [38], mangostanol [39], mangostenone F [40], allanxanthone E [41], mangostingone [42], garcinone D [43], γ -mangostin [44], mangosenone G [45], cudraxanthone [46], 1,5,8-trihydroxy-3-methoxy-2-(3-methylbut-2-enyl)xanthone [47], 8-deoxygartanin [48], gartanin [49] and smeathxanthone A [50], and oxoethylmangostine [51], from the pericarp extract of mangosteen. Among these isolates, compound 44 was found to exhibit the strongest anti-diabetic activity with the IC_{50} value of 1.5 μ M. In comparison with the standard anti-diabetic agent, deoxynorijirimycin (IC_{50} = 68.8 μ M), the other isolated compounds were also found to display a relatively good inhibitory activity showing IC_{50} values in the range of 5.0 to 63.5 μ M.

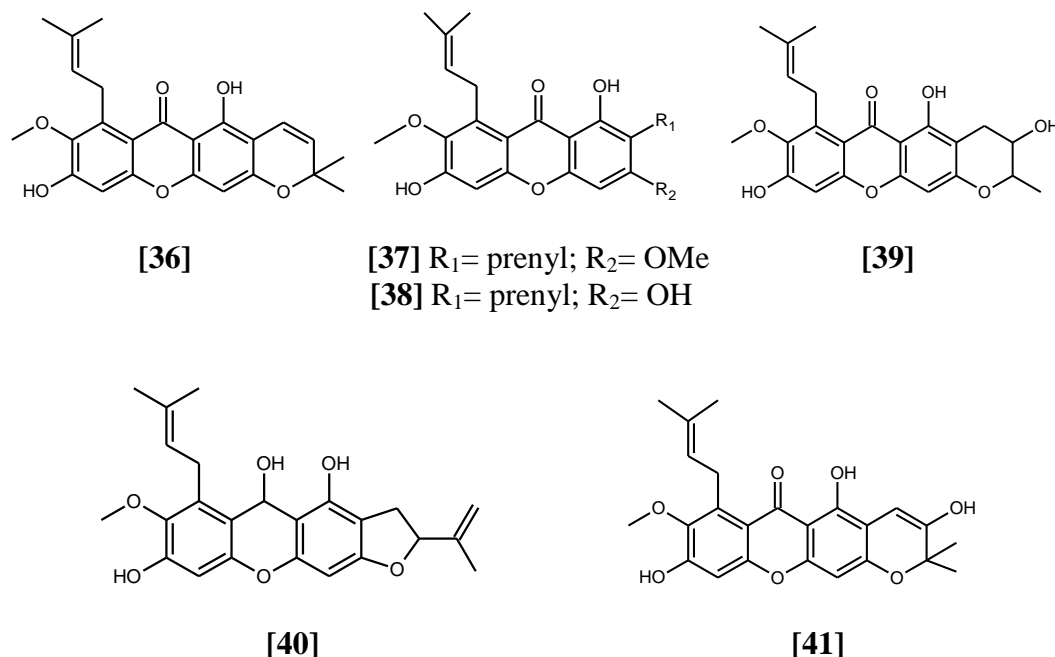


Figure 2.10: Structures of secondary metabolites isolated from *G. mangostana*

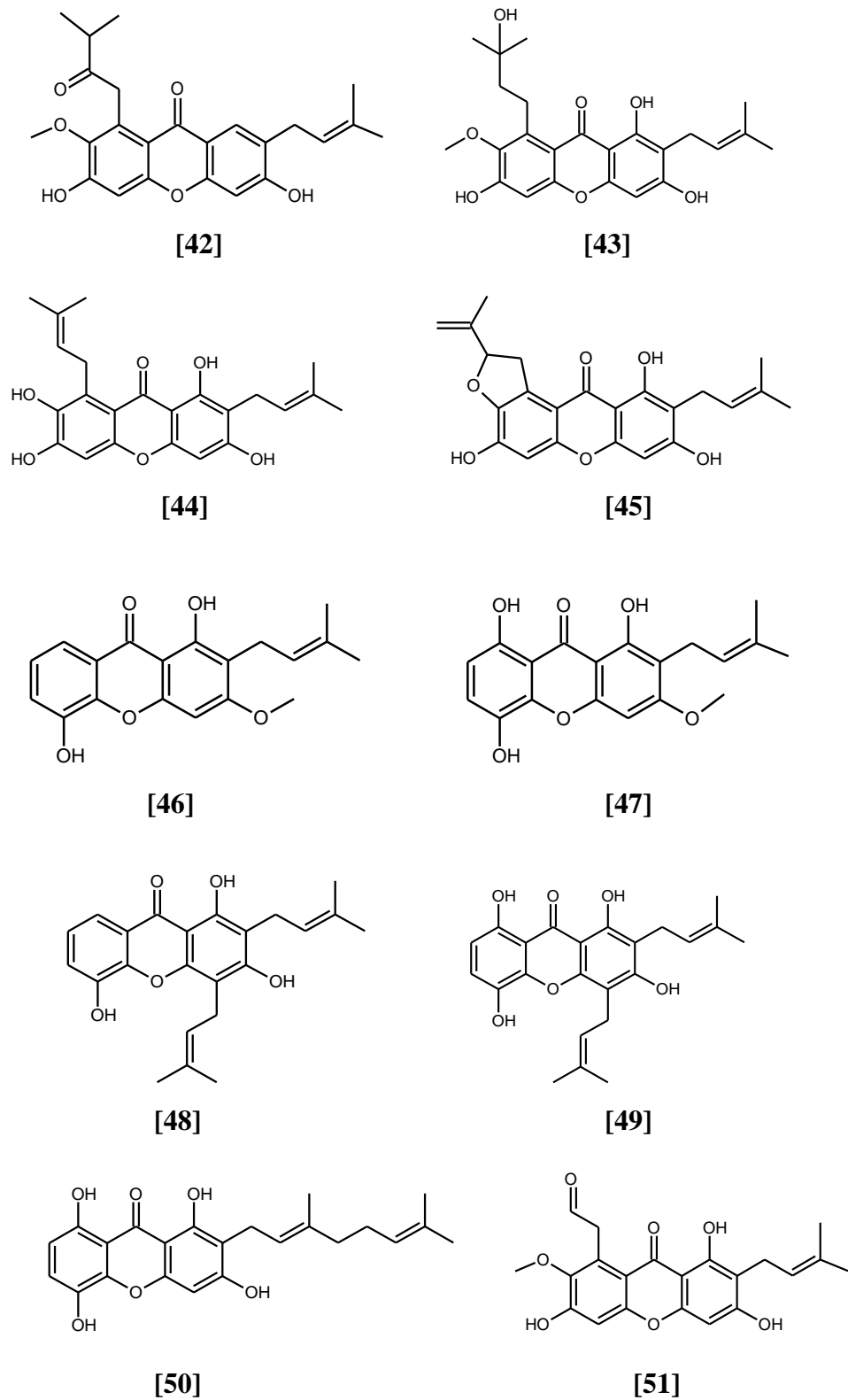


Figure 2.11: Structures of secondary metabolites isolated from *G. mangostana* (continued)

2.3.4 Summary of the Literature Reviews on the *Garcinia* Species

Besides *G. cowa*, *G. hombroniana* and *G. mangostana*, there are also other lesser-known species from the genus which had been studied for their phytochemical content and biological activities. The isolation of various classes of chemical constituents from the *Garcinia* species and their biological potentials are summarized in Table 2.2.

Table 2.2: Summary of the literature reviews on the *Garcinia* species

<i>Garcinia</i> Species	Class of Secondary Metabolites	Biological Activities	References
<i>G. amplexicaulis</i>	<ul style="list-style-type: none"> • Tocotrienols • Xanthones • Triterpene 	<ul style="list-style-type: none"> • Antioxidant 	<ul style="list-style-type: none"> • Lavaud, et al., 2015
<i>G. atroviridis</i>	<ul style="list-style-type: none"> • Triflavanones • Biflavonols 	<ul style="list-style-type: none"> • Acetylcholinesterase (AChE) and butyrylcholinesterase (BChE) enzymes inhibitory activity 	<ul style="list-style-type: none"> • Tan, et al., 2014
<i>G. benthami</i>	<ul style="list-style-type: none"> • Friedolanostanes • Friedocycloartanes • Benzophenones 	-	<ul style="list-style-type: none"> • Nguyen, et al., 2010b
<i>G. bracteata</i>	<ul style="list-style-type: none"> • Xanthones • Biphenyl derivatives 	<ul style="list-style-type: none"> • Anticancer 	<ul style="list-style-type: none"> • Thoison, et al., 2005 • Niu, et al., 2012 • Li, et al., 2015
<i>G. brasiliensis</i>	<ul style="list-style-type: none"> • Xanthones • Flavonoids • Prenylated benzophenones 	<ul style="list-style-type: none"> • Antioxidant • Anti-inflammatory • Antinociceptive 	<ul style="list-style-type: none"> • Gontijo, et al., 2012 • Santa-Cecilia, et al., 2011
<i>G. cambogia</i>	<ul style="list-style-type: none"> • Xanthones • Benzophenones 	<ul style="list-style-type: none"> • Anti-inflammatory • Anti-diabetic 	<ul style="list-style-type: none"> • Semwal, et al., 2015

	<ul style="list-style-type: none"> • Organic acids • Amino acids 	<ul style="list-style-type: none"> • Antioxidant • Antimicrobial • Antiulcer • Hepatoprotective 	
<i>G. cochonchinensis</i>	<ul style="list-style-type: none"> • Xanthonnes • Benzophenones 	<ul style="list-style-type: none"> • Anticancer 	<ul style="list-style-type: none"> • Nguyen, et al., 2011a • Trinh, et al., 2013
<i>G. cowa</i>	<ul style="list-style-type: none"> • Xanthonnes • Depsidones • Phloroglucinols • Flavonoids • Terpenes • Steroids 	<ul style="list-style-type: none"> • Antibacterial • Antioxidant • Anti-inflammatory • antimalarial 	<ul style="list-style-type: none"> • Panthong, et al., 2006 • Siridechakorn, et al., 2012 • Ritthiwigrom, et al., 2013
<i>G. cylindrocarpa</i>	<ul style="list-style-type: none"> • Xanthonnes 	<ul style="list-style-type: none"> • Anticancer 	<ul style="list-style-type: none"> • Sukandar, et al., 2016
<i>G. edulis</i>	<ul style="list-style-type: none"> • Xanthonnes 	<ul style="list-style-type: none"> • Anti-HIV • Cytotoxic 	<ul style="list-style-type: none"> • Magadula, 2010
<i>G. ferrea</i>	<ul style="list-style-type: none"> • Protostanes • Lanostanes • Xanthonnes 	-	<ul style="list-style-type: none"> • Bui, et al., 2014
<i>G. goudotiana</i>	<ul style="list-style-type: none"> • Prenylated benzoyl-phloroglucinols • Xanthonnes • Triterpenoids 	<ul style="list-style-type: none"> • Antimicrobial 	<ul style="list-style-type: none"> • Mahamodo, et al., 2014
<i>G. griffithii</i>	<ul style="list-style-type: none"> • Polyisoprenylated benzophenones 	<ul style="list-style-type: none"> • Antiprotozoal • Antibacterial 	<ul style="list-style-type: none"> • Nilar, et al., 2005 • Elfit, et al., 2009
<i>G. hanburyi</i>	<ul style="list-style-type: none"> • Xanthonnes 	<ul style="list-style-type: none"> • Anticancer • α-Glucosidase inhibitory activity 	<ul style="list-style-type: none"> • Deng, et al., 2013 • Chen, et al., 2015
<i>G. hombroniana</i>	<ul style="list-style-type: none"> • Benzophenones • Triterpenes • Flavonoids • Xanthonnes • Friedolanostanes • Lanostanes 	<ul style="list-style-type: none"> • Antioxidant • Anticancer • Antiplasmodial • Antibacterial • Antitrypanosomal 	<ul style="list-style-type: none"> • Jamila, et al., 2014 • Klaiklay, et al., 2012 • Dyary, et al., 2015

<i>G. indica</i> Choisy	<ul style="list-style-type: none"> • Polyisoprenylated benzophenones • Organic acids • Flavonoids 	<ul style="list-style-type: none"> • Antibacterial • Antifungal • Antioxidant • Antiaging • Neuroprotective • Gastroprotective • Anti-obesity • Anti-diabetic • Cardioprotective 	<ul style="list-style-type: none"> • Baliga, et al., 2011
<i>G. kola</i>	<ul style="list-style-type: none"> • Biflavanones 	<ul style="list-style-type: none"> • Antimalarial 	<ul style="list-style-type: none"> • Konziase, 2015
<i>G. livingstonei</i>	<ul style="list-style-type: none"> • Biflavonoids • Polyisoprenylated benzophenones • Terpenoids 	-	<ul style="list-style-type: none"> • Mulholland, et al., 2013
<i>G. malaccensis</i>	<ul style="list-style-type: none"> • Xanthonnes • Steroids 	<ul style="list-style-type: none"> • Anticancer • Antimicrobial • Antioxidant 	<ul style="list-style-type: none"> • Taher, et al., 2012
<i>G. mangostana</i>	<ul style="list-style-type: none"> • Diprenylated xanthonnes • Benzophenones • Xanthenones 	<ul style="list-style-type: none"> • Anthelmintic • Anti-inflammatory • Antioxidant 	<ul style="list-style-type: none"> • Nilar, et al., 2005 • Aukkanima rt, et al., 2005
<i>G. merguensis</i>	<ul style="list-style-type: none"> • Tetraoxygenated xanthonnes • Flavonoids 	<ul style="list-style-type: none"> • Antioxidant • Anticancer 	<ul style="list-style-type: none"> • Trisuwan, et al., 2013
<i>G. multiflora</i>	<ul style="list-style-type: none"> • Flavonoids • Xanthonnes • Steroids • Triterpenoids • Poylprenylated phloroglucinols 	<ul style="list-style-type: none"> • Anticancer 	<ul style="list-style-type: none"> • Chien, et al., 2008 • Lee, et al., 2013
<i>G. nigrolineata</i>	<ul style="list-style-type: none"> • Xanthonnes 	-	<ul style="list-style-type: none"> • Rukachaisir ikul, et al., 2003
<i>G. nujiangensis</i>	<ul style="list-style-type: none"> • Xanthonnes 	<ul style="list-style-type: none"> • Anticancer 	<ul style="list-style-type: none"> • Tang, et al., 2015
<i>G. oligantha</i>	<ul style="list-style-type: none"> • Xanthonnes 	<ul style="list-style-type: none"> • Anti-tobacco mosaic virus 	<ul style="list-style-type: none"> • Wu, et al., 2013
<i>G. parvifolia</i>	<ul style="list-style-type: none"> • Xanthonnes • Depsidones • Flavonoids • Alkaloids • Phloroglucinols 	<ul style="list-style-type: none"> • Anticancer • Antioxidant • Antiplatelet • Antiplasmodial • Larvicidal 	<ul style="list-style-type: none"> • Xu, et al., 2000; 2001 • Kardono, et al., 2006 • Rukachaisir

	<ul style="list-style-type: none"> • Benzoquinones 	<ul style="list-style-type: none"> • Antibacterial 	<ul style="list-style-type: none"> • ikul, et al., 2006; 200 • Lim, 2012
<i>G. paucinervis</i>	<ul style="list-style-type: none"> • Polyisoprenylated benzophenones 	<ul style="list-style-type: none"> • Cytotoxic 	<ul style="list-style-type: none"> • Gao, et al., 2010
<i>G. pedunculata</i>	<ul style="list-style-type: none"> • Xanthonnes • Triterpenoids 	<ul style="list-style-type: none"> • Anticancer 	<ul style="list-style-type: none"> • Vo, et al., 2012a; 2012b
<i>G. polyantha</i>	<ul style="list-style-type: none"> • Xanthonnes 	<ul style="list-style-type: none"> • Acetyl-cholinesterase (AChE) and butyryl-cholinesterase (BChE) enzymes inhibitory activity • Antioxidant 	<ul style="list-style-type: none"> • Lannang, et al., 2005 • Louh, et al., 2007
<i>G. porrecta</i>	<ul style="list-style-type: none"> • Xanthonnes • Triterpenoids 	<ul style="list-style-type: none"> • Anticancer 	<ul style="list-style-type: none"> • Kardono, et al., 2006
<i>G. rigida</i>	<ul style="list-style-type: none"> • Xanthonnes 	<ul style="list-style-type: none"> • Cytotoxic 	<ul style="list-style-type: none"> • Elya, et al., 2008
<i>G. schomburgkiana</i>	<ul style="list-style-type: none"> • Tetraoxygenated xanthonnes 	<ul style="list-style-type: none"> • Anticancer 	<ul style="list-style-type: none"> • Vo, et al., 2012b
<i>G. semseii</i>	<ul style="list-style-type: none"> • Polyisoprenylated benzophenones • Monocyclic triterpenes 	-	<ul style="list-style-type: none"> • Magadula, et al., 2008
<i>G. smeathmannii</i> (Oliver)	<ul style="list-style-type: none"> • Xanthonnes • Benzophenones • Triterpenes • cinnamates 	<ul style="list-style-type: none"> • Antibacterial • Anticandidal • Antimicrobial 	<ul style="list-style-type: none"> • Komguem, et al., 2005 • Kuete, et al., 2007
<i>G. speciosa</i> Wall	<ul style="list-style-type: none"> • Xanthonnes • Benzophenones • Steroids 	<ul style="list-style-type: none"> • Antioxidant • Anticancer 	<ul style="list-style-type: none"> • Sangsuwon and Jiratchariya kul, 2015
<i>G. staudtii</i>	<ul style="list-style-type: none"> • Prenylated xanthonnes 	<ul style="list-style-type: none"> • Antimicrobial 	<ul style="list-style-type: none"> • Ngoupayo, et al., 2009
<i>G. subelliptica</i>	<ul style="list-style-type: none"> • Triterpenoids • Phloroglucinols 	<ul style="list-style-type: none"> • Antiproliferative • Antioxidant 	<ul style="list-style-type: none"> • Lin, et al., 2012
<i>G. vieillardii</i>	<ul style="list-style-type: none"> • Xanthonnes • Benzophenones 	<ul style="list-style-type: none"> • Antileishmanial • Antimalarial 	<ul style="list-style-type: none"> • Hay, et al., 2004; 2008
<i>G. xanthocymus</i>	<ul style="list-style-type: none"> • Xanthonnes • Flavonoids • Mellein derivatives 	<ul style="list-style-type: none"> • Antibacterial • Antioxidant 	<ul style="list-style-type: none"> • Fu, et al., 2012 • Trisuwan, et al., 2014

CHAPTER 3

MATERIALS AND METHODS

3.1 Plant Material

The stem bark of *G. parvifolia* was collected from the jungle in Landeh district of Sarawak, in October 2014, and was authenticated by Mr. Tinjan Anak Kuda, botanist from the Forest Department, Sarawak. A voucher specimen (UITM 3018) was deposited at the herbarium of Universiti Teknologi MARA, Sarawak.

3.2 Materials and Solvents

The materials and solvents that had been used in the project were listed in Tables 3.1 to 3.8, along with their respective molecular formula, density and source, country.

Table 3.1: List of materials and industrial grade solvents used for extraction, isolation and purification of phytochemicals from *G. parvifolia*

Materials/ Solvents	Molecular formula	Density, ρ (g cm^{-3})	Source, Country
Acetone	CH_3COCH_3	0.791	QReC, Malaysia
Dichloromethane	CH_2Cl_2	1.325	Fisher Scientific, UK
Ethyl acetate	$\text{CH}_3\text{COOC}_2\text{H}_5$	0.902	Lab Scan, Ireland
Methanol	CH_3OH	0.791	Mallinckrodit Chemicals, Philipsburg
n-Hexane	$\text{CH}_3(\text{CH}_2)_4\text{CH}_3$	0.659	Merck, Germany

Table 3.2: List of materials and industrial grade solvents used for extraction, isolation and purification of phytochemicals from *G. parvifolia* (continued)

Sea sand	-	-	Merck, Germany
Sephadex® LH-20	-	-	New Jersey, USA
Silica gel (60Å) 230-400 Mesh	SiO ₂	-	Sigma-Aldrich, USA
Sodium sulphate anhydrous	Na ₂ SO ₄	2.66	Merck, Germany

Table 3.3: List of materials and analytical grade solvents used for TLC analysis

Materials/ Solvents	Molecular formula	Source, Country
TLC silica gel 60 F ₂₅₄	SiO ₂	Merck, Germany
Acetone	CH ₃ COCH ₃	QReC, Malaysia
Dichloromethane	CH ₂ Cl ₂	QReC, Malaysia
Ethyl acetate	CH ₃ COOC ₂ H ₅	Fisher Scientific, UK
n-Hexane	CH ₃ (CH ₂) ₄ CH ₃	R&M Chemicals, UK
Iodine	I ₂	Fisher Scientific, UK
Ferric chloride	FeCl ₃	Uni-chem, India

Table 3.4: Material and analytical grade chemical used for UV/Vis analysis

Materials/ Solvents	Molecular formula	Source, Country
Chloroform	CHCl ₃	Fisher Scientific, UK
Cuvette (quartz)	-	Membrane solution, USA

Table 3.5: Material used for IR analysis

Materials	Molecular formula	Density, ρ (g cm ⁻³)	Source, Country
Potassium Bromide	KBr	2.74	Merck, Germany

Table 3.6: List of material and deuterated solvents used for NMR analysis

Materials/ Solvents	Molecular formula	Source, Country
NMR tube	-	Norell®, US
Acetone-d ₄	CD ₃ COCD ₃	Acros Organics, Belgium
Deuterated chloroform (CDCl ₃)	CDCl ₃	Acros Organics, Belgium
Methanol-d ₆	CD ₃ OD	Acros Organics, Belgium

Table 3.7: Material and HPLC grade solvents used for LC- and GC-MS analysis

Materials/ Solvents	Molecular formula	Density, ρ (g cm⁻³)	Source, Country
Nylon syringe filter	-	-	Membrane solution, USA
Acetonitrile	CH ₃ CN	41.05	Fisher Scientific, UK
Methanol	CH ₃ OH	32.04	Fisher Scientific, UK

Table 3.8: List of material and reagents used in antioxidant assay

Materials/Reagents	Source, Country
96-well plate	Techno Plastic Products AG, Switzerland
1,1-diphenyl-2-picrylhydrazyl (DPPH)	Sigma-Aldrich, USA
Ascorbic acid (Vitamin C)	Sigma-Aldrich, USA
Kaempferol	Sigma-Aldrich, USA

3.3 Extraction, Isolation and Purification of Phytochemicals from *G. parvifolia*

Approximately 2.0 kg of stem bark of *G. parvifolia* was collected, air-dried and thoroughly pulverized. The stem bark powder was exhaustively extracted by percolation with dichloromethane in a conical flask at room temperature for 48 hours. Prior to sealing the conical flask with aluminium foil and paraffin film, the plant material was well-stirred and swirled to increase its extraction efficiency. Subsequently, filtration and concentration of the extract *in vacuo* gave a dark and gummy dichloromethane residue. The percolation was repeated twice using the pulpy residue and the resulting crude extracts were pooled together. The plant residue was further subjected to successive extraction with ethyl acetate and finally with methanol, twice for each of the solvents. Eventually, the dry weight of the dichloromethane and ethyl acetate crude extracts obtained was 53.85 and 52.27 g, respectively.

Next, the separation of the crude extracts by column chromatography on silica gel with suitable solvent system afforded a series of fractions. The chemical composition of each fraction was firstly monitored using TLC under UV light. The fractions that displayed more than one spot and similar chemical composition were combined and later subjected to repeated column chromatography until pure compounds were successfully isolated. Pure compounds which showed single spot on the TLC plate were structurally elucidated using various modern spectroscopic techniques including UV/Vis, IR spectroscopy, NMR and LC-MS.

3.4 Chromatography

3.4.1 Column Chromatography (CC)

Column chromatography is one of the solid-liquid separation techniques that can be used to isolate and purify chemical compounds from the crude extracts. Silica gel (60Å, 230-400 mesh) from Sigma-Aldrich, USA, and industrial grade solvents including n-hexane, dichloromethane, ethyl acetate, acetone and methanol, were employed as the stationary and mobile phase, respectively, during the separation of chemical compounds via column chromatography.

Prior to packing of silica gel in a cylindrical glass column, the sample must be prepared via dry packing method. The sample was first dissolved in a minimum amount of a mixture of dichloromethane and acetone (50:50). The sample was then added dropwise mixing with a suitable amount of silica gel and continuous stirring until a finely powdered sample was obtained.

There were several sizes of column available including 20, 30 and 40 mm internal diameter columns. Basically, the larger the amount of sample, the larger the size of column is required. After selection of the column size according to the amount of sample, the column was packed with silica gel using slurry method. A slurry of silica gel was prepared by mixing the silica gel and n-hexane in a beaker, and well-stirred. It was followed by a rapid introduction of the slurry through a filter

funnel into the column. The column was constantly tapped using rubber pipe so as to allow the silica gel to settle down and become more compact. This process was repeated until half of the column was filled up and packed with silica gel.

The powdered sample was subsequently applied onto the top of the packed silica gel to form a thin sample layer which was later fractionated into a series of colored bands during elution with a suitable solvent system of increasing polarity. Collection of the eluates based on separated color bands or by volume gave a series of fractions. A thin layer of sodium sulphate anhydrous was applied onto the top of sample layer as protection layer avoiding direct impact of solvent on sample layer during filling of solvent, and to absorb moisture in the solvent. The overall set up of column chromatography is shown in Figure 3.1.

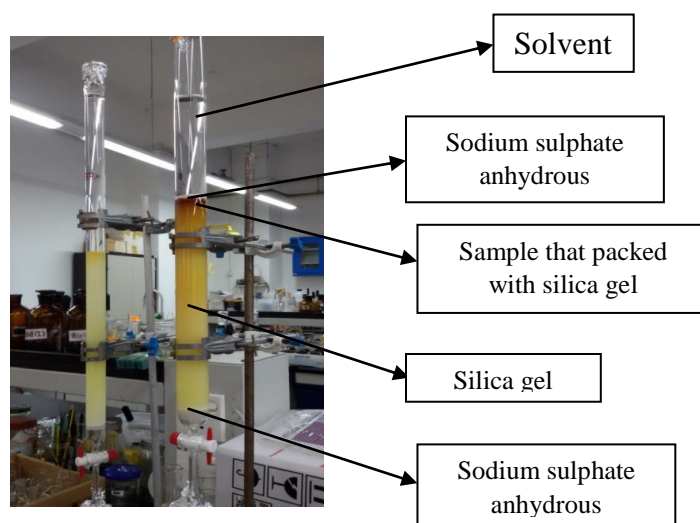


Figure 3.1: Overall set up of column chromatography

3.4.2 Gel Permeation Chromatography (GPC)

Another alternative chromatographic technique, in which a mixture of chemical constituents is separated according to their molecular size, is known as gel permeation chromatography. In this study, GPC had been used to further purify the mixtures that contained two different compounds. Sephadex® LH-20 from New Jersey, USA, was used as the stationary phase and well-packed in a 20 mm-column. Meanwhile, the sample was thoroughly dissolved in least amount of analytical grade methanol. It was later carefully applied onto the top of the packed column, and eluted with a solvent mixture of methanol and dichloromethane (90:10). The eluate was then collected in volumes of 2 to 3 mL for each fraction.

3.4.3 Thin Layer Chromatography (TLC)

The series of fractions collected from chromatographic column were monitored for their chemical composition and purity level using thin layer chromatography (TLC). It was performed on a thin layer of silica gel 60 F₂₅₄ precoated on an aluminium plate. A 8 cm × 4 cm plate was prepared, with both baseline and solvent front line which were drawn 0.6 cm from both ends of the plate. Subsequently, sample solution was introduced as a small spot on the baseline using a capillary tube until a sufficient amount of sample was loaded. At the meantime, 10 mL of a suitable solvent mixture was prepared as mobile phase in a developing chamber. After saturation with solvent vapor in the chamber, the TLC

plate was placed vertically into the chamber and tightly capped. The mobile phase was gradually drawn up to the solvent front line of the TLC plate by capillary action. The developed spots on the TLC were eventually marked down visualizing under UV light and in the iodine chamber. The retention factor, R_f , of each spot was calculated using the equation below:

$$R_f = \frac{\text{Distance travelled by the analyte (cm)}}{\text{Distance travelled by the solvent front (cm)}}$$

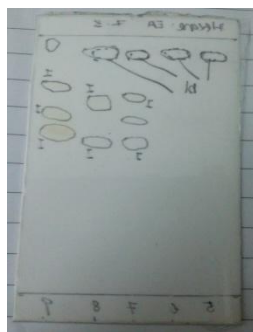


Figure 3.2: Developed TLC plate

3.5 TLC Visualization Methods

3.5.1 Ultraviolet (UV) Light

After the development of the TLC plates, the separated components of each fraction was visualized under UV light of both long (365 nm) and short (254 nm) wavelengths. All the spots appeared were lightly outlined using a pencil. The components containing extended conjugation and aromatic rings can be easily detected using this visualization technique.

3.5.2 Iodine Vapor Stain

A closed chamber containing 1.5 g of iodine crystals was prepared. After saturation with the iodine vapor in a chamber, the TLC plate was subsequently propped vertically in the chamber and tightly closed. After a while, the colorless components on the TLC plate turned into brown color. These brown-colored spots were marked down with pencil immediately because these spots do not persist over a long period of time after the TLC plate was removed from the chamber. This method is an excellent way for the detection of a wide range of unsaturated and aromatic components including terpenoids.

3.5.3 Ferric Chloride Reagent

Ferric chloride test is a common confirmatory test to determine the presence of phenols and hydroxamic acids. A ferric chloride solution was prepared by dissolving 1.0 g ferric chloride in 100 mL of methanol. The solution was sprayed on the developed TLC plate to form colored metal complexes. The dark blue or greenish, and red spots on the TLC plate indicate the presence of phenolic constituents and hydroxamic acids, respectively.

3.6 Instruments

3.6.1 Nuclear Magnetic Resonance (NMR) Spectroscopy

Nuclear magnetic resonance (NMR) is an indispensably and non-destructive spectroscopic technique which is used to provide a wide range of information, including types, relative amounts and environments of nuclei, purity level and isomerism, of the organic compounds. A NMR sample was prepared by completely dissolving the pure compound in a suitable deuterated solvent such as chloroform, acetone or methanol. Meanwhile tetramethylsilane (TMS) was used as internal reference. Next, the sample solution was transferred into a clean, dry NMR tube up to about 4 cm height. The NMR tube was then capped, labeled and sealed with parafilm, and experimentally analyzed using a JEOL JNM-ECX 400 MHz NMR spectrometer. A series of spectra including ^1H -, ^{13}C -NMR, DEPT, HMQC and HMBC was obtained to assist in structural elucidation of organic compounds.

3.6.2 Infrared (IR) Spectroscopy

IR spectroscopy was used to provide information regarding the functional groups present in a compound, position of substituents on the aromatic ring as well as to access the purity of organic compounds. The IR sample was prepared in potassium bromide (KBr) pellet. It was done by mixing sample and KBr in a ratio

of 1:10 and grinding them together until a homogenous powdered mixture was formed. The KBr pellet was then obtained by compressing the mixture using a hydraulic press. The IR spectra of the compounds were recorded in a range between 4000 and 400 cm^{-1} on a Perkin Elmer 2000-FTIR spectrophotometer.

3.6.3 Ultraviolet-Visible (UV-Vis) Spectroscopy

The presence of conjugated chromophores in a compound gives characteristic absorption peaks in the region between 200 and 800 nm which can be detected using a UV/Vis spectrophotometer. After dissolving a small amount of sample in chloroform, the UV/Vis absorption of sample was measured on a double beam Perkin Elmer Lambda 35 spectrophotometer, with chloroform as the solvent blank. The absorption maxima of the samples were determined over a range from 200 to 400 nm.

3.6.4 Liquid Chromatography- Mass Spectrometry (LC-MS)

The mass spectra which provide structural information regarding molecular weight and molecular formula of isolated compounds were recorded on an Agilent Technologies 6520 LC/MS. Approximately 1.0 mg of sample was weighed into the vials and then dissolved in 1 mL of HPLC grade solvent such as acetonitrile or methanol, in a sample vial. The sample solution was later sonicated for 5 minutes. After that, 15 μL of the sample solution was introduced into the

column and eluted with a solvent mixture of water and methanol (70:30, v/v) at a flow rate of 0.6 mL/min. The separated components were ionized via electrospray ionization to give HRESI mass spectra.

3.6.5 Melting Point Apparatus

Melting point determination of the compounds was carried out using a Stuart SMP 10 melting point apparatus. A hematocrit capillary tube was filled in with a solid sample up to about 3 mm height. Subsequently, the solid sample was heated until it was entirely melted. The melting range at which the solid sample started to liquefy and completely melted was recorded. It was used to assess the purity of the test compounds and to compare their melting points with literature values. Pure crystalline or powdered compound melts in a narrow and sharp melting range, whereas the impure compound tends to give a much wider temperature range.

3.6.6 Polarimeter

Polarimetry is widely used to examine the optical activity of compounds that consist of one or more chiral centers by measuring the degree through which the plane polarized light is being rotated. Firstly, 5 mg of optically active sample in 10 mL chloroform was prepared in a volumetric flask. The sample solution was poured into a polarimeter cell and the optical rotation was determined on a Jasco

Europe P-2000 digital polarimeter. The specific rotation of the sample was later calculated using the following equation:

$$[\alpha]_{\lambda}^T = \frac{\alpha}{c \times l}$$

where $[\alpha]$ = Specific rotation

α = Observed optical rotation

l = Optical path length (1.0 dm)

c = Concentration of the sample in g/mL

T = Temperature (25°C)

λ = Wavelength (589 nm)

3.7 Antioxidant Assay

Isolated compounds and reference standards (vitamin C and kaempferol) were separately dissolved in methanol to prepare their master stocks at concentration of 1 mg/mL. At the meantime, 2 mg/mL DPPH solution was prepared by dissolving 4 mg of DPPH powder in 2 mL of methanol. All the solutions prepared were later sonicated for 5 minutes to produce homogenous solutions. The solutions were then placed in a 4 °C chiller in dark condition because they are light sensitive.

From the stock solutions, the isolates and standard compounds were prepared at various concentrations of 240, 120, 60, 30, 15, 7.5 and 3.75 µg/mL in methanol through serial dilution in 96-well plate. 10 µL of DPPH solution and 90 µL of methanol were then added into each well to give a final volume of 200 µL. On the

other hand, the wells in row H were filled with only DPPH solution and methanol to serve as negative control. The antioxidant assay was performed in three individual replicates for each of the isolated compounds and standards.

After that, the plate was instantly wrapped with aluminium foil to avoid solvent evaporation and light exposure, and kept in dark at room temperature for 30 minutes. It was followed by measurement of absorbance of the mixtures in each well at 520 nm using a Bio-Rad Model 680 microplate reader. Inhibition rate of the test compound was calculated using the following equation:

$$\text{Inhibition Rate (\%)} = \frac{A_0 - A_1}{A_0} \times 100\%$$

where A_0 = Absorbance of the negative control (without plant extract)

A_1 = Absorbance of the test compound

A graph of inhibition rate against concentration of the test compound was plotted. From the graph, the concentration of the sample that required to scavenge the free radicals by 50 % was determined. It is known as half maximal inhibitory concentration (IC_{50}).

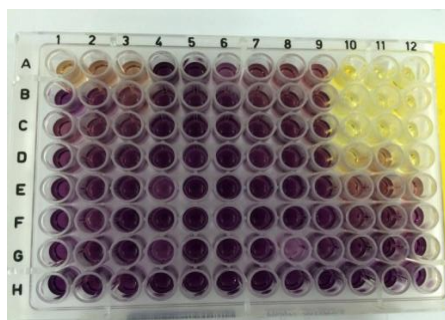


Figure 3.3: 96-well plate used in DPPH assay

CHAPTER 4

RESULTS AND DISCUSSION

4.1 Isolation of Compounds from the Dichloromethane Stem Bark Extract of *G. parvifolia*

About 53.85 g of the dichloromethane stem bark extract was fractionated by column chromatography over silica gel into a total of 6 fractions (LW4_1-6), eluted with solvent mixtures of increasing polarity, including hexane-ethyl acetate, ethyl acetate-acetone and acetone-methanol. From these fractions, fractions LW4_1-3 were pooled together for further separation by column chromatography using linear gradient elution of hexane and ethyl acetate (95:0- 0:100, v/v) to afford 24 subfractions (LW4A_1-24). Due to the similar physical appearance and chemical composition between subfractions LW4A_14 and LW4A_15, they were combined and then subjected to silica gel column chromatography using a hexane-acetone gradient system (95:0- 0:100, v/v). As a result, a total of 17 subfractions (LW4A14A_1-17) were collected. Among these subfractions, subfraction LW4A14A_8 was found to give a pure greenish gum. After spectroscopic and spectrometric analyses (IR, UV/Vis, NMR and MS), this compound was identified as [2*E*,6*E*,10*E*]-(+)-4 β -hydroxy-3-methyl-5 β -(3,7,11,15-tetramethyl-2,6,10,14-hexadecatetraenyl)-2-cyclohexen-1-one [52] and was given the trivial name as tetraprenyltoluquinone (TPTQ). The isolation pathway of tetraprenyltoluquinone was shown in Figure 4.1.

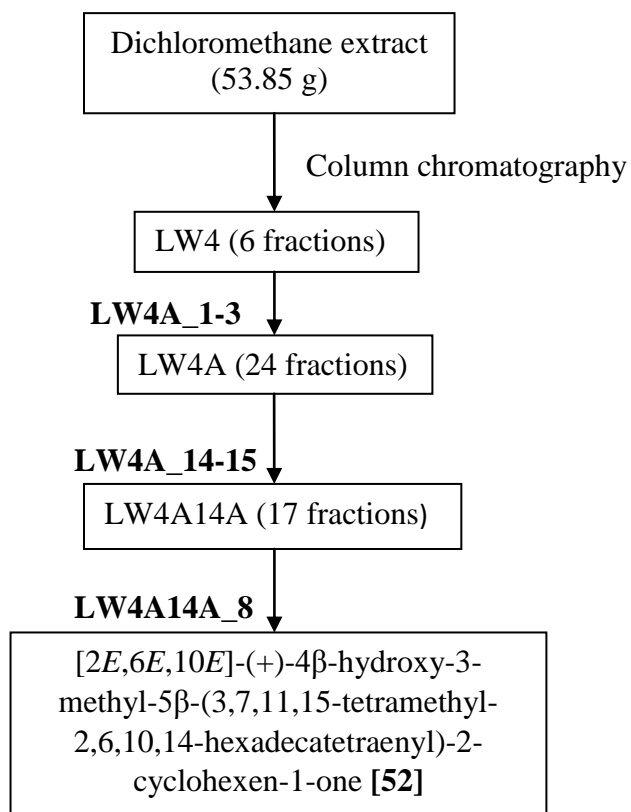


Figure 4.1: Isolation pathway of [2*E*,6*E*,10*E*]-(+)-4β-hydroxy-3-methyl-5β-(3,7,11,15-tetramethyl-2,6,10,14-hexadecatetraenyl)-2-cyclohexen-1-one [52]

4.1.1 Characterization and Structural Elucidation of [2*E*,6*E*,10*E*]-(+)-4 β -hydroxy-3-methyl-5 β -(3,7,11,15-tetramethyl-2,6,10,14-hexadecatetraenyl)-2-cyclohexen-1-one [52]

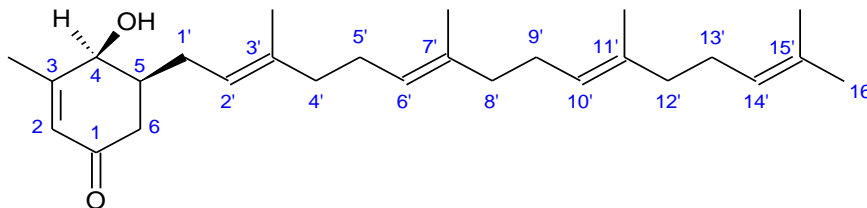


Figure 4.2: Structure of [2*E*,6*E*,10*E*]-(+)-4 β -hydroxy-3-methyl-5 β -(3,7,11,15-tetramethyl-2,6,10,14-hexadecatetraenyl)-2-cyclohexen-1-one [52]

Compound **52** was isolated as a viscous greenish gum with a mass of 524.8 mg. This compound is relatively polar showing a R_f value of 0.6 when using a solvent mixture of dichloromethane and acetone (9:1, v/v) as the mobile phase in TLC analysis. It appeared as a dark spot on the developed TLC plate under UV light and as a yellow spot when staining with iodine vapor. In addition, it appeared as a dark blue spot when sprayed with ferric chloride solution, indicating the presence of enol group which is formed in equilibrium with keto group in compound **52**. It exists as an equilibrium mixture of two different structures as given in Figure 4.3. The enol form of compound **52** is responsible for the light blue color when reacted with ferric chloride. Besides that, the HRESI mass spectrum (Figure 4.4) of this compound displayed a pseudo-molecular ion, $[M+H]^+$ at m/z 399.3258 which is corresponding to the molecular formula of $C_{27}H_{42}O_2$. In addition, it has a $[\alpha]_D^{25}$ value of $+47^\circ$, which is close to the reported literature value of $+50^\circ$ (Wahyuni, et al., 2015).

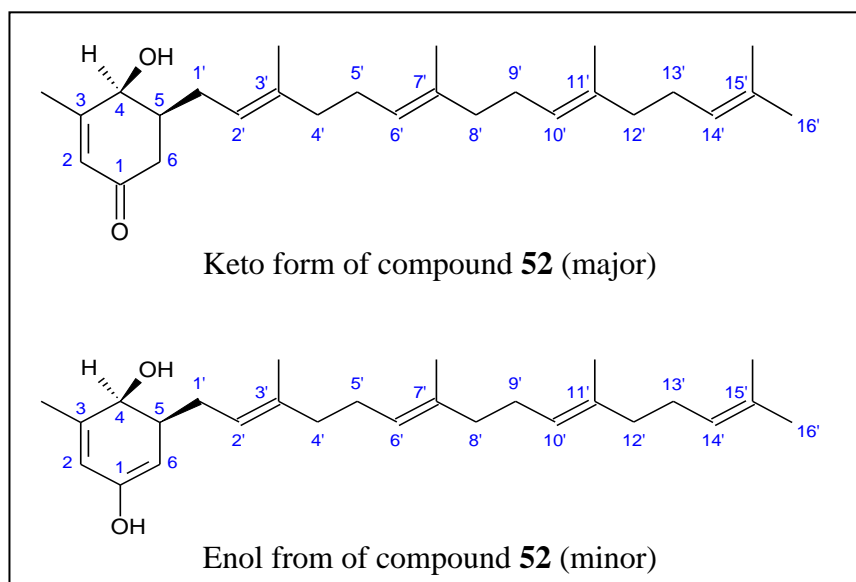


Figure 4.3: An equilibrium mixture of keto and enol forms of compound 52

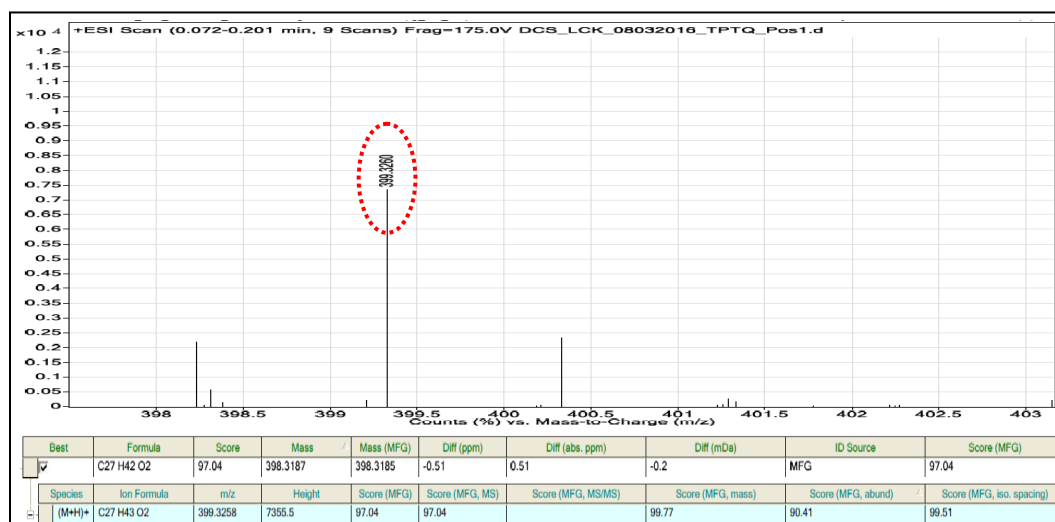


Figure 4.4: HRESI Mass spectrum of compound 52

The structure of compound **52** was successfully elucidated based on the NMR spectral data obtained. From the ¹H NMR spectra (Figures 4.5 & 4.6), a highly deshielded singlet at δ_{H} 5.82 was assigned as the olefinic proton, which had to be H-2. Meanwhile, the signals at δ_{H} 4.12 and 2.11, each integrating for one hydrogen were attributed to methine protons, H-4 and H-5, respectively. The

methine proton, H-4 appeared to be more deshielded than H-5 due to the presence of electron withdrawing hydroxyl group at carbon C-4. The spectrum also displayed a pair of signals at δ_{H} 2.51 and 2.08, both were assigned to the methylene protons, H-6 because the two protons in the methylene group experienced different magnetic environment as they are rigidly placed in the cyclic ring. As a result, each proton in the methylene group gave signal with different chemical shift values. In addition, a singlet integrated for three protons at δ_{H} 2.02 was assigned as the methyl protons, 3-CH₃. The presence of geranylgeranyl group was revealed by a series of characteristic proton signals including δ_{H} 5.16 (1H, t, $J = 7.0$ Hz), 5.07 (3H, d, $J = 5.5$ Hz), 2.34 (1H, m), 2.15 (1H, d, $J = 1.2$ Hz), 2.05 (6H, m), 1.96 (6H, m), 1.66 (3H, s), 1.61 (3H, s) and 1.58 (9H, s).

The ¹³C NMR spectrum (Figure 4.7) displayed a total of 27 carbons signals, which was in consistent with the total number of carbons in the proposed structure. The most downfield carbon signal at δ_{C} 198.9 was attributed to the presence of carbonyl carbon, C-1. The spectrum also displayed two signals at δ_{C} 163.6 and 126.8 corresponding to the pair of olefinic carbons, C-3 and C-2, respectively. Besides that, presence of two methine and one methylene carbons were indicated by the signals at δ_{C} 73.6 (C-4) and 43.7 (C-5), and 41.4 (C-6), respectively. The presence of geranylgeranyl group was further evidenced by the four protonated olefinic carbon signals at δ_{C} 120.8 (C-2'), 124.5 (C-6'), 124.2 (C-10'), 123.9 (C-14'); four substituted olefinic carbon signals at δ_{C} 138.5 (C-3'), 135.5 (C-7'),

135.0 (C-11'), 131.4 (C-15'); five methyl carbon signals at δ_C 17.8 (C-16'), 16.4 (3'-CH₃), 16.1 (7'-CH₃), 16.1 (11'-CH₃), 25.8 (15'-CH₃); seven methylene carbon signals at δ_C 30.9 (C-1'), 39.9 (C-4'), 26.7 (C-5'), 39.8 (C-8'), 26.8 (C-9'), 39.8 (C-12'), 26.6 (C-13'). The ¹³C NMR spectral data of compound **52** was found to be in agreement with the literature data (Wahyuni, et al., 2014). The DEPT spectrum (Figure 4.8) further revealed the presence of six methyl, eight methylene, seven methine and six quaternary carbons, which were in agreement with the proposed structure.

The chemical structure of compound **52** was then deduced from HMQC and HMBC analyses. HMQC spectral data provided the information about ¹J correlation between protons and their immediate carbons. From the HMQC spectrum (Figure 4.9), there were 21 proton signals including H-2, 3-CH₃, H-4, H-5, H-6, H-1', H-2', 3'-CH₃, H-4', H-5', H-6', 7'-CH₃, H-8', H-9', H-10', 11'-CH₃, H-12', H-13', H-14', 15'-CH₃ and H-16', which were found to correlate to their respective carbons. Meanwhile, HMBC spectral data provided further information about ²J and ³J correlation between protons and their neighboring carbons. From the HMBC spectrum (Figure 4.10), the placement of geranylgeranyl group at carbon C-5 was evident from the correlations of the methylene protons, H-1' with carbon C-5 via ²J coupling, and with carbon C-6 via ³J coupling. Moreover, the HMBC correlations from proton H-2 to carbons 3-CH₃ (δ_C 20.5), C-4 (δ_C 73.6) and C-6 (δ_C 41.4); proton H-4 to carbons C-3 (δ_C 163.6) and C-5 (δ_C 43.7); proton H-5 to carbons C-1 (δ_C 198.9); proton H-6 to carbons C-

2 (δ_C 126.8), C-4 (δ_C 73.6) and C-5 (δ_C 43.7) suggested the presence of 4-hydroxy-3-methyl-2-cyclohexen-1-one moiety in the assigned structure. The summary of NMR assignment of compound **52** is shown in Table 4.1.

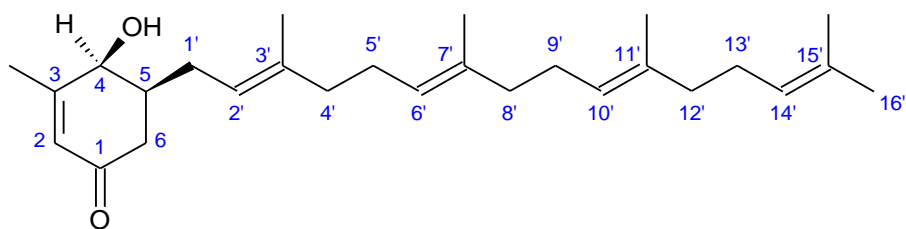
The UV/Vis spectrum (Figure 4.11) displayed UV absorption maximum at 252 nm, assignable to the presence of conjugated enone group in the compound. Meanwhile, the FT-IR spectrum (Figure 4.12) revealed the absorption bands at 3424, 2924 and 1662 cm^{-1} , which confirmed the presence of hydroxyl, sp^3 C-H (stretch) and carbonyl functionalities in the structure. Based on all the spectral evidence above, compound **52** was identified as [2*E*,6*E*,10*E*]-(+)-4 β -hydroxy-3-methyl-5 β -(3,7,11,15-tetramethyl-2,6,10,14-hexadecatetraenyl)-2-cyclohexen-1-one [**52**].

Table 4.1: Summary of NMR assignment of [2*E*,6*E*,10*E*]- (+)-4 β hydroxy -3-methyl-5 β -(3,7,11,15-tetramethyl-2,6,10,14-hexadeca-tetraenyl)-2-cyclohexen-1-one [52**] in comparison with the literature data**

Position	δ_H (ppm)	δ_C (ppm)	δ_C^* (ppm)	DEPT	HMBC	
					2J	3J
1	-	198.9	199.9	C	-	-
2	5.82 (1H,s)	126.8	126.4	CH	-	3-CH ₃ , C-4, 6
3	-	163.6	164.1	C	-	-
4	4.12 (1H, d, $J = 6.1$ Hz)	73.6	73.1	CH	C-3, 5	-
5	2.11 (1H, m)	43.7	43.5	CH	-	C-1
6	2.51 (1H, d, $J = 12.2$ Hz)	41.4	41.1	CH ₂	-	C-1', 4
	2.08 (1H, m)				C-5	C-2, 4
3-CH ₃	2.02 (3H,s)	20.5	20.4	CH ₃	C-3	C-2, 4

1'	2.34 (1H, m)	30.9	30.5	CH ₂	C-2'	C-6
	2.15 (1H, d, <i>J</i> = 1.2 Hz)				C-5	-
2'	5.16 (1H, t, <i>J</i> = 7.0 Hz)	120.8	120.5	CH	C-1'	C-4', 3'-CH ₃
3'	-	138.5	138.2	C	-	-
4'	1.96 (2H, m)	39.9	39.8	CH ₂	C-5'	3'-CH ₃ , C-6'
5'	2.05 (2H, m)	26.7	39.6	CH ₂	C-4', 6'	C-3', C-7'
6'	5.07 (1H, d, <i>J</i> = 5.5 Hz)	124.5	124.3	CH	C-5'	7'-CH ₃ , C-4'
7'	-	135.5	-	C	-	-
8'	1.96 (2H, m)	39.8	39.6	CH ₂	C-9'	7'-CH ₃ , C- 10'
9'	2.05 (2H, m)	26.8	26.6	CH ₂	C-8', 10'	C-7', 11'
10'	5.07 (1H, d, <i>J</i> = 5.5 Hz)	124.2	124.1	CH	C-9'	11'-CH ₃ , C- 8'
11'	-	135.0	-	C	-	-
12'	1.96 (2H, m)	39.8	26.5	CH ₂	C-13'	11'-CH ₃ , C- 14'
13'	2.05 (2H, m)	26.6	26.4	CH ₂	C-12', 14'	C-11', 15'
14'	5.07 (1H, d, <i>J</i> = 5.5 Hz)	123.9	123.8	CH	C-13'	C-12'
15'	-	131.4	-	C	-	-
16'	1.61 (3H, s)	17.8	-	CH ₃	-	15'-CH ₃
3'-CH ₃	1.58 (3H, s)	16.4	-	CH ₃	-	C-4'
7'-CH ₃	1.58 (3H, s)	16.1	-	CH ₃	C-7'	C-6'
11'-CH ₃	1.58 (3H, s)	16.1	-	CH ₃	-	C-10'
15'-CH ₃	1.66 (3H, s)	25.8	-	CH ₃	C-15'	C-14', 16'

* Wahyuni, et al., 2015.



[52]

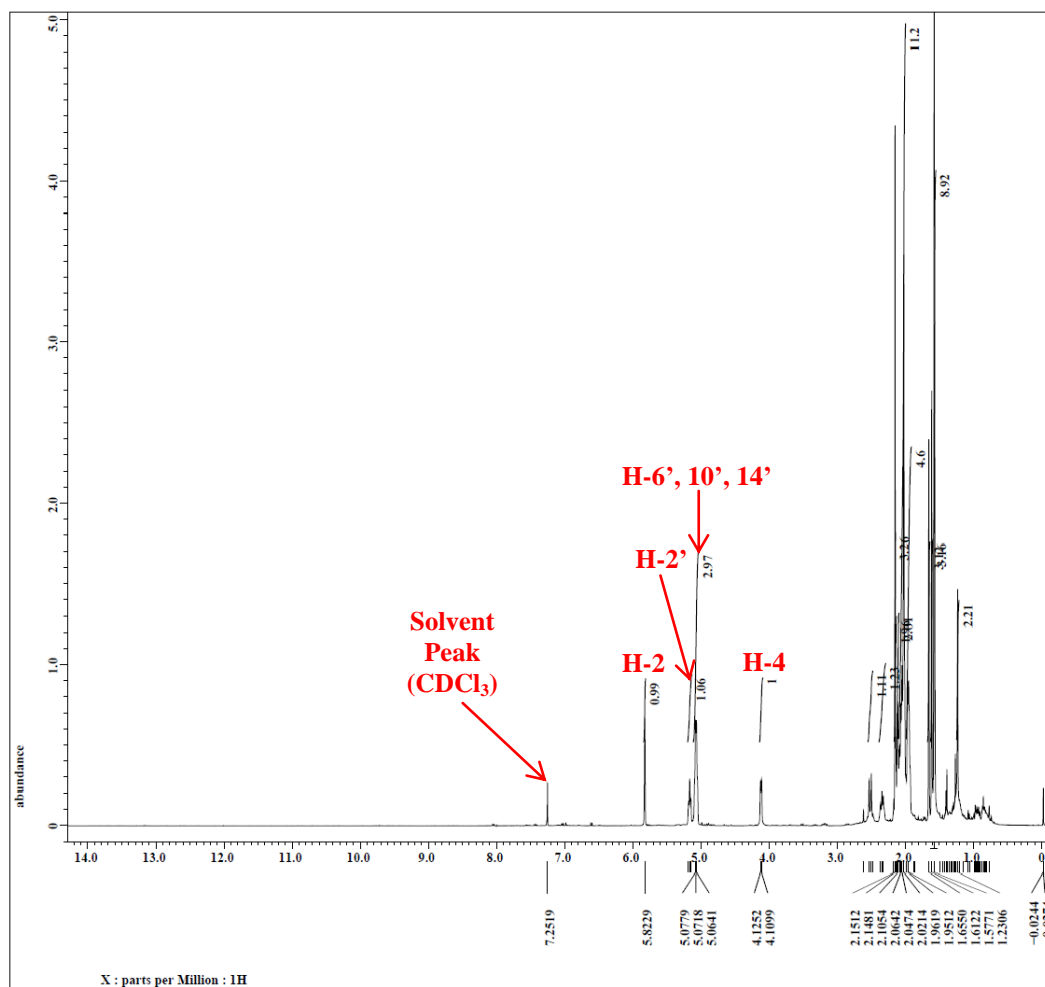
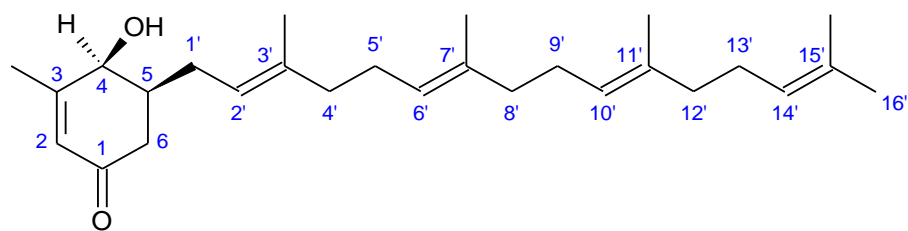


Figure 4.5: ¹H NMR spectrum of compound 52 (400 MHz, CDCl₃)



[52]

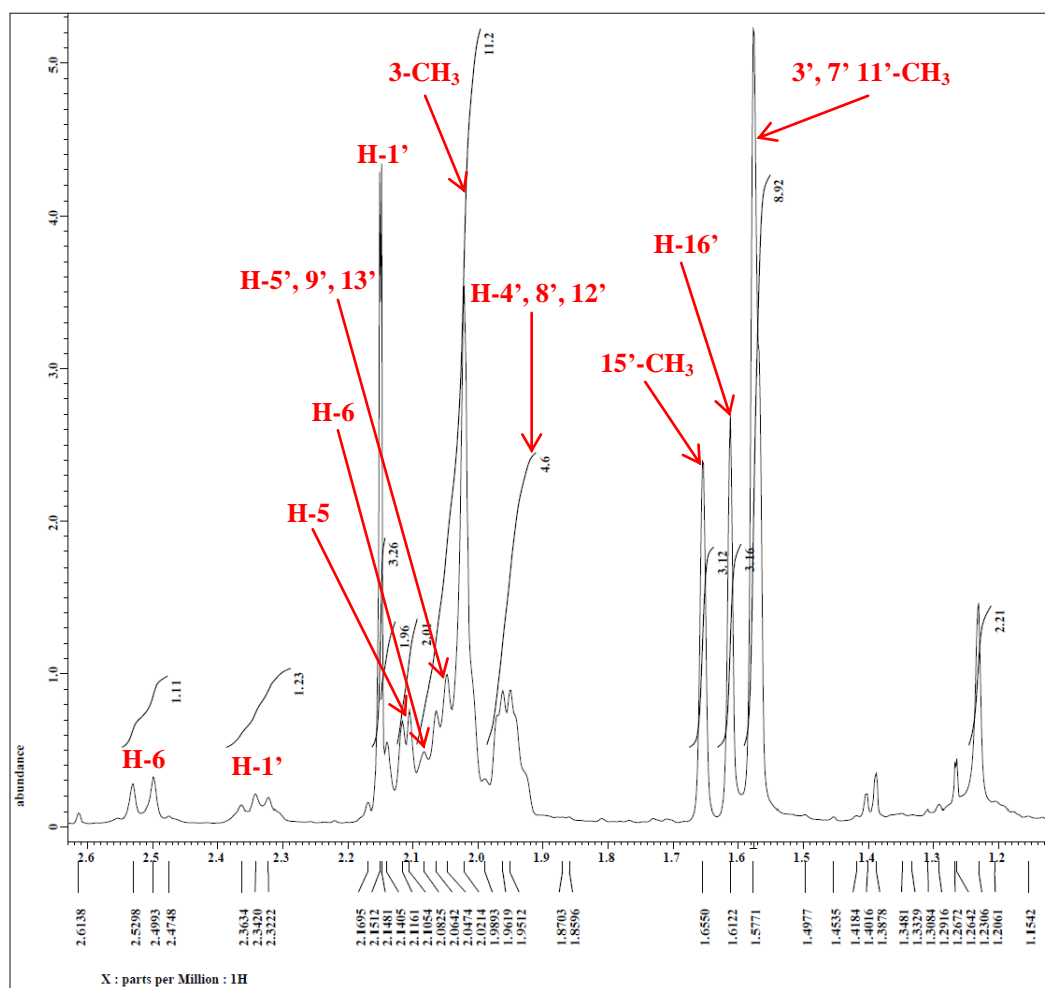
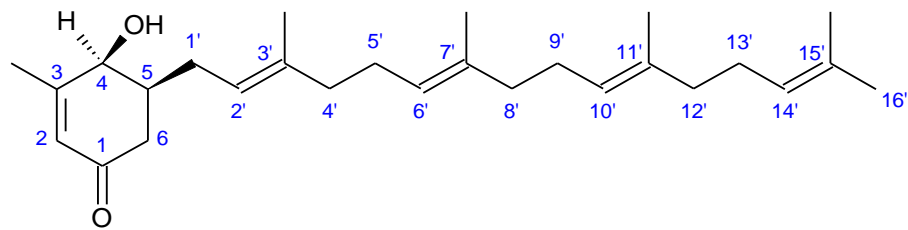


Figure 4.6: Expanded ^1H NMR spectrum of compound 52 (400 MHz, CDCl_3)



[52]

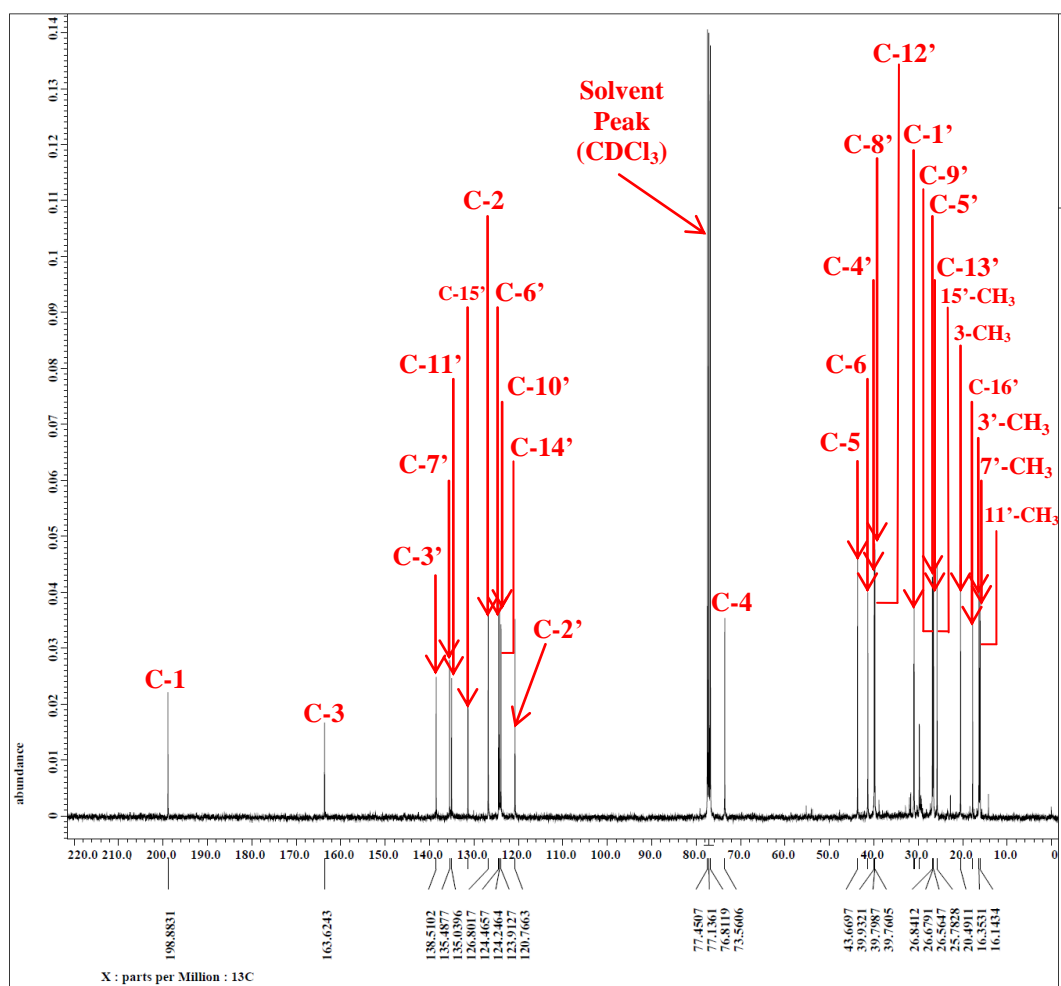
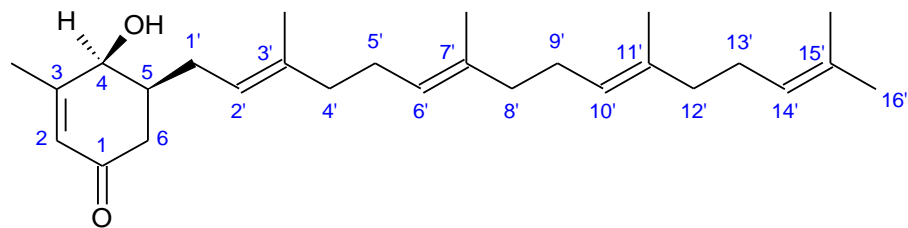


Figure 4.7: ¹³C NMR spectrum of compound 52 (100 MHz, CDCl₃)



[52]

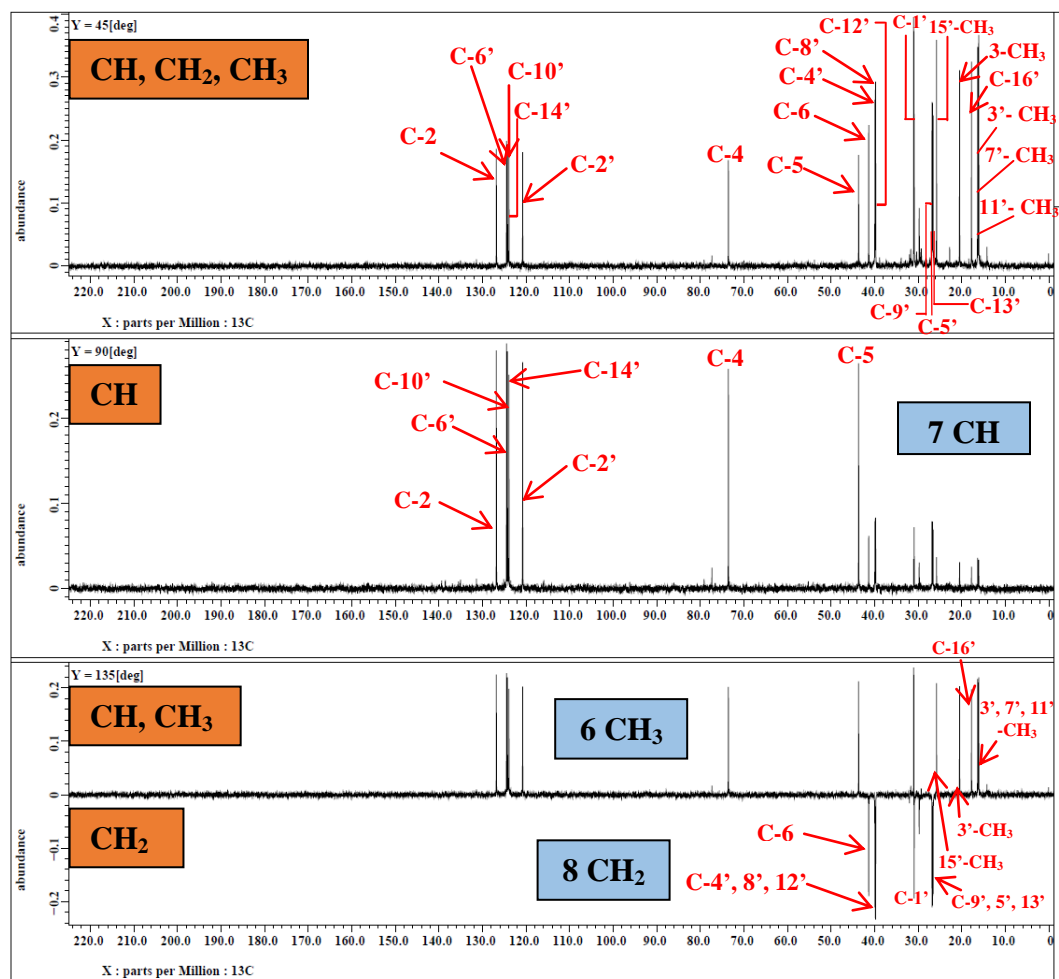
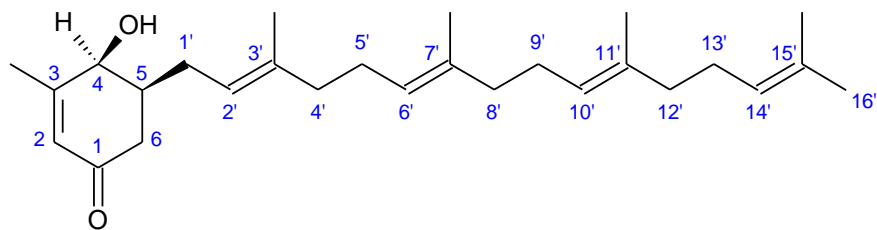


Figure 4.8: DEPT spectrum of compound 52 (100 MHz, CDCl₃)



[52]

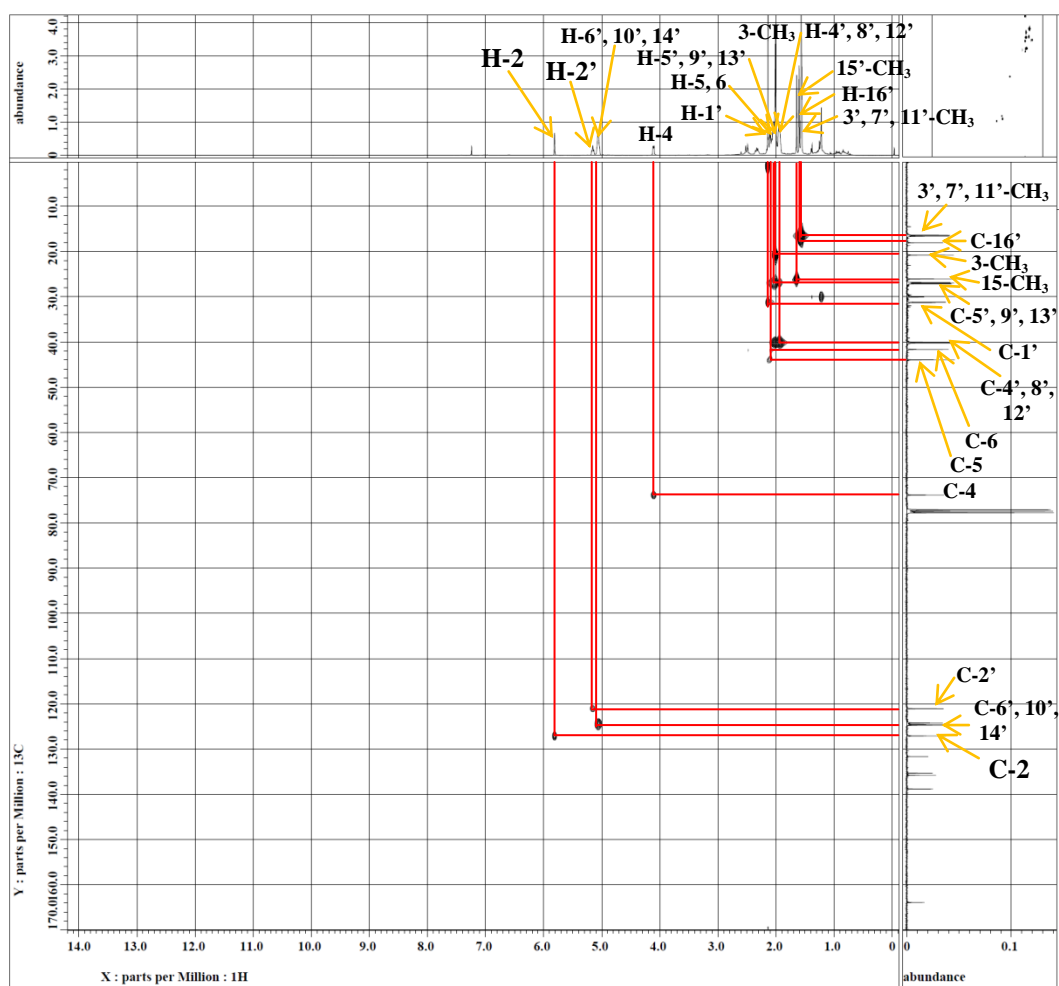
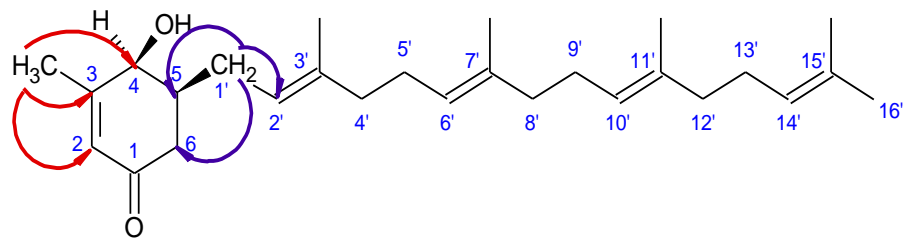


Figure 4.9: HMQC spectrum of compound 52



[52]

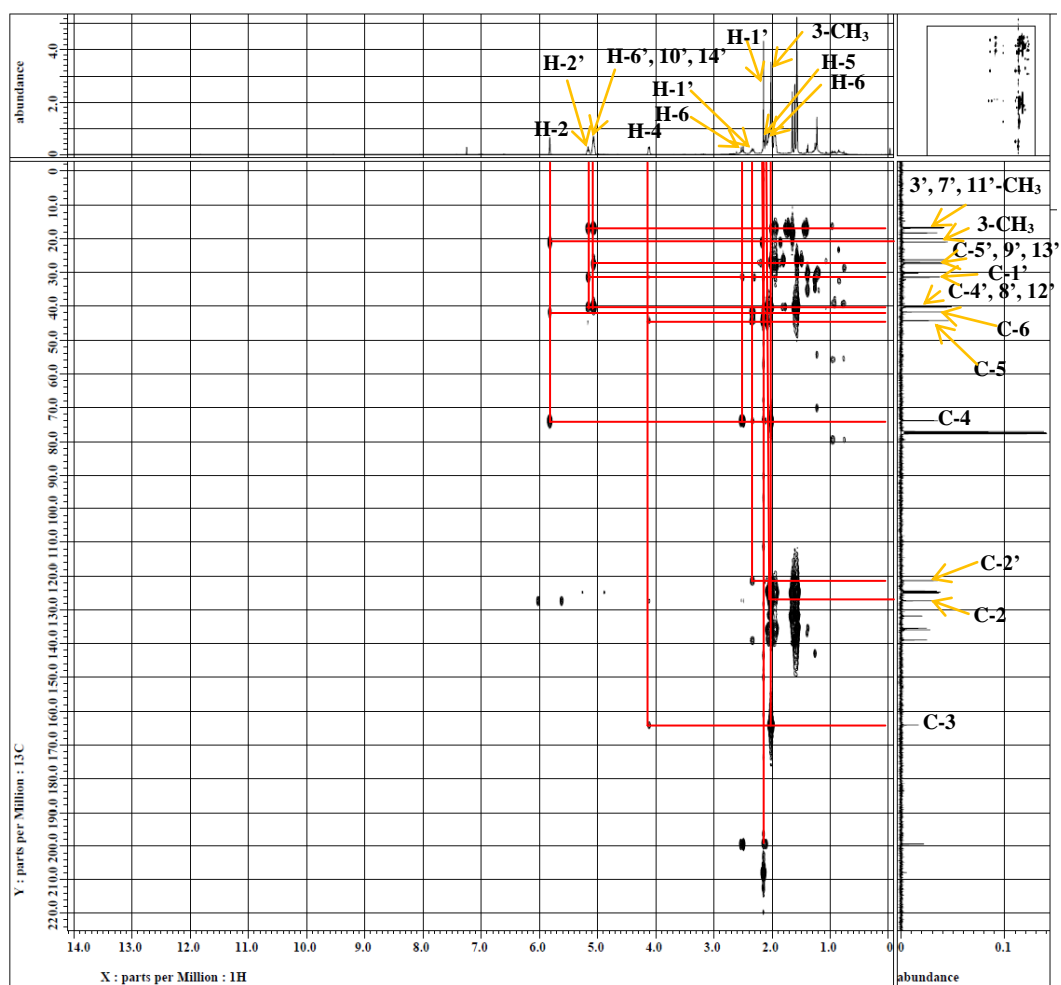


Figure 4.10: HMBC spectrum of compound 52

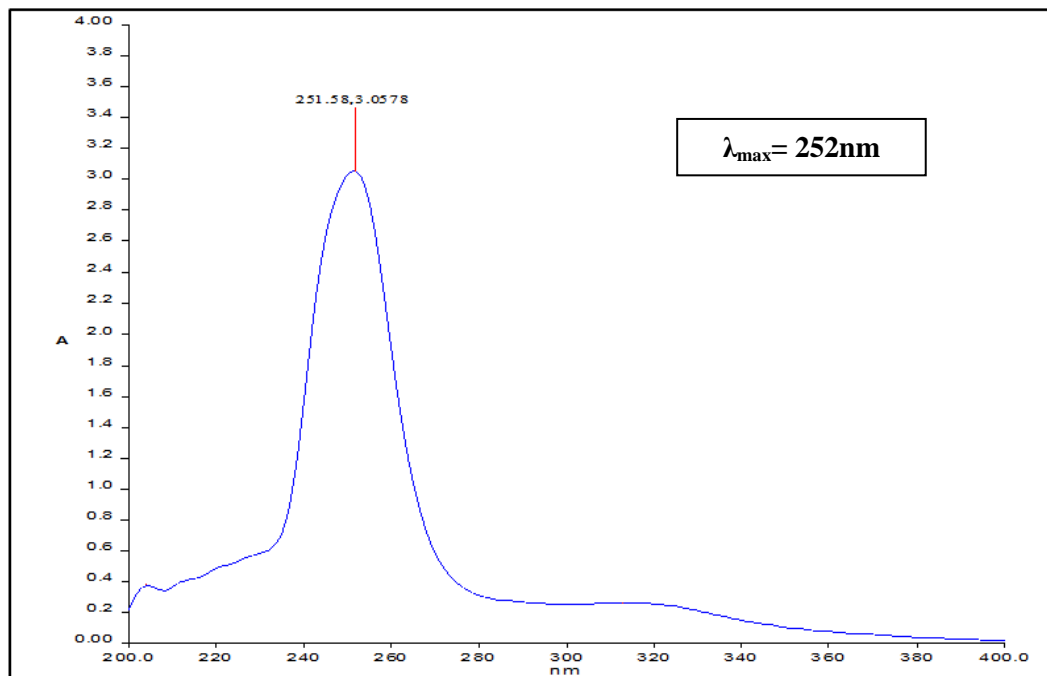


Figure 4.11: UV/Vis spectrum of compound 52

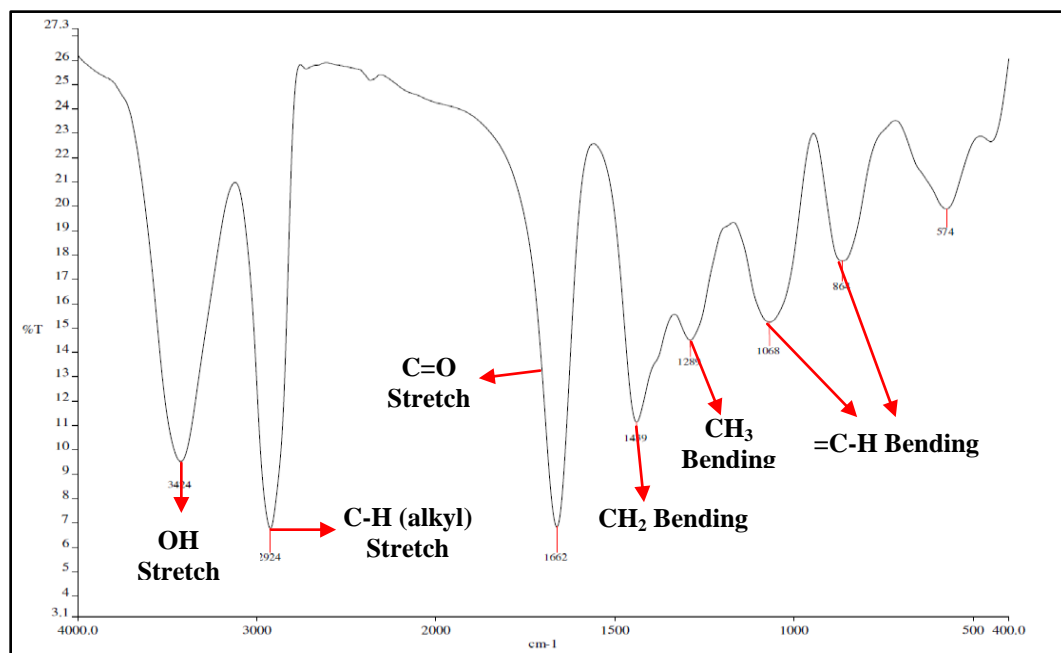


Figure 4.12: FT-IR spectrum of compound 52

4.2 Isolation of Compounds from the Ethyl Acetate Stem Bark Extract of *G. parvifolia*

Column chromatography on ethyl acetate stem bark extract had led to the isolation of three xanthone derivatives and a steroid. About 52.27 g of ethyl acetate extract was subjected to column chromatography packed with silica gel and eluted with solvent mixtures of increasing polarity: hexane-ethyl acetate, ethyl acetate-acetone and acetone-methanol to yield 24 fractions (A1-24). After TLC analysis on the fractions, fractions A10 and A11 were combined, and further purified by a series of silica gel column chromatography to afford 33 subfractions (LWE102B_1-33). Among these subfractions, subfraction LWE102B_8 was further fractionated over Sephadex® LH-20 using analytical grade methanol as the eluting solvent to give 70 subfractions (LWE102B8_1-70). Subfractions LWE102B8_57-59 were found to give a single spot on TLC plate and combined for spectroscopic analysis. The pure compound was determined to be α -mangostin [53].

On the other hand, fraction A13 was further subjected to column chromatography over silica gel to yield 23 subfractions (LW2A_1-23). Only subfraction LW2A_13 showed a single spot on TLC plate and was later identified as rubraxanthone [54]. Meanwhile, subfractions LW2A_11 and LW2A_12 were analyzed by TLC to show similar chemical composition, and were combined for further purification by column chromatography eluted with a solvent mixture of hexane-acetone in increasing polarity. The purification of this combined fractions

led to the isolation of two pure compounds, namely 1,3,7-trihydroxy-2,4-*bis*(3-methylbut-2-enyl)xanthone [55] and stigmasterol [56] from subfractions LW2B_18 and LW2B_9, respectively. The structures of pure compounds were elucidated based on the spectral data. The isolation pathway of α -mangostin [53], rubraxanthone [54], 1,3,7-trihydroxy-2,4-*bis*(3-methylbut-2-enyl)xanthone [55] and stigmasterol [56] is shown in Figure 4.13.

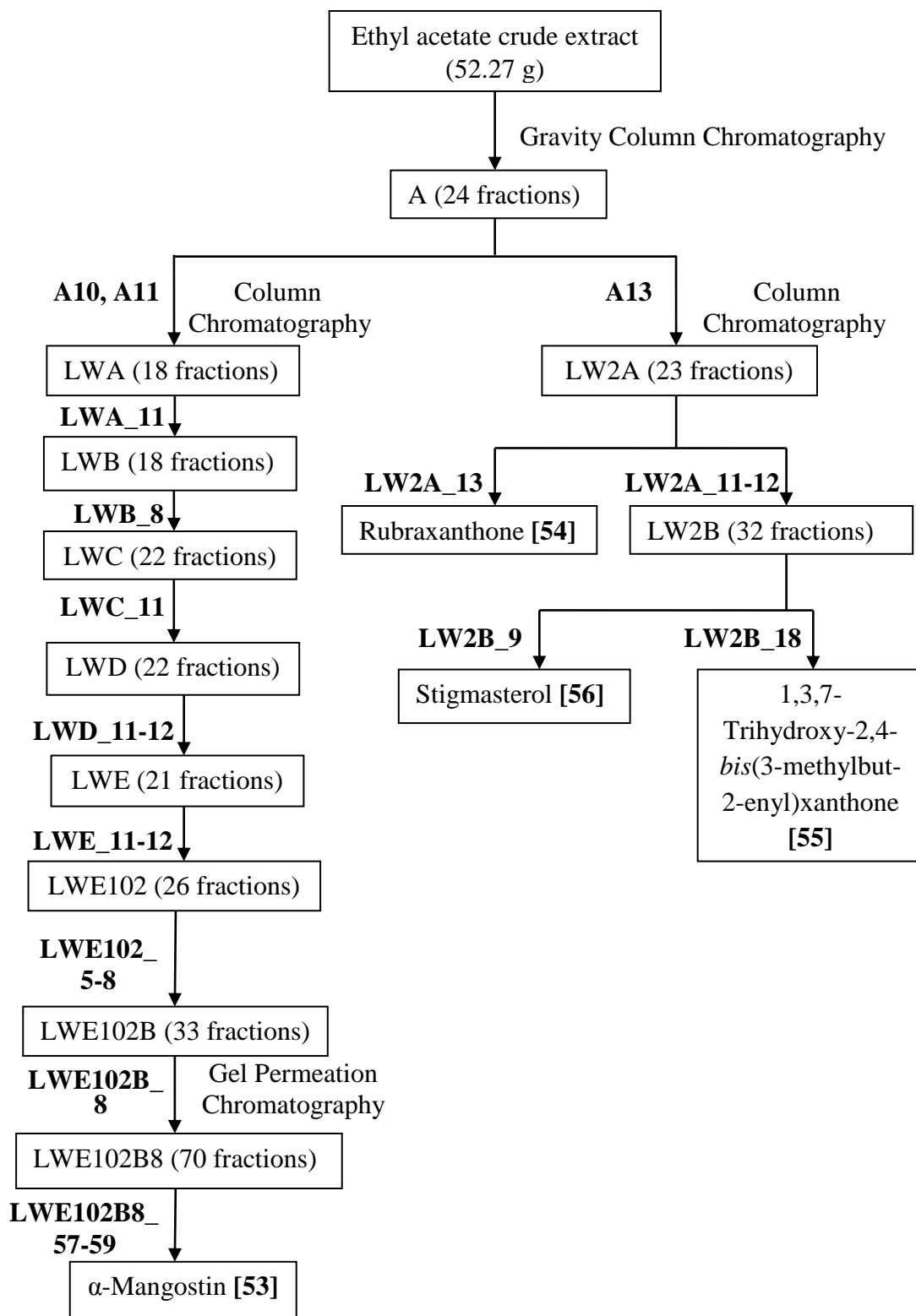


Figure 4.13: Isolation pathway of α -mangostin [53], rubraxanthone[54], 1,3,7-trihydroxy-2,4-bis(3-methylbut-2-enyl)xanthone [55] and stigmasterol [56]

4.2.1 Characterization and Structural Elucidation of α -Mangostin [53]

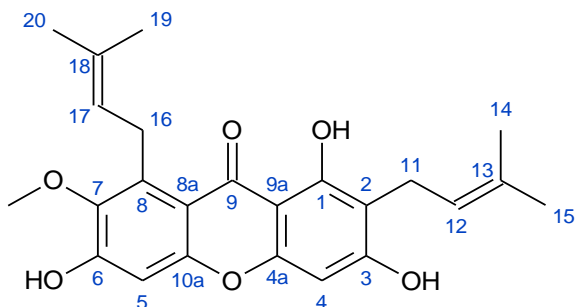


Figure 4.14: Structure of α -mangostin [53]

Compound **53** was obtained as yellow solid with an amount of 16.7 mg. It has a melting range of 176-178 °C (Lit. 175-177 °C, Ahmad, et al., 2013). The TLC analysis indicated that this compound gave a R_f value of 0.75 using a solvent mixture of dichloromethane and acetone (8:2, v/v) as the mobile phase. It appeared as an orange spot under UV light at 365 nm wavelength and as a yellow spot when treated with iodine vapor. The spot turned from yellow to dark blue after sprayed with ferric chloride solution, indicating the phenolic nature of this compound. It has a molecular weight of 410.1741 g mol⁻¹ which is corresponding to a molecular formula of C₂₄H₂₆O₆ based on the pseudo-molecular ion observed at m/z 411.1802 in the HRESI mass spectrum (Figure 4.15).

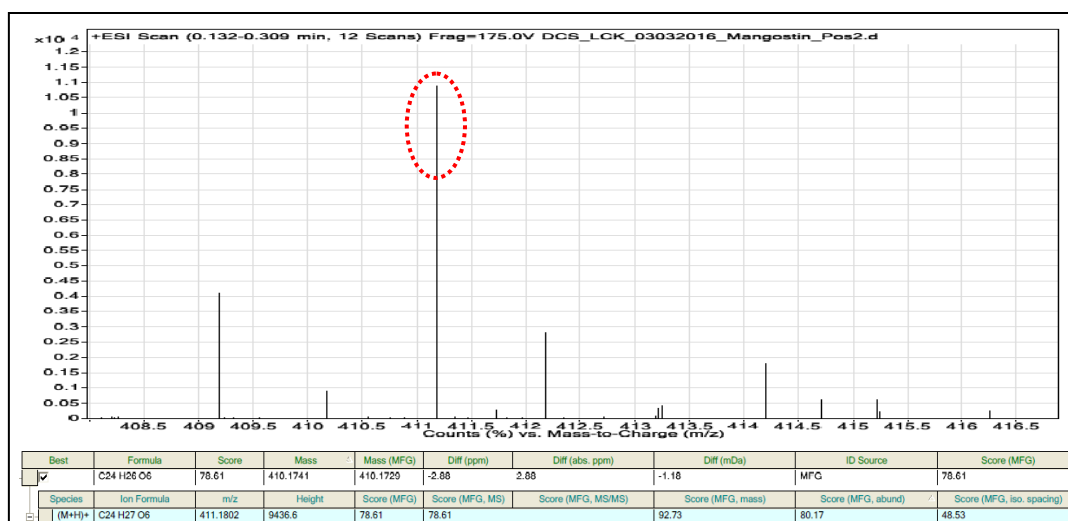


Figure 4.15: HRESI mass spectrum of compound 53

In the ¹H NMR spectrum (Figure 4.16), a sharp singlet at δ_{H} 13.77 was assigned to the chelated hydroxyl proton, 1-OH. The two singlet signals at δ_{H} 6.28 and 6.81 were attributed to the lone aromatic protons, H-4 and H-5, respectively. The presence of methoxy group, 7-OCH₃ was revealed by the singlet signal at δ_{H} 3.80, integrating for three protons. Meanwhile, the presence of two prenyl groups in the proposed structure was indicated by the two sets of characteristic proton signals: δ_{H} 5.27 (1H, m), 3.44 (2H, d, $J = 7.3$ Hz), 1.83 (3H, s), 1.76 (3H, s), and δ_{H} 5.27 (1H, m), 4.08 (2H, d, $J = 6.1$ Hz), 1.82 (3H, s), 1.68 (3H, s).

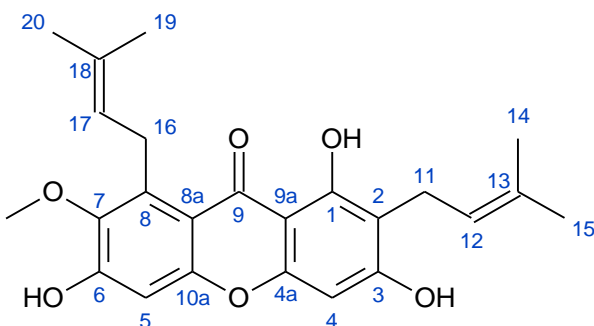
The ¹³C NMR spectrum (Figure 4.17) displayed a total of 24 carbon signals, which was in correspondence with the total number of carbon in the proposed structure. Among these carbon signals, the most deshielded carbon signal at δ_{C} 182.1 was assigned to the carbonyl carbon, C-9. In the aromatic region of the spectrum, two relatively more shielded carbon signals found at δ_{C} 93.4 and 101.7 were attributed to the two protonated aromatic carbons, C-4 and C-5, respectively.

Besides that, the presence of six oxygenated aromatic carbons gave relatively more deshielded carbon signals in the aromatic region at δ_C 160.7 (C-1), 161.7 (C-3), 155.1 (C-4a), 154.6 (C-10a), 155.9 (C-6) and 142.6 (C-7). In the meantime, the remaining quaternary aromatic carbons displayed signals at δ_C 108.6 (C-2), 132.2 (C-8), 112.3 (C-8a) and 103.7 (C-9a). The carbon signal at δ_C 62.1 was assigned to the methoxy carbon, 7-OCH₃. In addition, two sets of carbon signals at δ_C 21.5 (C-11), 121.5 (C-12), 135.8 (C-13), 18.3 (C-14), 26.7 (C-15), and δ_C 26.7 (C-16), 123.2 (C-17), 132.2 (C-18), 18.0 (C-19), 25.8 (C-20), corroborated the presence of two 3-methylbut-2-enyl units.

The chemical structure of compound **53** was further determined based on the HMQC and HMBC analyses. From the HMQC spectrum (Figure 4.18), a total of 11 protonated carbon signals were observed. They were carbons C-4, C-5, C-11, C-12, C-14, C-15, C-16, C-17, C-19, C-20 and 7-OCH₃ which showed correlations with their respective protons in the HMQC spectrum. From the HMBC spectrum (Figure 4.19), the chelated hydroxyl proton, 1-OH showed 2J correlation with carbon C-1, and 3J correlations with carbons C-2 and C-9a, indicating the attachment of 1-OH to carbon C-1. The methoxy group, 7-OCH₃ was found to attach to carbon C-7 based on the cross peak observed between its methyl protons and carbon C-7 via 3J coupling. Apart from that, the placement of two isoprene units in the xanthone skeleton was also determined based on the HMBC spectral data. First isoprene unit was suggested to link to carbon C-2 based on the 2J correlation observed between the methylene protons, H-11, and

quaternary aromatic carbon, C-2. The second isoprene unit was deduced to attach to carbon C-8 based on the correlations of methylene proton, H-16 with carbon C-8 via 2J coupling, and with carbons C-7 and C-8a via 3J coupling. The summary of NMR assignment of compound **53** is shown in Table 4.2.

The proposed structure of compound **53** was further supported by UV/Vis and IR analyses. The UV/Vis spectrum (Figure 4.20) displayed absorption maxima at 250 and 308 nm, indicating the presence of conjugated structure in compound **53**. Besides that, the FT-IR spectrum (Figure 4.21) revealed the absorption bands at 3426 and 1642 cm^{-1} , which confirmed the presence of hydroxyl and carbonyl groups, respectively. The presence of aromatic ring and ethereal group in the compound were further supported by the bands appeared at 1610 and 1459, and 1281 cm^{-1} , respectively. Based on all the spectral evidence, compound **53** was identified as 1,3,6-trihydroxy-7-methoxy-2,8-bis(3-methylbut-2-enyl)xanthone or α -mangostin [**53**].

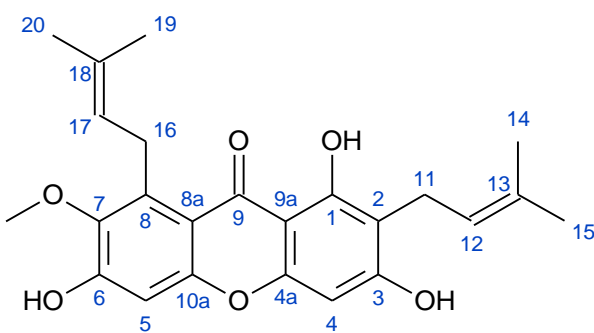


[53]

Table 4.2: Summary of NMR assignment of α -mangostin [53]

Position	δ_{H} (ppm)	δ_{C} (ppm)	HMBC	
			2J	3J
1	-	160.7	-	-
2	-	108.6	-	-
3	-	161.7	-	-
4	6.28 (1H, s)	93.4	C-3, 4a	C-2, 9a
4a	-	155.1	-	-
5	6.81 (1H, s)	101.7	C-6	C-7, 8a
6	-	155.9	-	-
7	-	142.6	-	-
8	-	137.1	-	-
8a	-	112.3	-	-
9	-	182.1	-	-
9a	-	103.7	-	-
10a	-	154.6	-	-
11	3.44 (2H, d, $J = 7.3$ Hz)	21.5	C-2, 12	C-13
12	5.27 (1H, m)	121.5	C-11	C-14, 15
13	-	135.8	-	-
14	1.83 ^a (3H, s)	18.3 ^b	C-13	C-15
15	1.76 (3H, s)	25.9	C-13	C-12, 14
16	4.08 (2H, d, $J = 6.1$ Hz)	26.7	C-8, 17	C-7, 8a, 18
17	5.27 (1H, m)	123.2	-	C-19, 20
18	-	132.2	-	-
19	1.82 ^a (3H, s)	18.0 ^b	C-18	C-20
20	1.68 (3H, s)	25.8	C-18	C-17, 19
1-OH	13.77 (1H, s)	-	C-1	C-2, 9a
7-OCH ₃	3.80 (3H, s)	62.1	-	C-7

^a Interchangeable; ^b Interchangeable



[53]

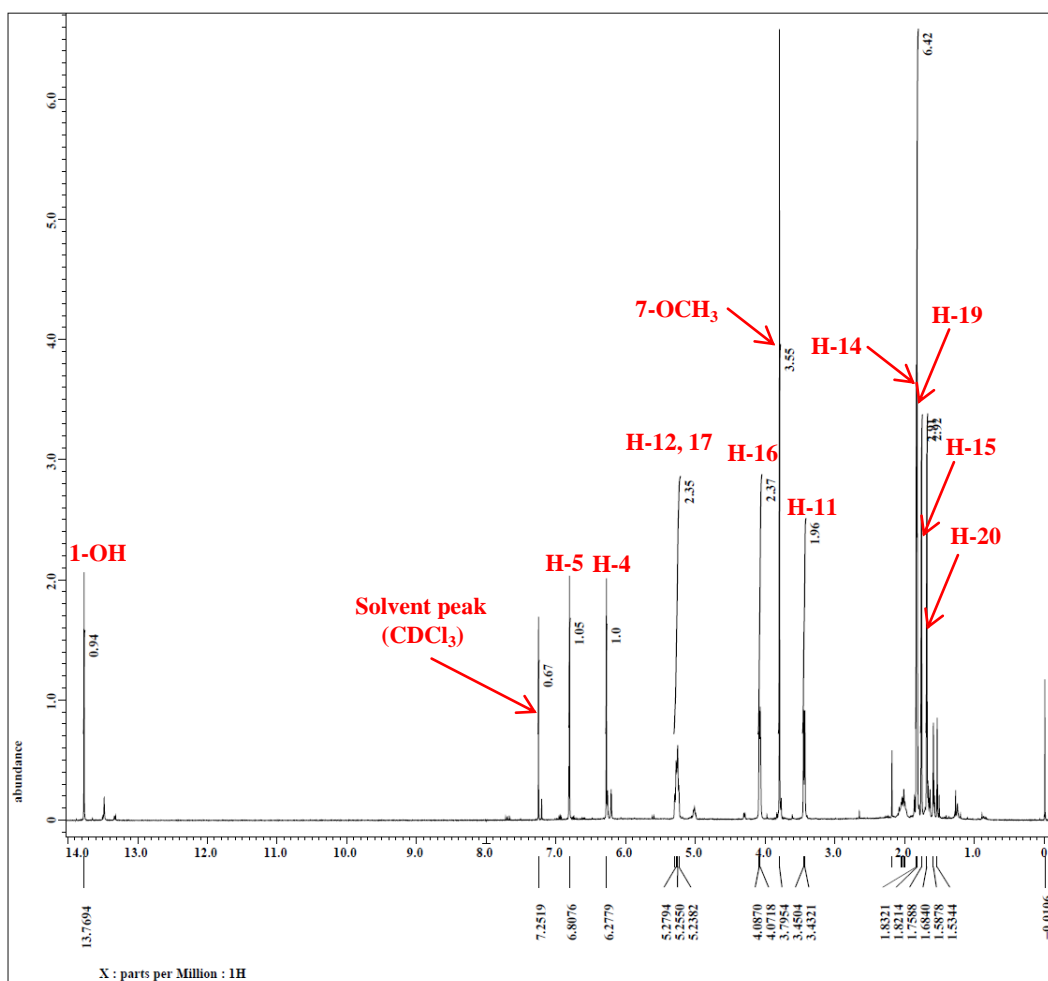
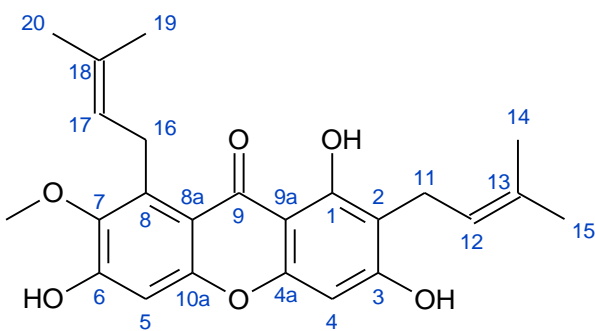


Figure 4.16: ¹H NMR spectrum of compound 53 (400 MHz, CDCl₃)



[53]

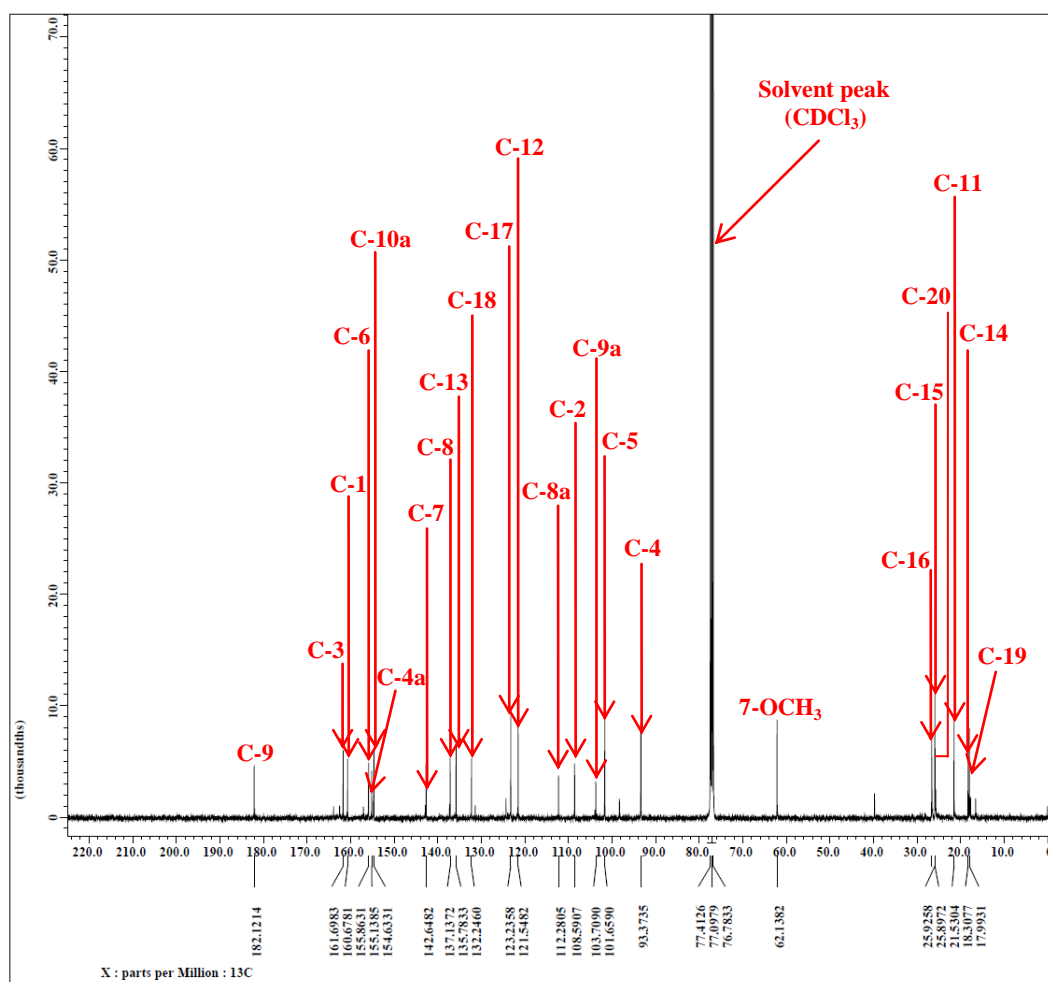
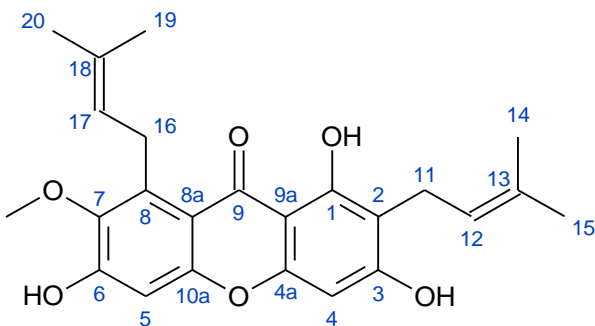


Figure 4.17: ^{13}C NMR spectrum of compound 53 (100 MHz, CDCl_3)



[53]

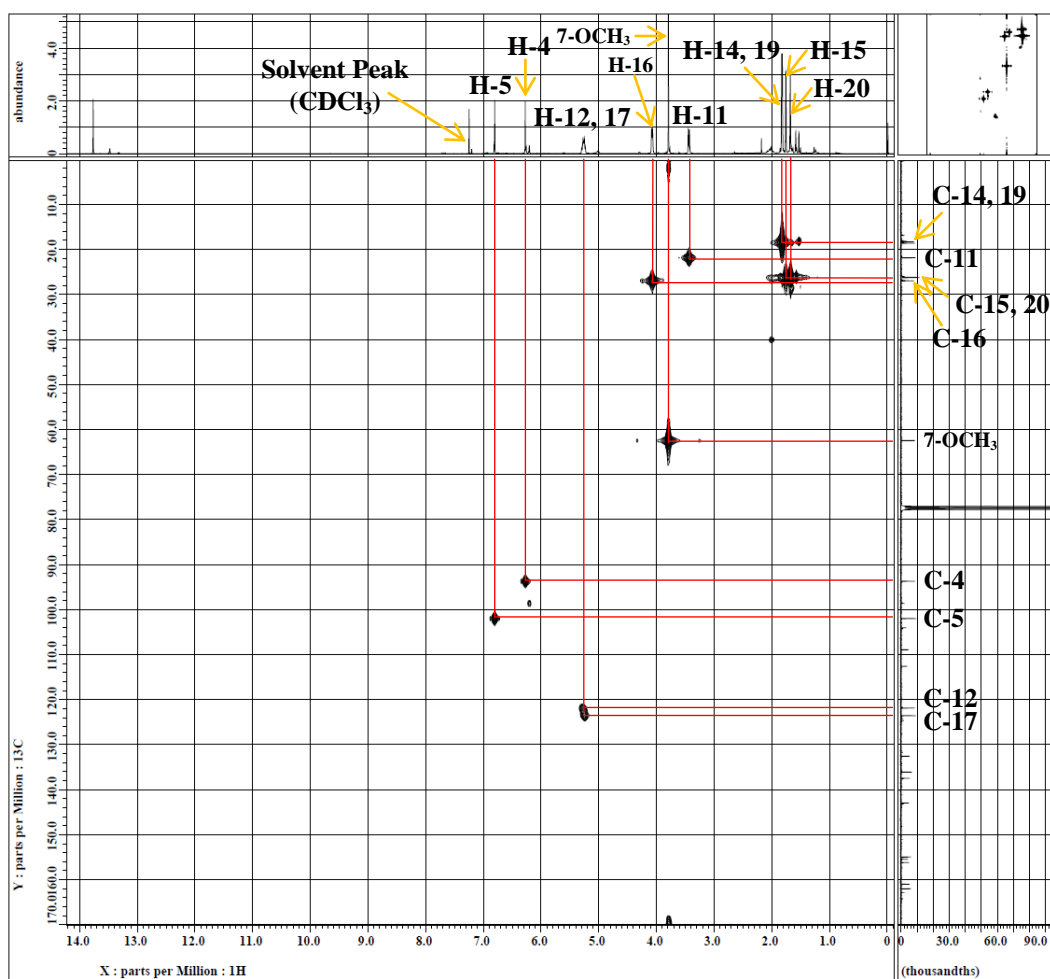
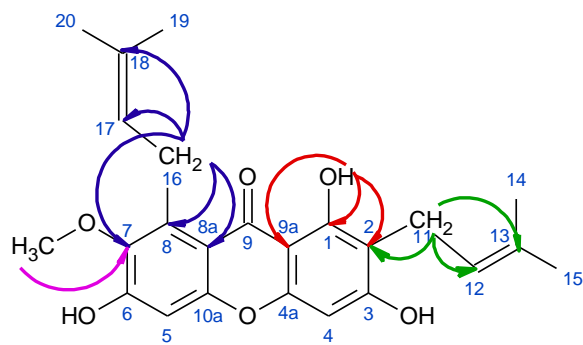


Figure 4.18: HMQC spectrum of compound 53



[53]

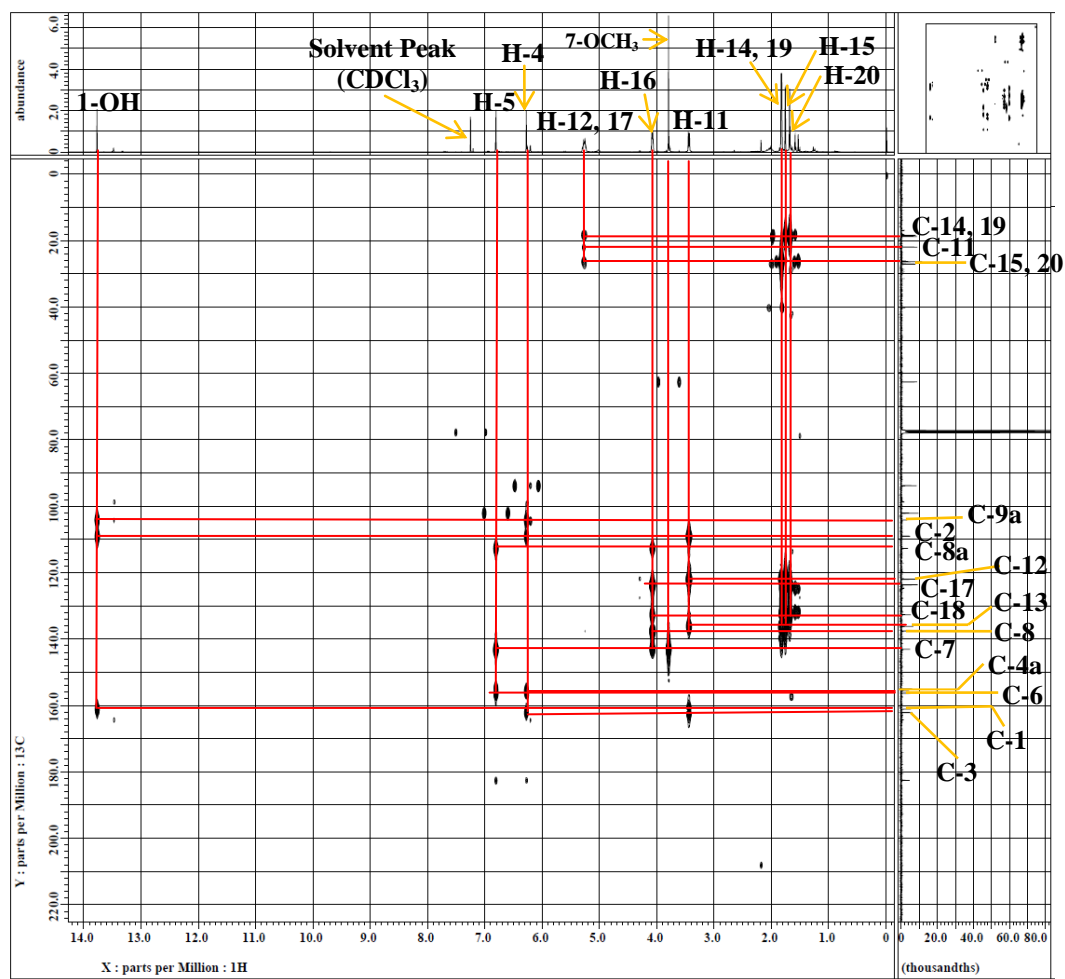


Figure 4.19: HMBC spectrum of compound 53

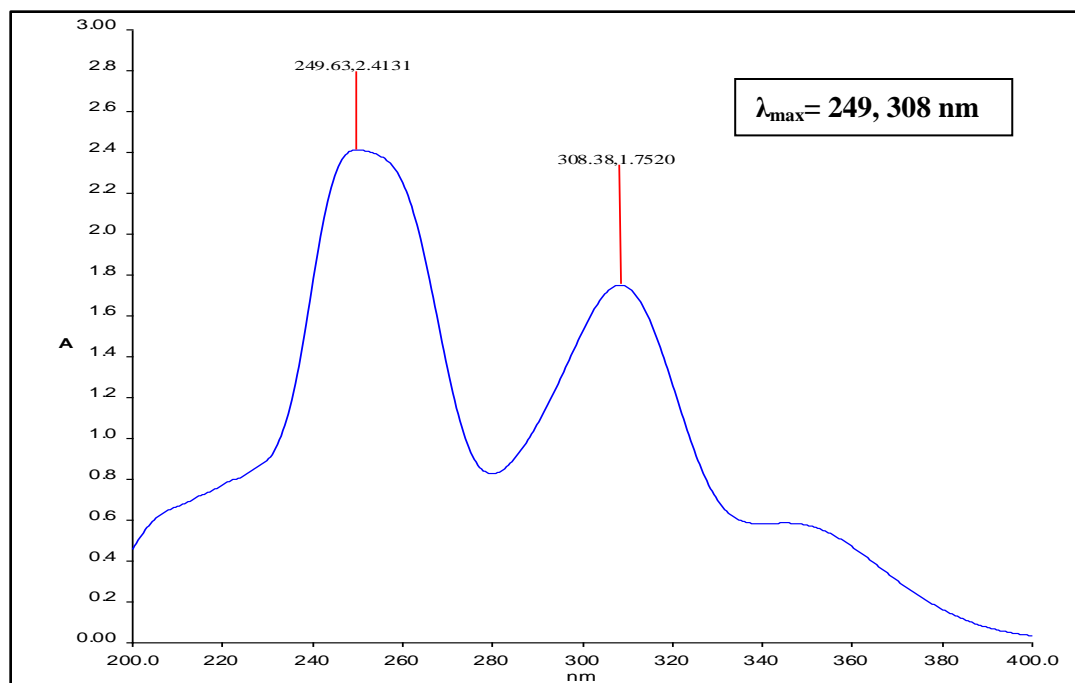


Figure 4.20: UV/Vis spectrum of compound 53

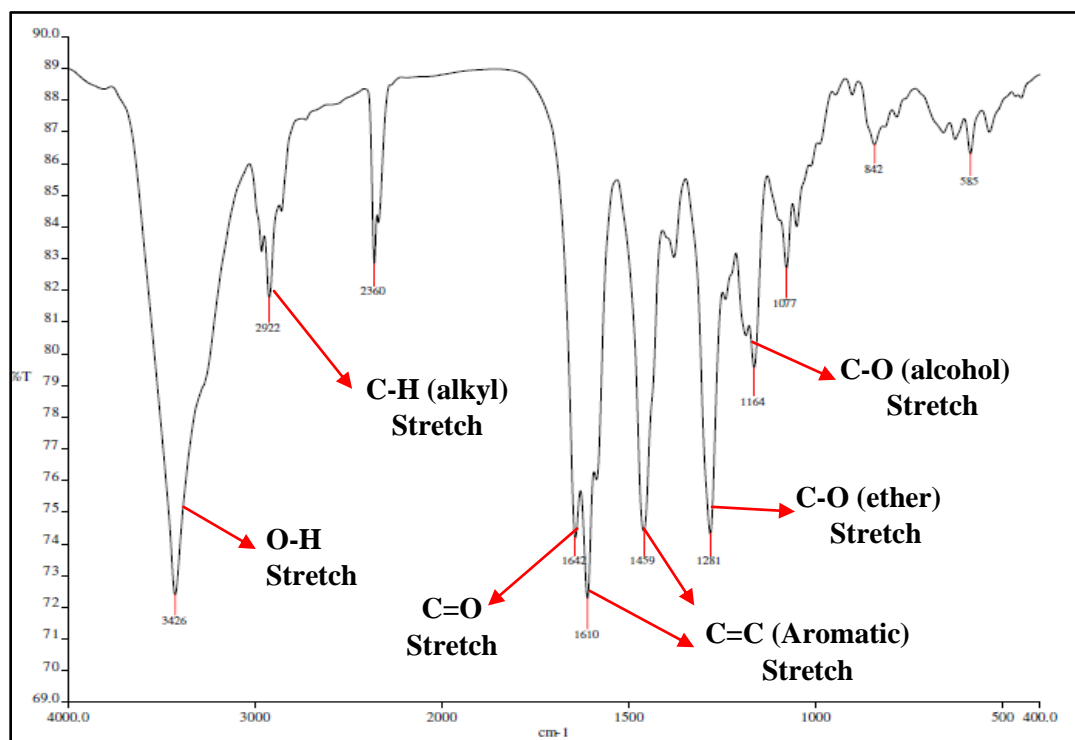


Figure 4.21: FT-IR spectrum of compound 53

4.2.2 Characterization and Structural Elucidation of Rubraxanthone [54]

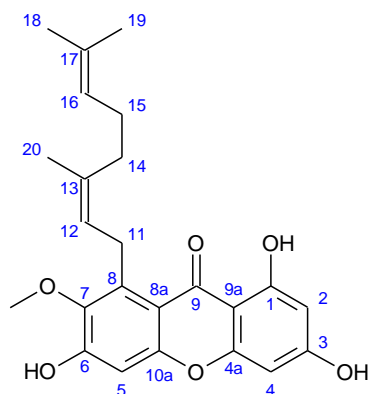


Figure 4.22: Chemical structure of Rubraxanthone [54]

Compound **54** was isolated as yellow crystals with a weight of 422.9 mg, showing a melting point of 199-201 °C (Lit. 201-202 °C, Ee, et al., 2005). Based on the TLC analysis, it gave a R_f value of 0.47 when using 90% dichloromethane and 10% acetone as the mobile phase. Meanwhile, it appeared as a yellow spot under UV light at 365 nm wavelength and when treated with iodine vapor. This compound gave dark blue spot in the ferric chloride test, indicating its phenolic nature. Compound **54** has a molecular weight of 410.1744 g mol⁻¹ which is in agreement with a molecular formula of C₂₄H₂₆O₆ based on the HRESI mass spectrum (Figure 4.23).

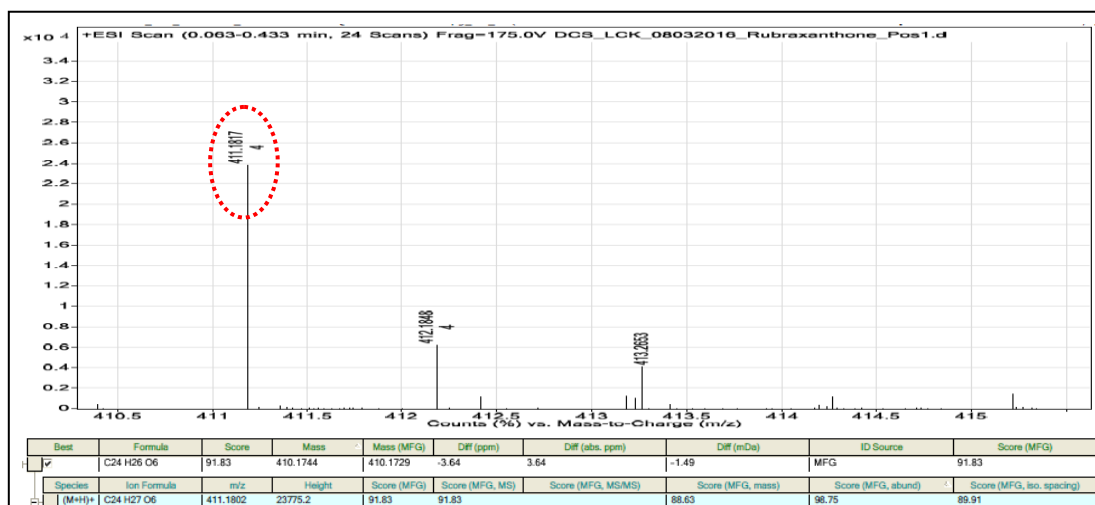


Figure 4.23: HRESI mass spectrum of compound 54

The structure of compound **54** was also determined based on the NMR spectral data. By comparing the ^1H NMR spectrum of compound **54** (Figure 4.24) to that of compound **53**, the only salient difference between these two compounds was that compound **53** has two prenyl groups attached to carbons C-2 and C-8, whereas compound **54** has a geranyl group attached to carbon C-8. Both of these compounds were found to have same xanthonic nucleus with similar oxygenated pattern. The presence of geranyl moiety in compound **54** was revealed by the characteristic signals at δ_{H} 5.25 (1H, t, $J = 5.8$ Hz), 5.00 (1H, t, $J = 7.0$ Hz), 4.07 (2H, d, $J = 6.7$ Hz), 2.02 (2H, m), 1.94 (2H, t, $J = 7.3$ Hz), 1.79 (3H, s), 1.52 (3H, s) and 1.48 (3H, s). Besides, a broad singlet signal at δ_{H} 9.54, integrating for two protons, was assigned to the two hydroxyl protons, 3-OH and 6-OH in the structure. The remaining proton signals at δ_{H} 13.46, 6.76, 6.24 and 3.76 were found to be identical to that of the proton signals in ^1H NMR spectrum of compound **53**, which were assigned to protons 1-OH, H-5, H-4 and 7-OCH₃, respectively.

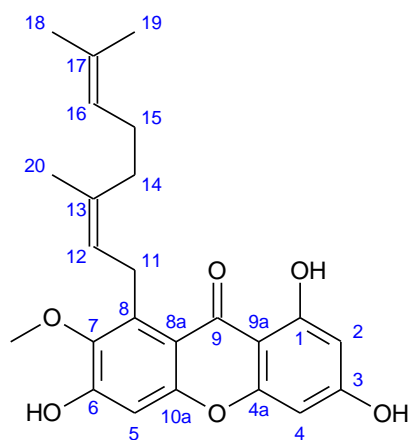
The ^{13}C NMR spectrum (Figure 4.25) revealed compound **54** to have a total of 24 carbons. The presence of geranyl group was further verified via ^{13}C NMR experiment. Structurally, the geranyl group consists of three methyl, three methylene, two methine and two quaternary carbons, which were revealed by the characteristic signals at δ_{C} 25.0 (C-18), 16.9 (C-19), 15.8 (C-20), 39.6 (C-14), 26.5 (C-15), 26.0 (C-11), 124.4 (C-16), 124.0 (C-12), 134.2 (C-13) and 130.7 (C-17). Apart from that, the carbon signal at δ_{C} 97.9 was assigned to the protonated aromatic carbon, C-2. Meanwhile, the remaining carbon assignment to the other parts of xanthone nucleus for compound **54** was found to be identical to that of compound **53**. The DEPT spectrum (Figure 4.26) revealed the presence of four methyl, three methylene, five methine and 12 quaternary carbons, which were in agreement with the proposed structure.

From the HMQC spectrum (Figure 4.27), the carbons C-2, C-4, C-5, C-11, C-12, C-14, C-15, C-16, C-18, C-19, C-20 and 7-OCH₃ were protonated as the carbon signals showed their correlations with protons in the HMQC spectrum. From the HMBC spectrum (Figure 4.28), the placement of geranyl group to carbon C-8 was established based on the correlations observed between the methylene proton, H-11 and the three quaternary carbons, C-7 (δ_{C} 143.7), C-8 (δ_{C} 137.4) and C-8a (δ_{C} 111.1). The summary of NMR assignment of rubraxanthone [**54**] is shown in Table 4.3.

The proposed structure of compound **54** was further analyzed using UV/Vis and FT-IR spectroscopies. The UV/Vis spectrum (Figure 4.29) gave absorption maxima at 248, 305, 345 nm, indicating the phenolic nature of this compound. The FT-IR spectrum (Figure 4.30) showed the absorption bands at 3422, 2921 and 1613 nm, which were in consistent with the presence of hydroxyl, sp^3 C-H and carbonyl groups in the proposed structure. Based on the spectral data above, compound **54** was finally determined to be 1,3,6-trihydroxy-7-methoxy-1-(3,7-dimethylocta-2,6-dienyl)xanthone or rubraxanthone [**54**].

Table 4.3: Summary of NMR assignment of rubraxanthone [54]

Position	δ_{H} (ppm)	δ_{C} (ppm)	DEPT	HMBC	
				2J	3J
1	-	164.0	C	-	-
2	6.14 (1H, d, $J = 1.8$ Hz)	97.9	CH	C-1	C-4, 9a
3	-	164.5	C	-	-
4	6.24 (1H, d, $J = 1.8$ Hz)	93.0	CH	C-3, 4a	C-2, 9a
4a	-	157.1	C	-	-
5	6.76 (1H, s)	102.0	CH	C-6, 10a	C-7, 8a
6	-	156.6	C	-	-
7	-	143.7	C	-	-
8	-	137.4	C	-	-
8a	-	111.1	C	-	-
9	-	181.8	C	-	-
9a	-	102.9	C	-	-
10a	-	155.4	C	-	-
11	4.07 (2H, d, $J = 6.7$ Hz)	26.0	CH ₂	C-8, 12	C-7, 8a, 13
12	5.25 (1H, t, $J = 5.8$ Hz)	124.0	CH	-	C-14, 20
13	-	134.2	C	-	-
14	1.94 (2H, t, $J = 7.3$ Hz)	39.6	CH ₂	C-15, 13	C-12, C-20
15	2.02 (2H, m)	26.5	CH ₂	C-14, 16	C-13, 17
16	5.00 (1H, t, $J = 7.0$ Hz)	124.4	CH	-	C-19
17	-	130.7	C	-	-
18	1.52 (3H, s)	25.0	CH ₃	-	C-16, 19
19	1.48 (3H, s)	16.9	CH ₃	C-17	C-18
20	1.79 (3H, s)	15.8	CH ₃	C-13	C-12, 14
1-OH	13.46 (1H, s)	-	-	C-1	C-2, 9a
3-OH, 6-OH	9.54 (2H, brs)	-	-	-	-
7-OCH ₃	3.76 (3H, s)	60.6	CH ₃	-	C-7



[54]

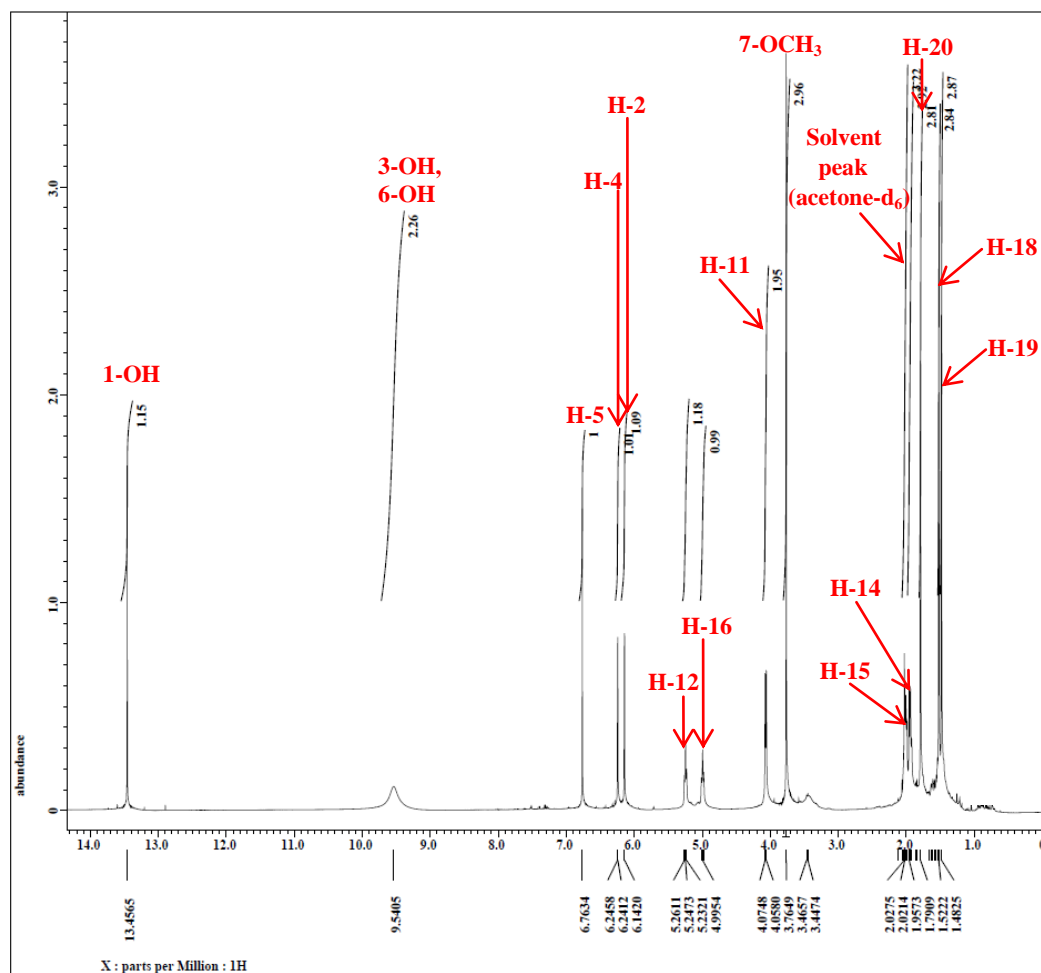
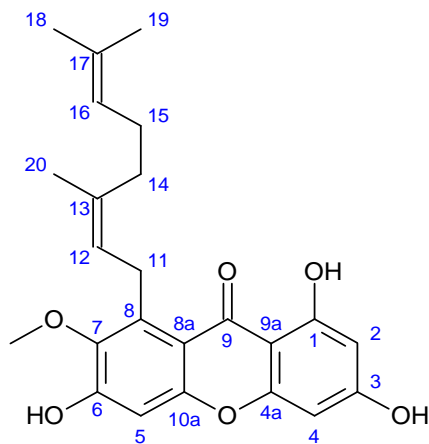


Figure 4.24: ¹H NMR spectrum of compound 54 (400 MHz, acetone-d₆)



[54]

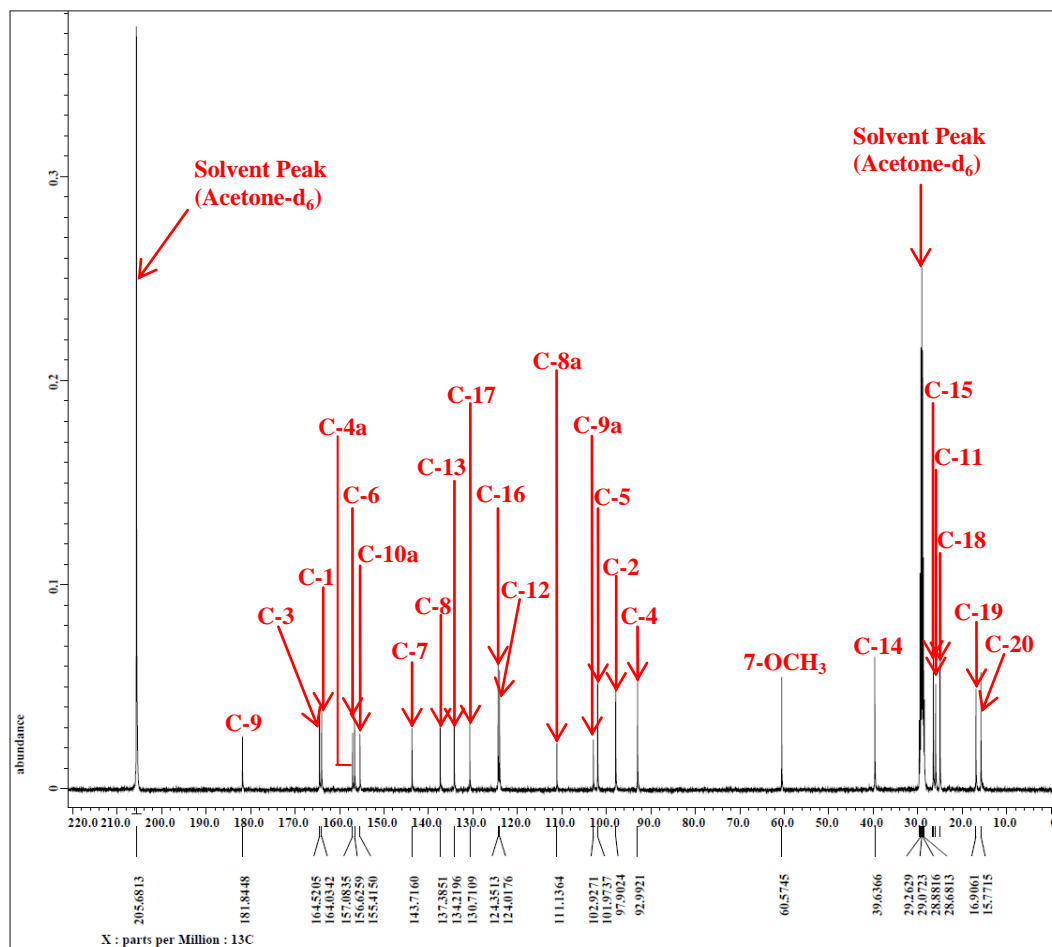


Figure 4.25: ¹³C NMR spectrum of compound 54 (100 MHz, acetone-d₆)

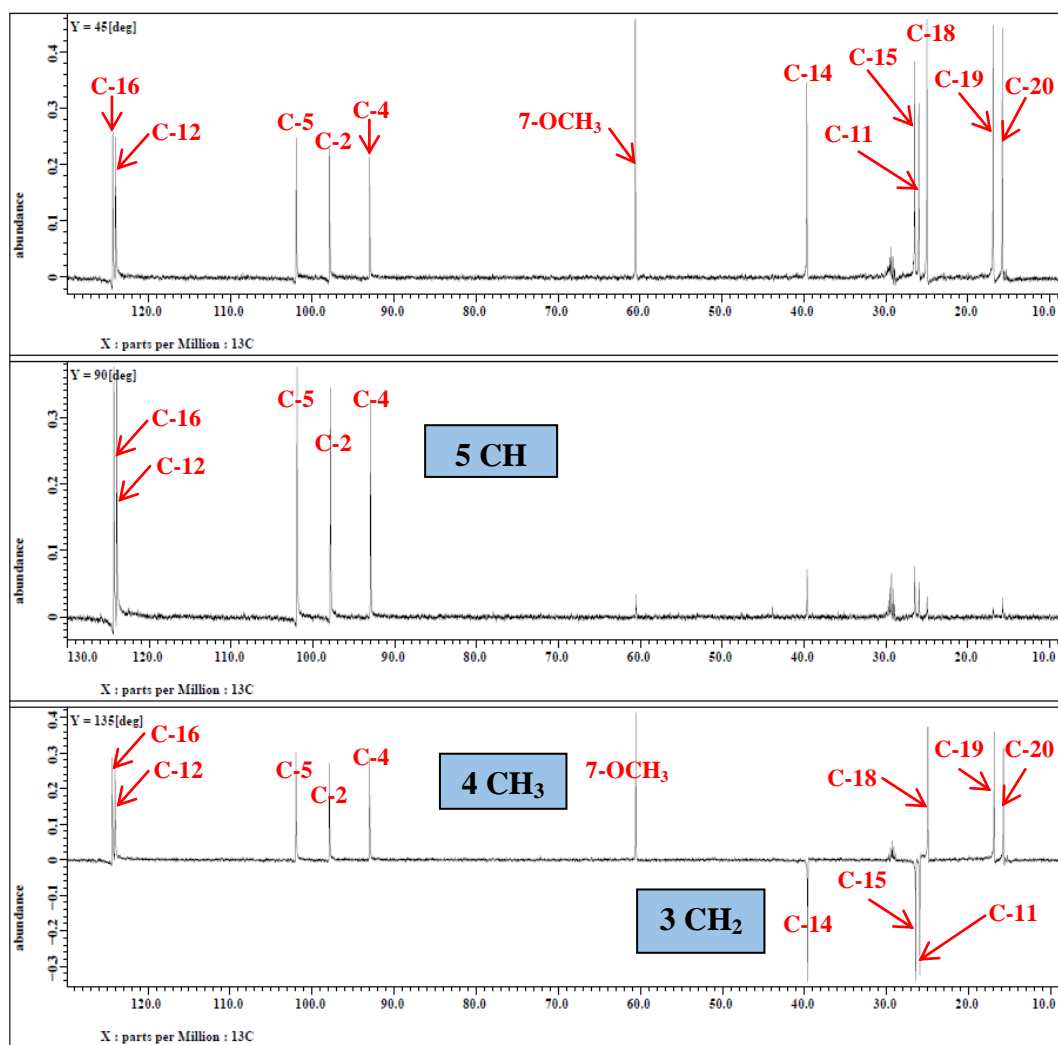
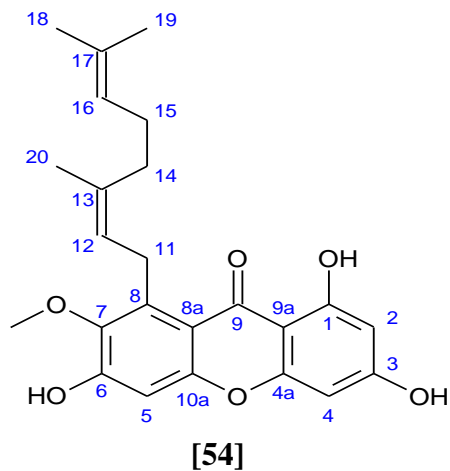
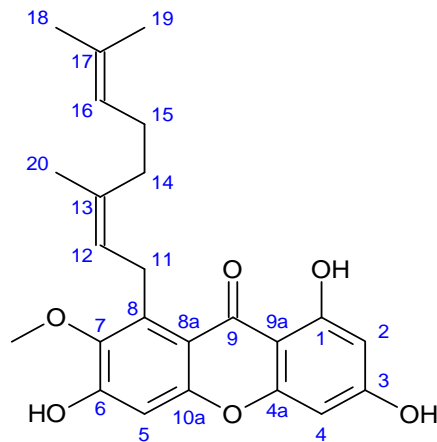


Figure 4.26: DEPT spectrum of compound 54 (100 MHz, acetone-d₆)



[54]

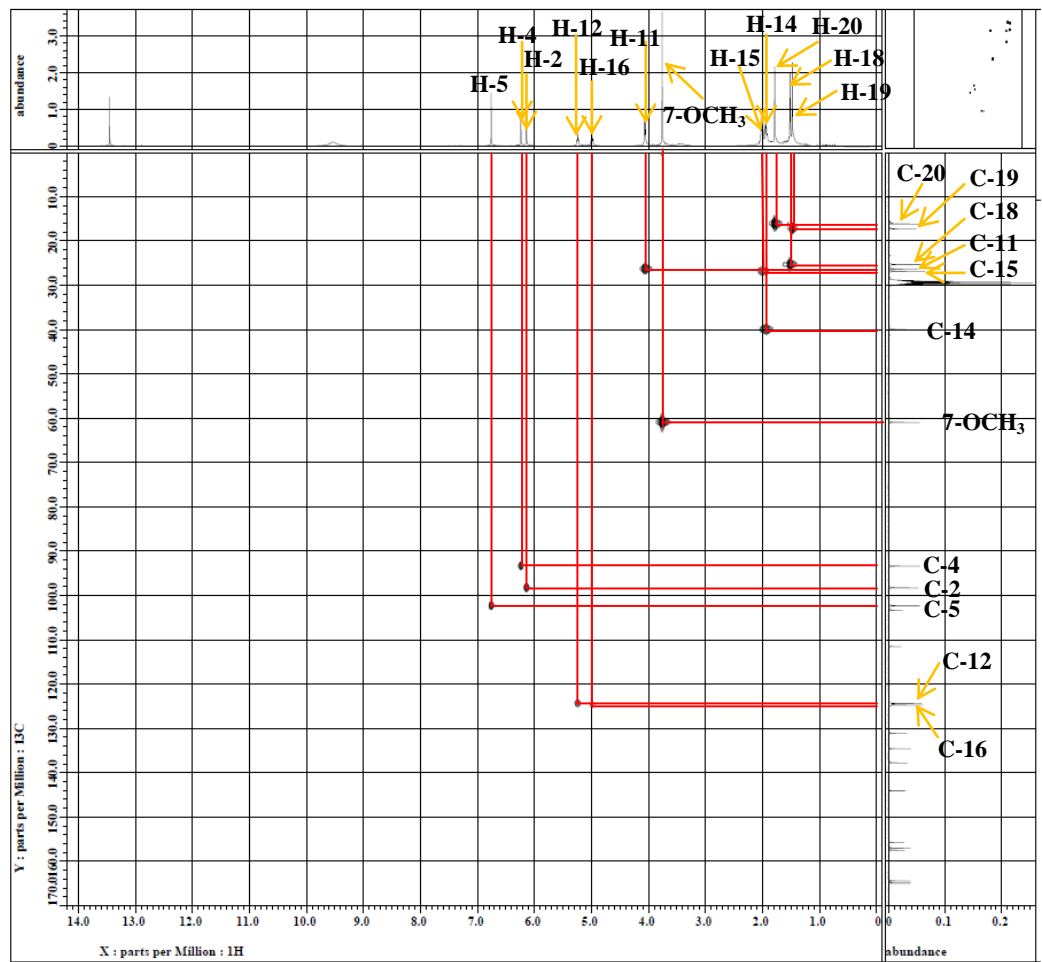
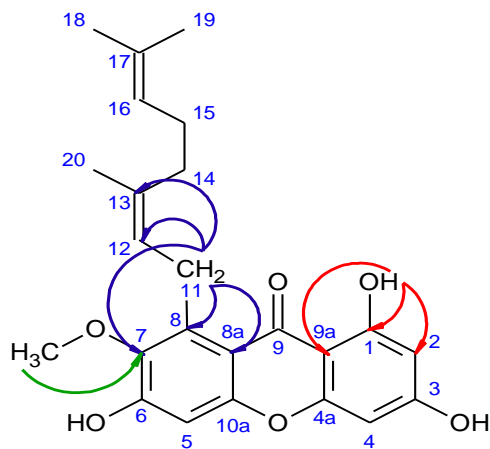


Figure 4.27: HMQC spectrum of compound 54



[54]

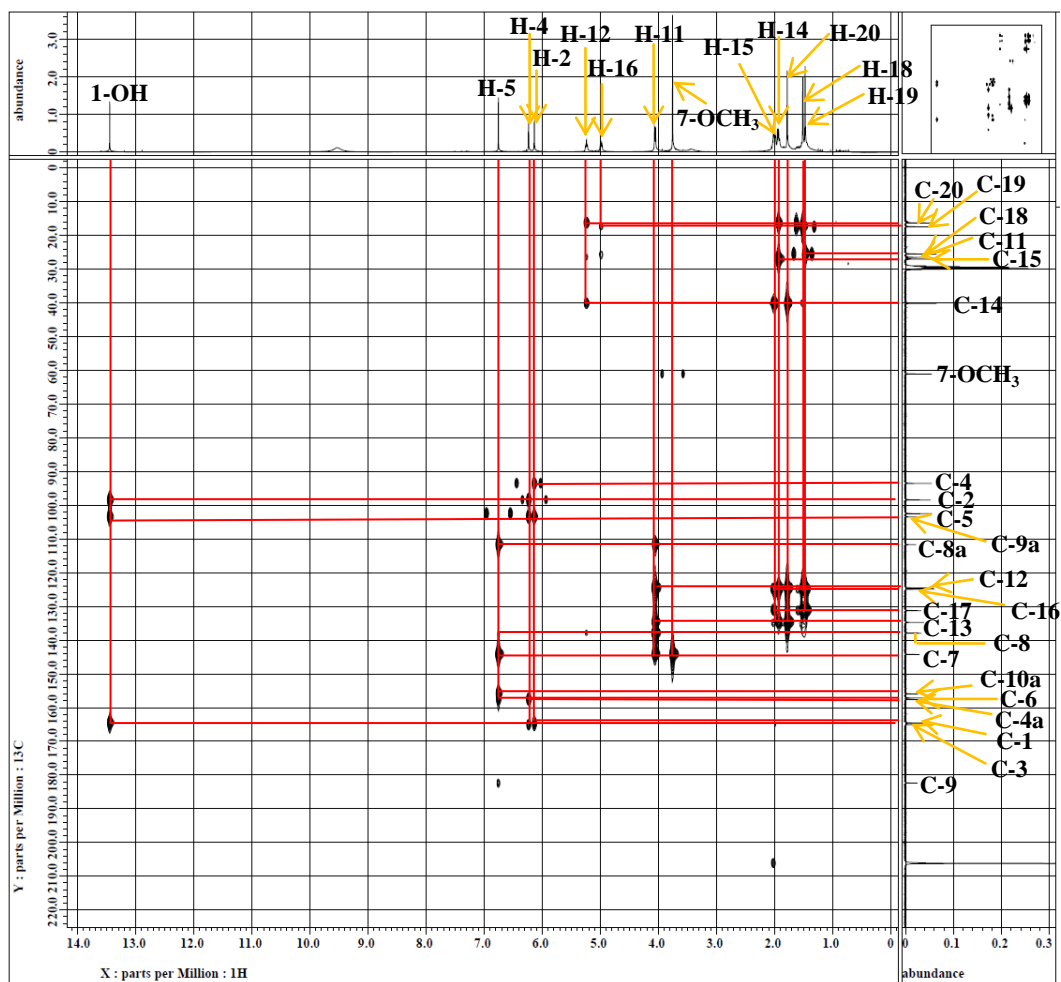


Figure 4.28: HMBC spectrum of compound 54

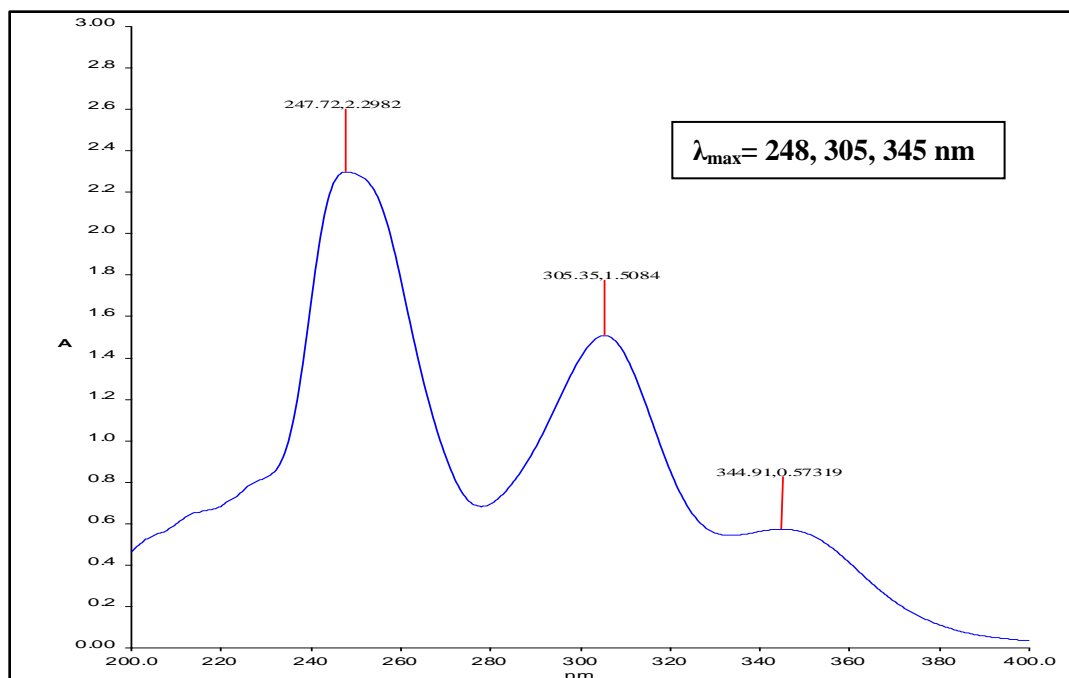


Figure 4.29: UV/Vis spectrum of compound 54

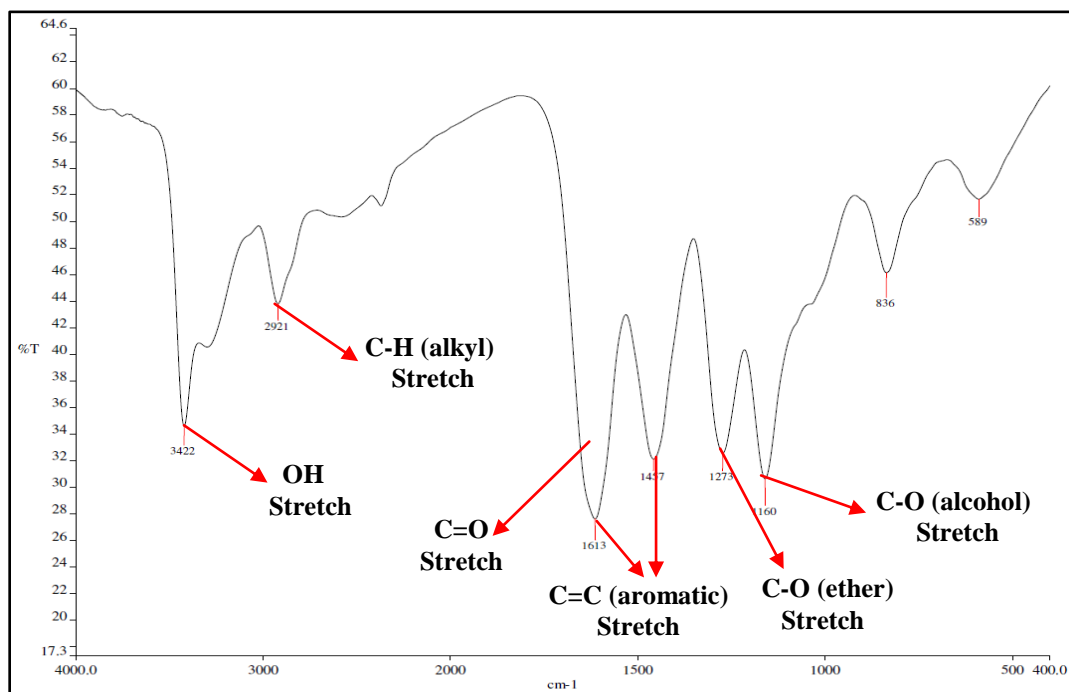


Figure 4.30: FT-IR spectrum of compound 54

4.2.3 Characterization and Structural Elucidation of 1,3,7-Trihydroxy-2,4-bis(3-methylbut-2-enyl)xanthone [55]

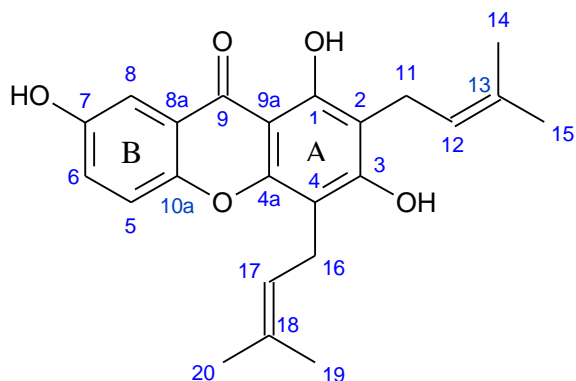


Figure 4.31: Chemical structure of 1,3,7-trihydroxy-2,4-bis(3-methylbut-2-enyl)xanthone [55]

Compound **55** was isolated as yellow solids with a weight of 29.2 mg, showing a melting point of 130-131 °C (Lit. 128-129 °C, Ee, et al., 2005). After subjecting this compound to TLC analysis, it gave a R_f value of 0.65 when using 90% dichloromethane and 10% acetone. On top of that, compound **55** was found to give a purple spot under UV light at 365 nm wavelength and a yellow spot when treated with iodine vapor. This compound appeared as a dark blue spot in the ferric chloride test, establishing its phenolic nature. In addition, this compound has a molecular weight of $380.1633 \text{ g mol}^{-1}$ which is corresponding to a molecular formula of $\text{C}_{23}\text{H}_{24}\text{O}_5$ based on the pseudo-molecular ion at m/z 381.1697 in the HRESI mass spectrum (Figure 4.32).

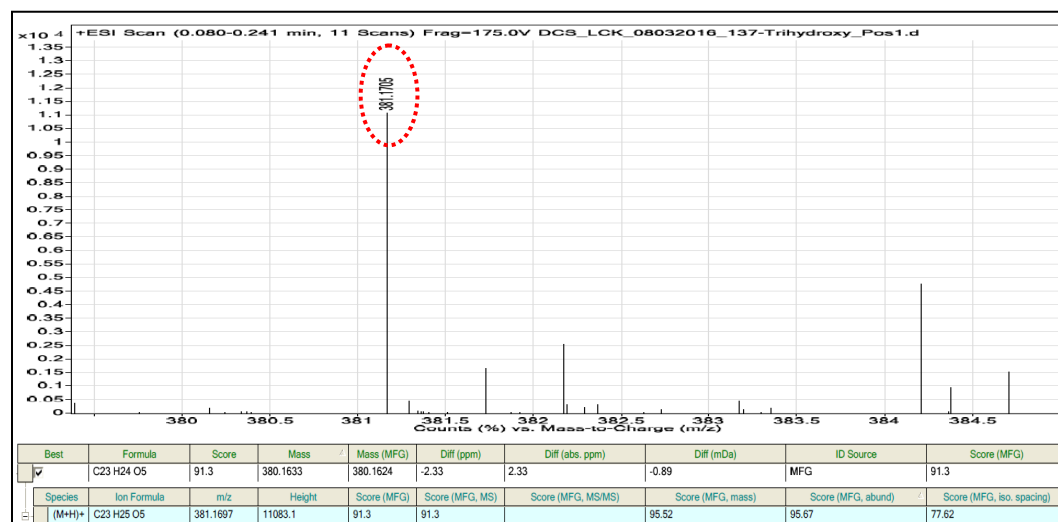


Figure 4.32: HRESI mass spectrum of compound 55

The chemical structure of compound **55** was subsequently elucidated according to the 1D- and 2D-NMR spectral data. The ^1H NMR spectrum of compound **55** (Figure 4.33) displayed two broad singlet signals at δ_{H} 9.10 and 8.51 which were assigned to the hydroxyl protons, 3-OH and 7-OH, respectively. Two pairs of signals at δ_{H} 7.45/7.32 ($J = 9.2$ Hz) and 7.54/7.32 ($J = 3.1$ Hz), suggesting presence of one *ortho*- and one *meta*-coupled aromatic protons in ring B. In addition, the presence of two prenyl groups in the proposed structure was indicated by two sets of proton signals: δ_{H} 3.42 (2H, d, $J = 6.7$ Hz), 5.20 (1H, m), 1.86 (3H, s), 1.63 (3H, s), and δ_{H} 3.56 (2H, d, $J = 7.4$ Hz), 5.20 (1H, m), 1.76 (3H, s), 1.63 (3H, s).

The ^{13}C NMR spectrum of compound **55** (Figure 4.34) displayed a total of 23 carbon signals, which was in agreement with the proposed structure. The carbon signals at δ_{C} 124.6, 119.3 and 108.8 were assigned to the protonated aromatic carbons, C-6, C-5 and C-8, respectively. Besides that, 10 quaternary aromatic

carbons were evident from the carbon signals at δ_C 181.2 (C-9), 160.8 (C-3), 158.7 (C-1), 154.3 (C-7), 153.4 (C-4a), 150.3 (C-10a), 121.1 (C-8a), 110.4 (C-2), 106.3 (C-4) and 103.1 (C-9a). Meanwhile, two sets of carbon signals at δ_C 21.6 (C-11), 122.6 (C-12), 131.8 (C-13), 17.6 (C-14), 25.4 (C-15), and δ_C 22.0 (C-16), 122.6 (C-17), 132.0 (C-18), 17.5 (C-19), 25.4 (C-20) confirmed the presence of two 3-methylbut-2-enyl units.

Based on the HMQC spectrum (Figure 4.35), a total of 11 protonated carbon signals were observed. There were carbons C-5, C-6, C-8, C-11, C-12, C-14, C-15, C-16, C-17, C-19 and C-20 which showed correlations with their respective protons in the HMQC spectrum. On the other hand, the position of the two prenyl groups in the xanthone nucleus was confirmed based on the HMBC spectrum (Figure 4.36). The placement of first prenyl group at C-2 was deduced based on the correlations of methylene proton, H-11 with carbon C-2 via 2J coupling, and carbons C-1 and C-3 via 3J coupling. At the meantime, the second prenyl group was found to attach to carbon C-4 based on the cross peaks observed between the methylene proton, H-16 and the substituted aromatic carbons, C-3, C-4 and C-4a. The summary of NMR assignment of 1,3,7-trihydroxy-2,4- *bis*(3-methylbut-2-enyl)xanthone **[55]** is shown in Table 4.5.

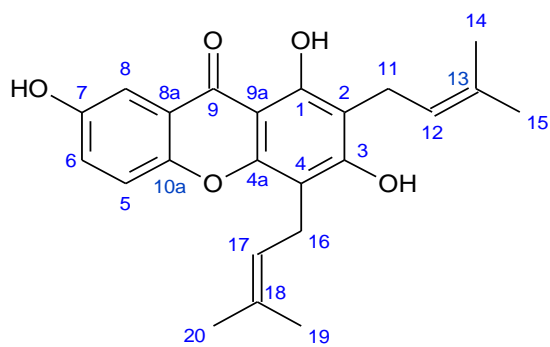
The UV/Vis spectrum (Figure 4.37) displayed the absorption maxima at 265, 315 and 378 nm, indicating the presence of conjugated structure in this compound. Meanwhile, the FT-IR spectrum (Figure 4.38) displayed the absorption bands at

3389, 2927 and 1630 cm^{-1} , which were in consistent with the presence of the hydroxyl, sp^3 C-H (stretch) and carbonyl groups in the proposed structure. Compound **55** was eventually identified as 1,3,7-trihydroxy-2,4-bis(3-methylbut-2-enyl)xanthone [55].

Table 4.4: Summary of NMR assignment of 1,3,7-trihydroxy-2,4-bis(3-methylbut-2-enyl)xanthone [55]

Position	δ_{H} (ppm)	δ_{C} (ppm)	HMBC	
			2J	3J
1	-	158.7	-	-
2	-	110.4	-	-
3	-	160.8	-	-
4	-	106.3	-	-
4a	-	153.4	-	-
5	7.45 (1H, d, $J = 9.2$ Hz)	119.3	C-10a	C-7, 8a
6	7.32 (1H, dd, $J = 9.2, 3.1$ Hz)	124.6	-	C-10a
7	-	154.3	-	-
8	7.54 (1H, d, $J = 3.1$ Hz)	108.8	-	C-6, 10a
8a	-	121.1	-	-
9	-	181.2	-	-
9a	-	103.1	-	-
10a	-	150.3	-	-
11	3.42 (2H, d, $J = 6.7$ Hz)	21.6	C-2, 12	C-1, 3, 13
12	5.20 (1H, m)	122.6	-	C-14, 15
13	-	131.8	-	-
14	1.86 (3H, s)	17.6	C-13	C-12, 15
15	1.63 (3H, s)	25.4	C-13	C-12, 14
16	3.56 (2H, d, $J = 7.4$ Hz)	22.0	C-4, 17	C-3, 4a, 18
17	5.20 (1H, m)	122.6	-	C-19, 20
18	-	132.0	-	-
19	1.76 (3H, s)	17.5	C-18	C-17, 20
20	1.63 (3H, s)	25.4	-	C-17, 19
1-OH	13.25 (1H, s)	-	C-1	C-2, 9a
3-OH	9.10 ^a (1H, s)	-	-	-
7-OH	8.51 ^a (1H, s)	-	-	-

^a Interchangeable



[55]

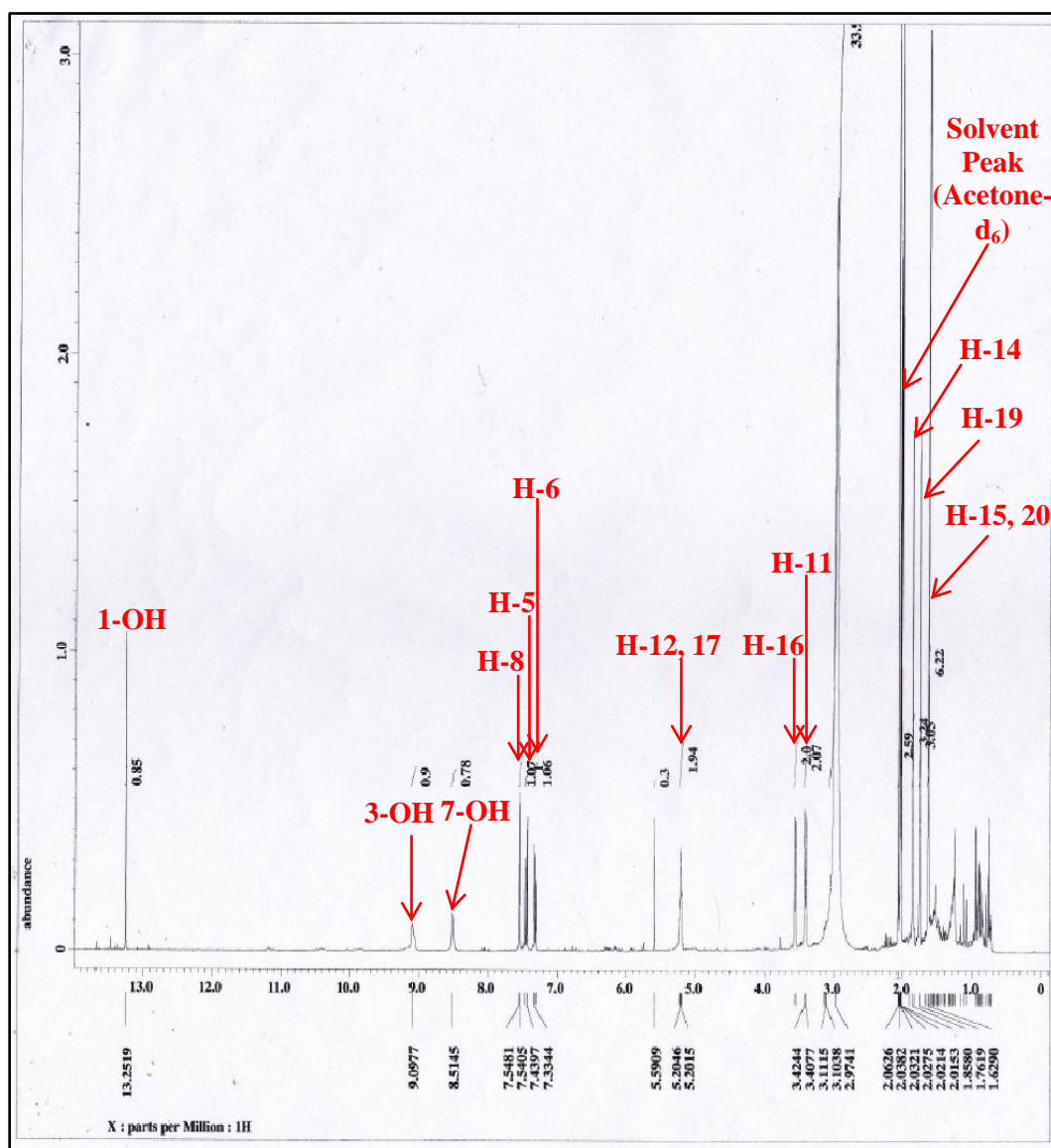


Figure 4.33: ¹H NMR spectrum of compound 55 (400 MHz, acetone-d₆)

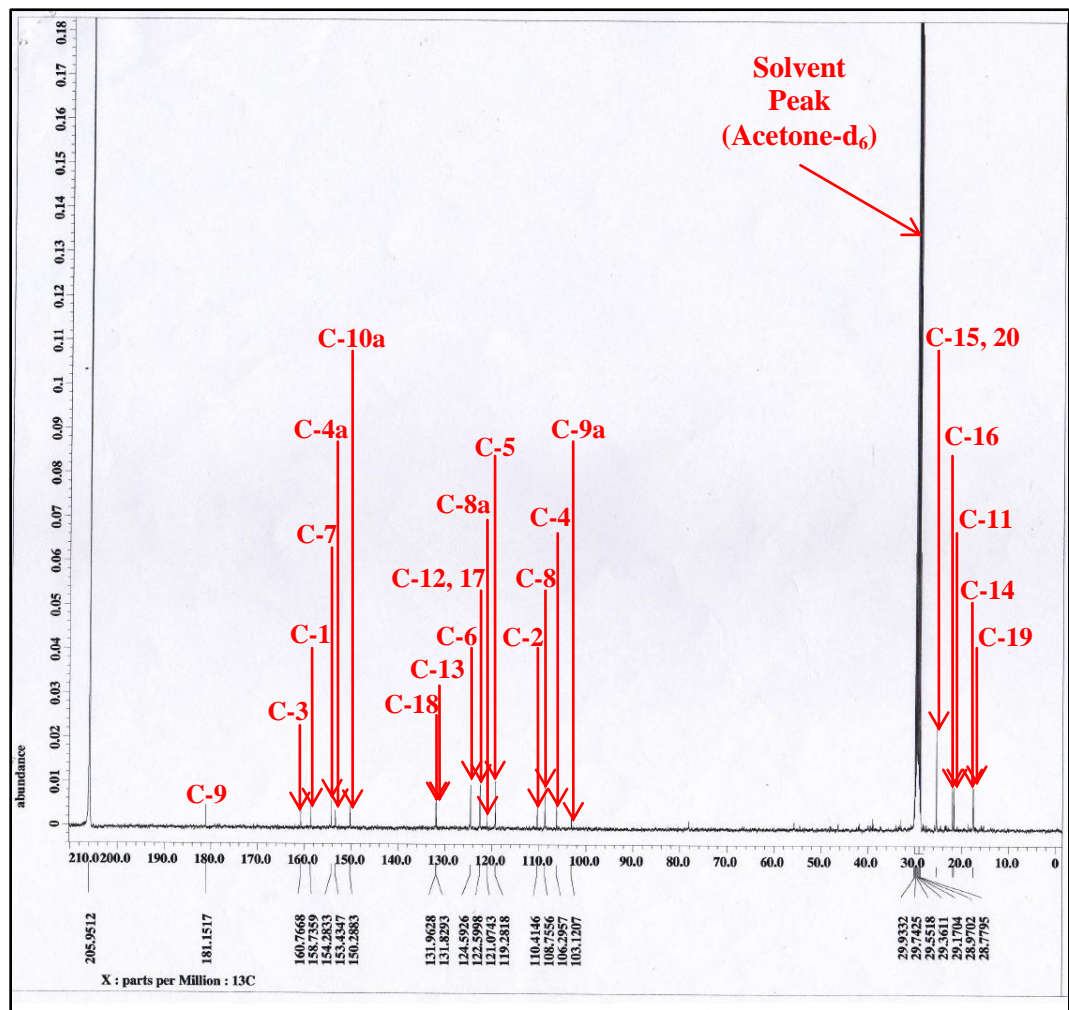
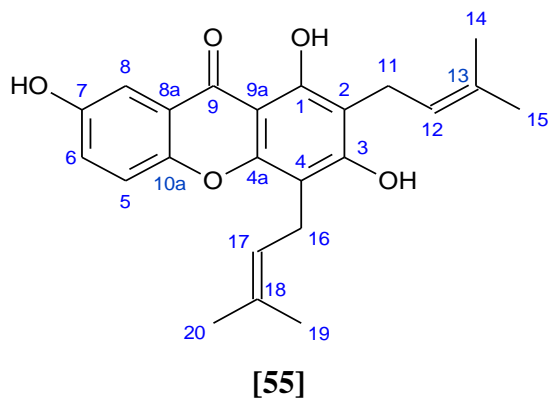


Figure 4.34: ¹³C NMR spectrum of compound 55 (100 MHz, acetone-d₆)

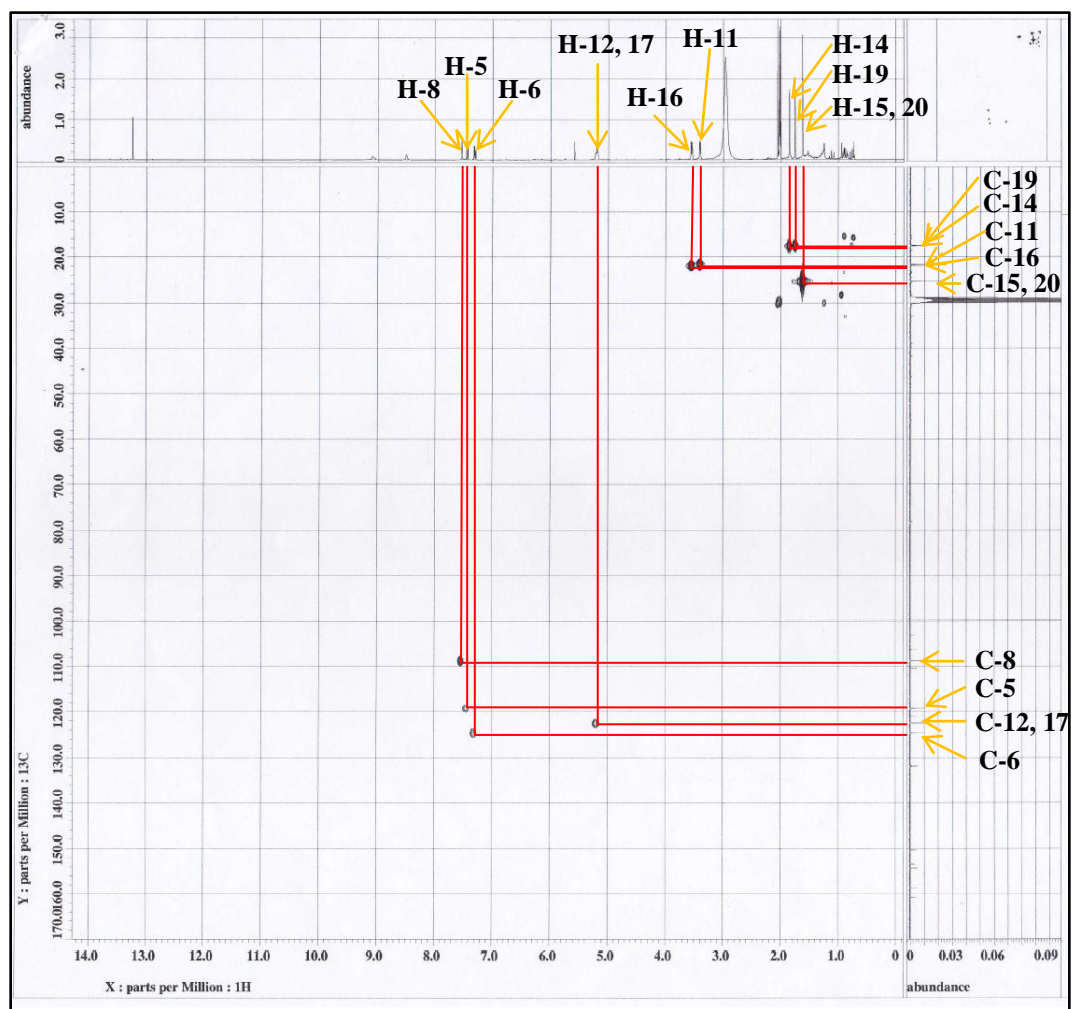
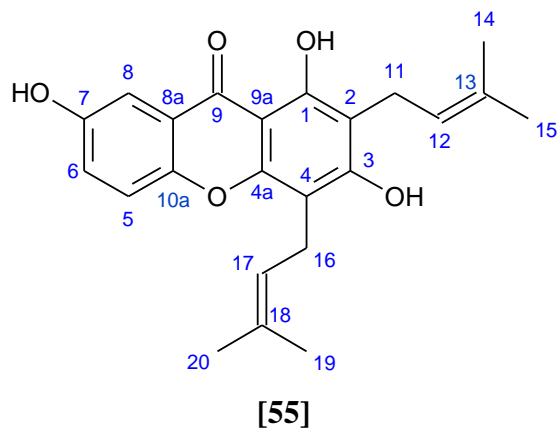
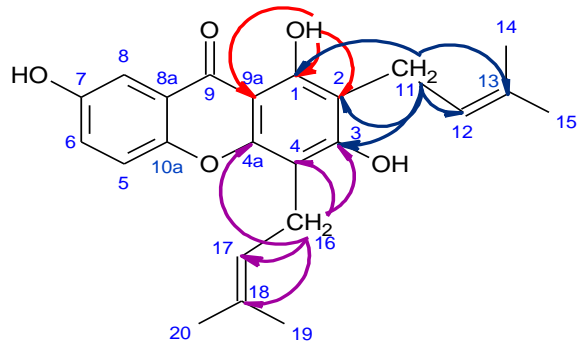


Figure 4.35: HMBC spectrum of compound 55



[55]

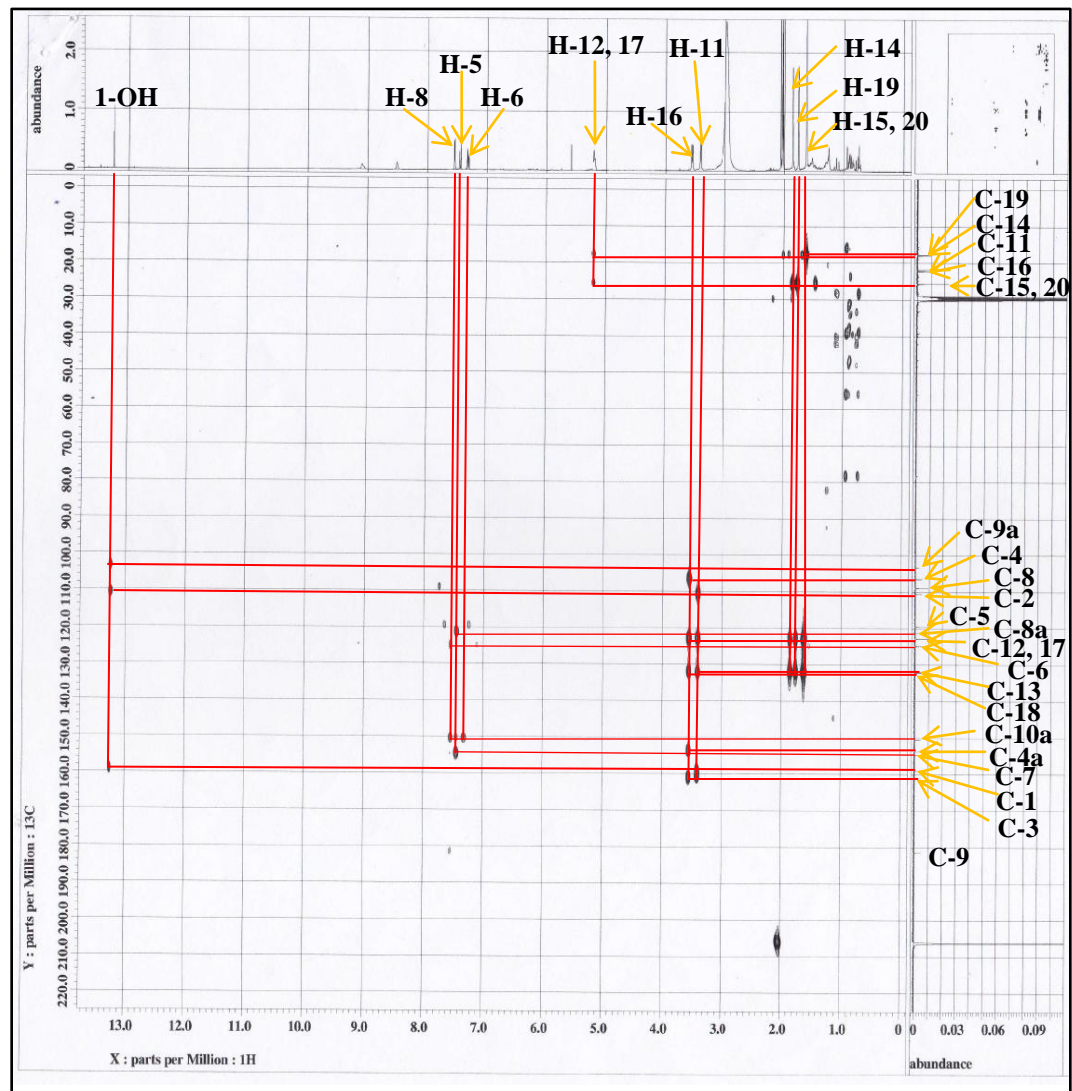


Figure 4.36: HMBC spectrum of compound 55

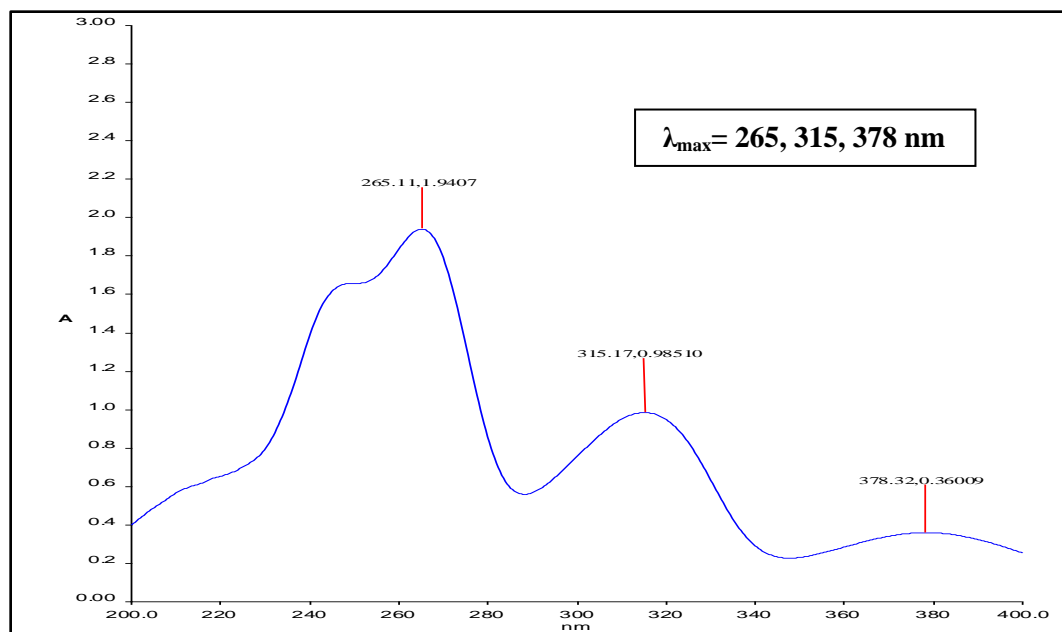


Figure 4.37: UV/Vis spectrum of compound 55

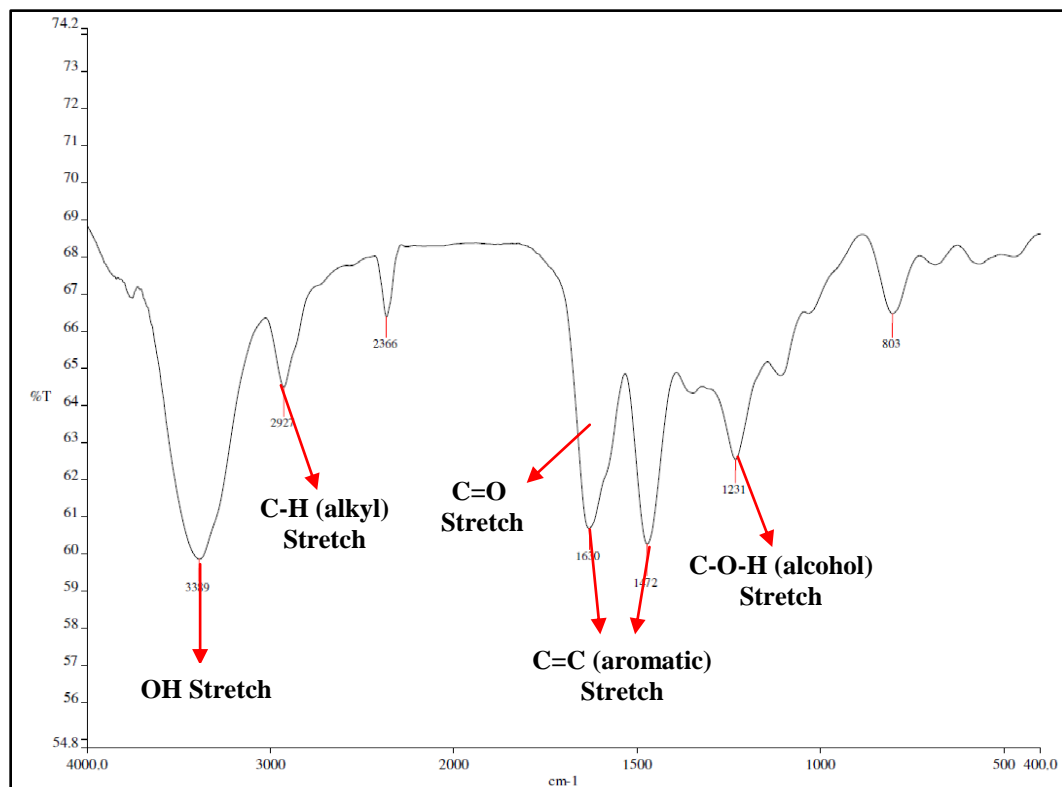


Figure 4.38: FT-IR spectrum of compound 55

4.2.4 Characterization and Structural Elucidation of Stigmasterol [56]

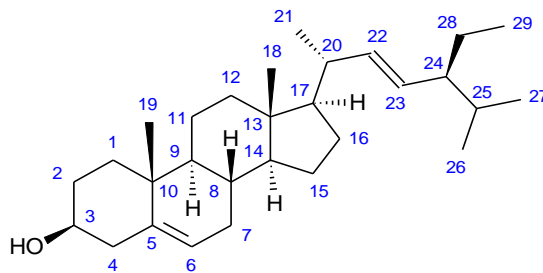


Figure 4.39: Chemical structure of stigmasterol [56]

Compound **56** was isolated as white needle crystals with an amount of 13.9 mg. It has a melting range of 133-136 °C (Lit. 135-136 °C, Lukitaningsih, 2012). The TLC analysis revealed this compound to have a R_f value of 0.09 when eluted with a solvent mixture of hexane and dichloromethane (4:6, v/v). Besides that, it gave no visible spot when visualizing under UV light, and a yellow spot when treated with iodine vapor. Meanwhile, this compound showed negative result in the ferric chloride test, indicating the absence of phenolic moiety in this compound. In addition, it showed $[\alpha]_D^{25}$ value of -14° , which is close to the reported literature value of -16.63° (Mawa and Said, 2012).

In the ^1H NMR spectrum (Figures 4.40 & 4.41), three highly deshielded signals at δ_{H} 5.34, 5.14 and 5.00, each integrating for one proton, were assigned to the olefinic protons, H-6, H-23 and H-22, respectively. Among these olefinic protons, the signals at δ_{H} 5.14 and 5.00 appeared as doublet-of-doublet signals with similar coupling constants of 15.2 and 8.6 Hz, indicating the presence of a *trans* olefinic group. Furthermore, the ^1H NMR spectrum also displayed a multiplet signal at δ_{H} 3.51, which was assigned to the oxymethine proton, H-3. The methyl protons

were indicated by the remaining signals at δ_{H} 1.02 (H-18), 1.00 (H-21), 0.83 (H-29), 0.80 (H-27), 0.78 (H-26) and 0.69 (H-19).

In the ^{13}C NMR spectrum (Figure 4.42), a total of 29 carbon signals were observed, and were found to be in agreement with the proposed structure. The presence of four olefinic carbons was indicated by the signals at δ_{C} 140.8 (C-5), 138.4 (C-22), 129.3 (C-23) and 121.8 (C-6). Besides that, a relatively more deshielded carbon signal at δ_{C} 71.9 was assigned to carbon C-3 which was linked to a hydroxyl group. Meanwhile, there were six methyl carbons which appeared at δ_{C} 21.3 (C-26), 21.2 (C-21), 19.5 (C-19), 19.1 (C-27), 12.3 (C-29) and 12.1 (C-18). Other than that, a series of methylene carbon signals was also observed at δ_{C} 42.4 (C-4), 39.8 (C-12), 37.3 (C-1), 32.0 (C-2), 32.0 (C-7), 29.0 (C-16), 25.5 (C-28), 24.4 (C-15) and 21.2 (C-11), whereas the presence of methine carbons was evident from the signals at δ_{C} 57.0 (C-14), 56.0 (C-17), 51.3 (C-24), 50.2 (C-9), 40.6 (C-20), 32.0 (C-25) and 31.7 (C-8). The remaining signals at δ_{C} 42.3 and 36.6 were assigned to the quaternary carbons, C-13 and C-10, respectively. The ^{13}C NMR spectral data of compound **56** was found to be in agreement with the literature data (Pierre and Moses, 2015). The summary of NMR assignment of stigmasterol [**56**] in comparison with the literature values is shown in Table 4.4.

The proposed structure was further supported by UV/Vis and FT-IR spectroscopies. The UV/Vis spectrum (Figure 4.43) displayed a single absorption wavelength, 243 nm, which was the cutoff wavelength of chloroform, indicating

the absence of conjugated moiety in the compound. Meanwhile, the FT-IR spectrum (Figure 4.44) gave the absorption bands at 3398 and 2919 cm^{-1} corresponding to the presence of hydroxyl and sp^3 C-H group, respectively. Based on all the spectral evidence above, compound **56** was determined to be stigmasterol [56].

Table 4.5: Summary of NMR assignment of stigmasterol [56] in comparison with the literature data

Position	δ_{H} (ppm)	δ_{C} (ppm)	δ_{C}^* (ppm)
1	-	37.3	37.2
2	-	32.0	31.6
3	3.51 (1H, m)	71.9	71.7
4	-	42.4	42.2
5	-	140.8	140.8
6	5.34 (1H, d, $J = 4.9$ Hz)	121.8	121.6
7	-	32.0	31.6
8	-	31.7	31.8
9	-	50.2	50.0
10	-	36.6	36.2
11	-	21.2	21.1
12	-	39.8	39.6
13	-	42.3	42.1
14	-	57.0	56.8
15	-	24.4	24.3
16	-	29.0	28.8
17	-	56.0	55.8
18	1.02 (3H, s)	12.1	12.2
19	0.69 (3H, s)	19.5	19.9
20	-	40.6	40.5
21	1.00 (3H, s)	21.2	21.0
22	5.00 (1H, dd, $J = 15.2, 8.6$ Hz)	138.4	138.2
23	5.14 (1H, dd, $J = 15.2, 8.6$ Hz)	129.3	129.4
24	-	51.3	51.2
25	-	32.0	31.9
26	0.78 (3H, d, $J = 6.7$ Hz)	21.3	21.2
27	0.80 (3H, d, $J = 7.9$ Hz)	19.1	19.0
28	-	25.5	25.5
29	0.83 (3H, t)	12.3	12.3

*Pierre and Moses, 2015.

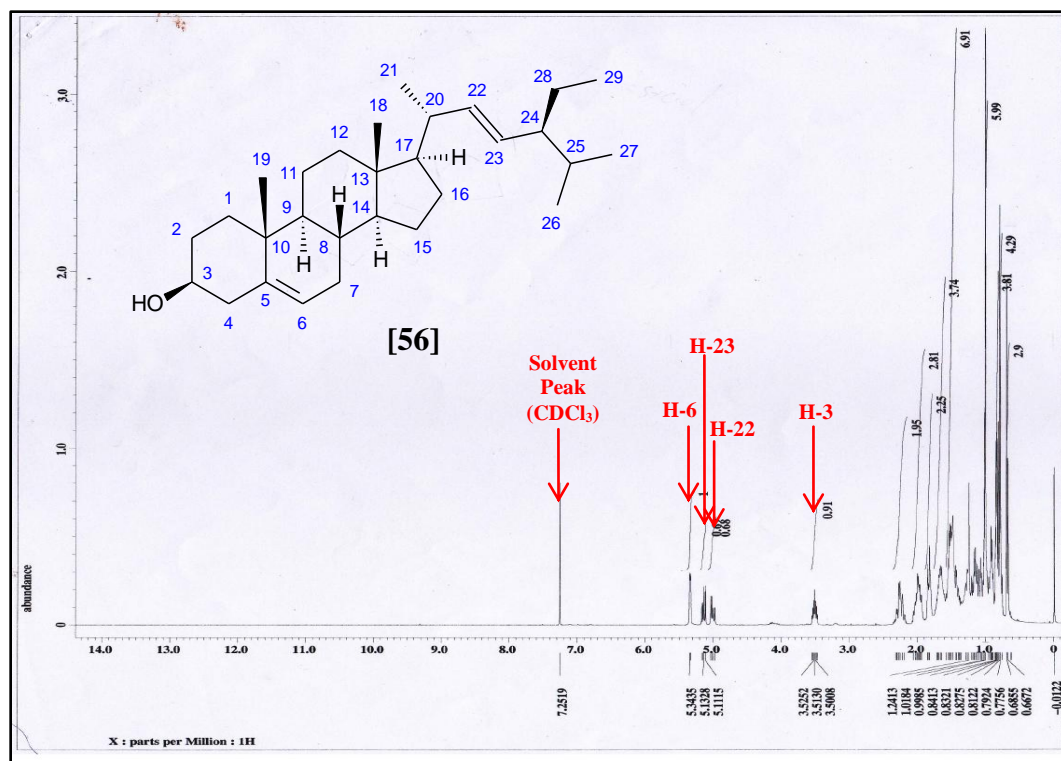


Figure 4.40: ^1H NMR spectrum of compound 56 (400 MHz, CDCl_3)

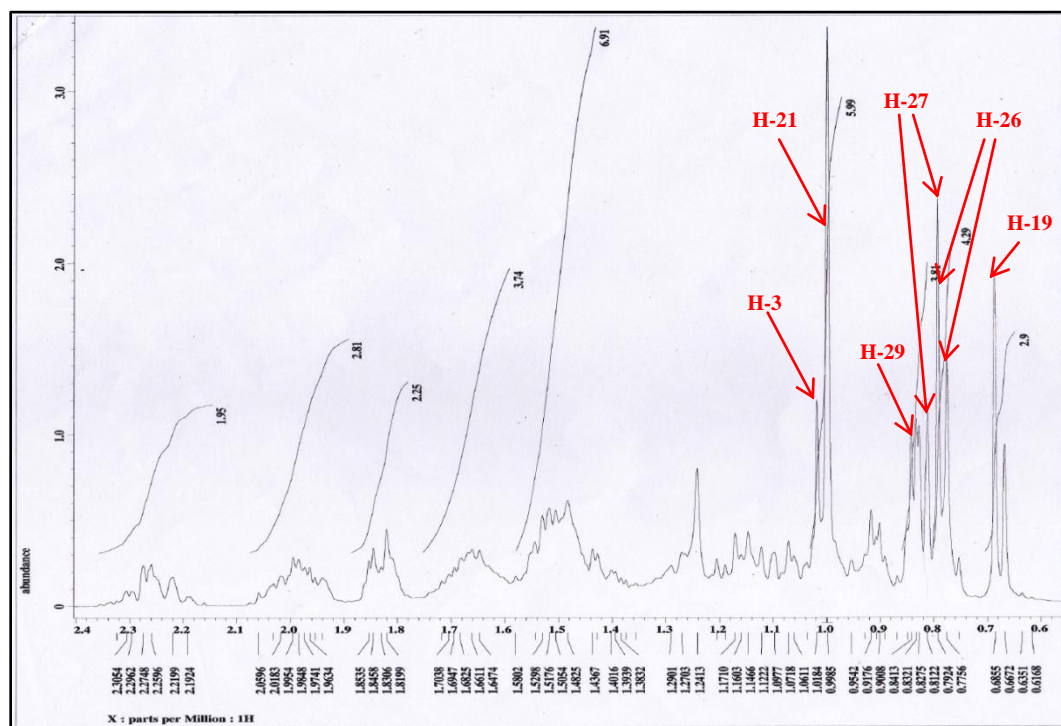
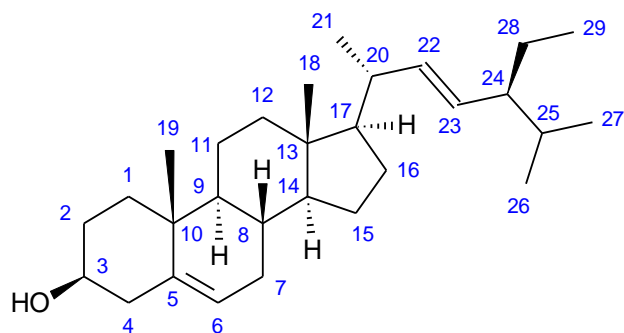


Figure 4.41: Expanded ^1H NMR spectrum of compound 56 (400 MHz, CDCl_3)



[56]

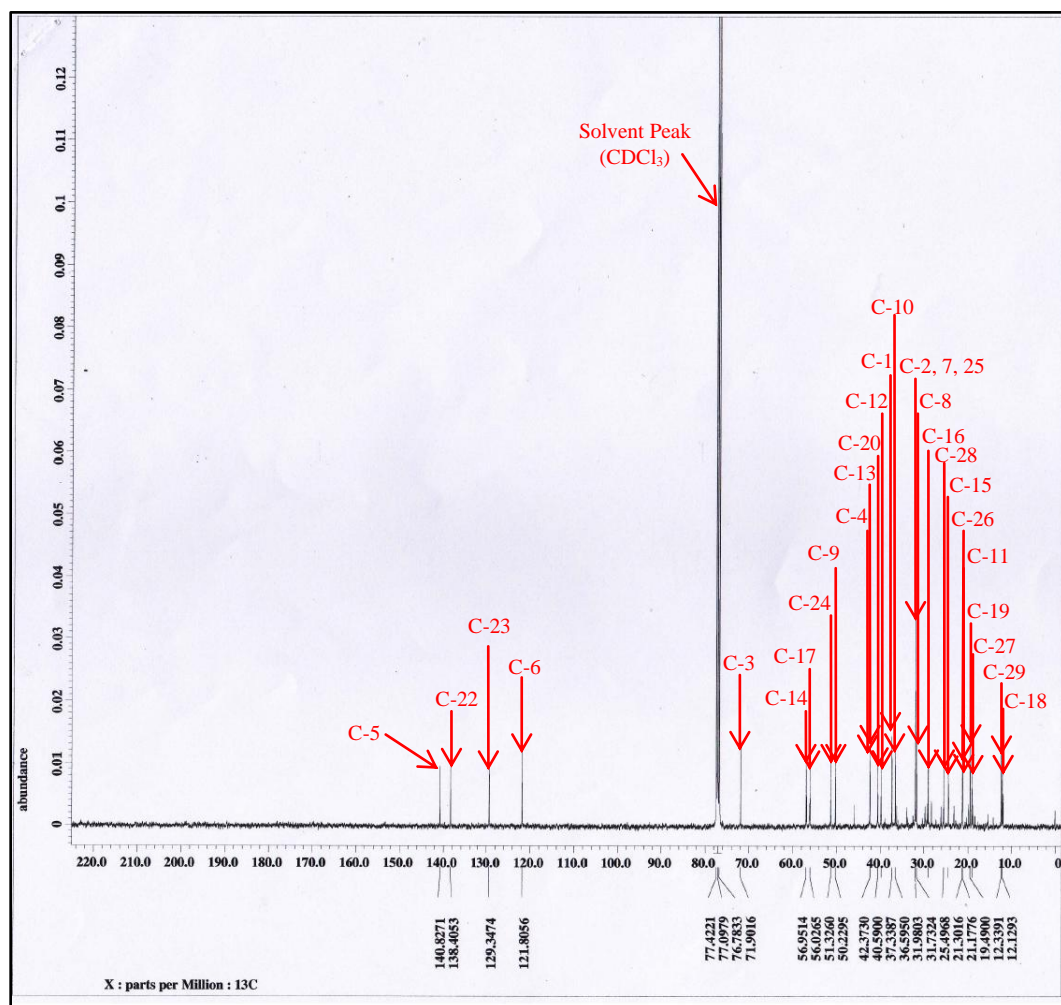


Figure 4.42: ¹³C NMR spectrum of compound 56 (100 MHz, CDCl₃)

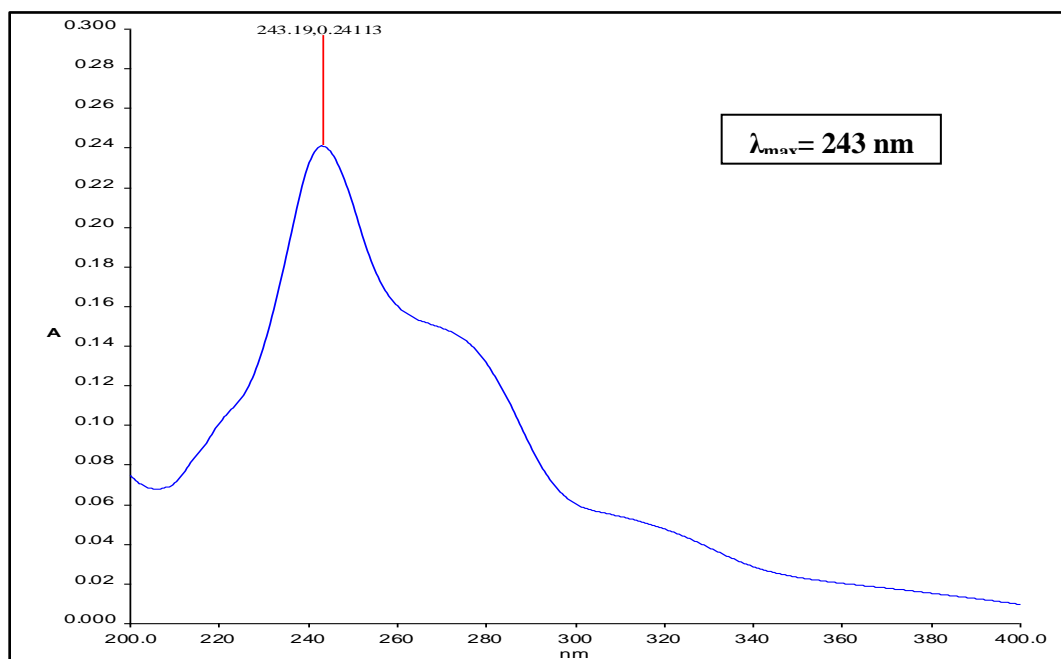


Figure 4.43: UV/Vis spectrum of compound 56

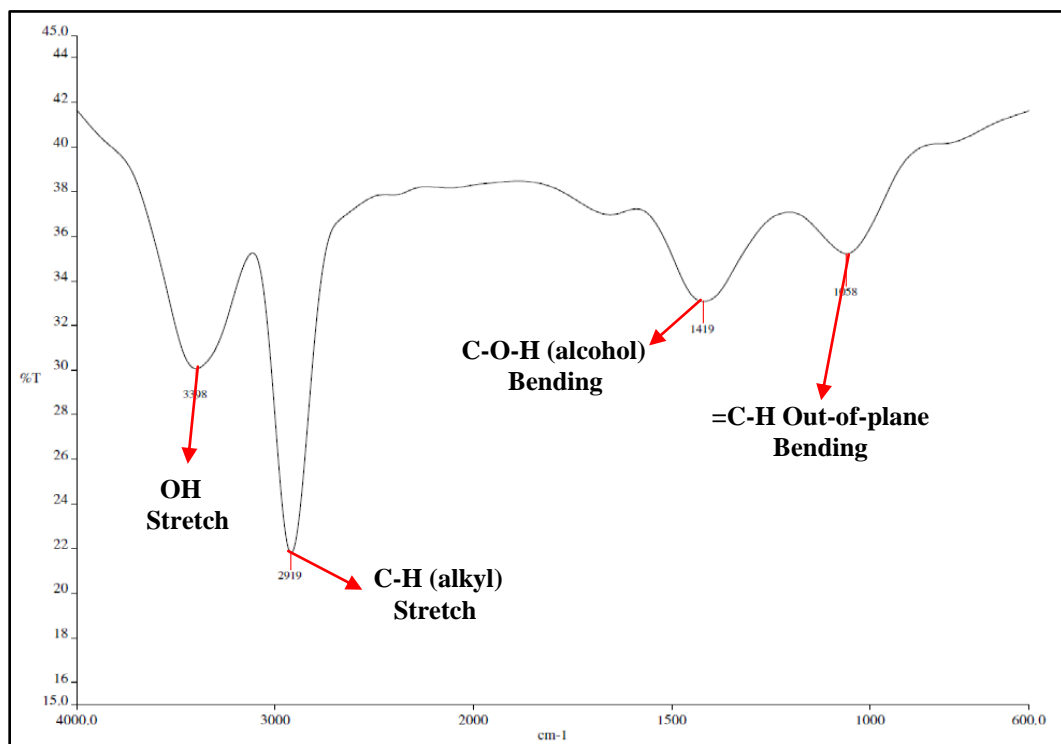


Figure 4.44: FT-IR spectrum of compound 56

4.3 Antioxidant Assay

Table 4.6: Inhibitory concentration (IC₅₀) of positive controls, crude extracts and isolated compounds in DPPH assay

Samples	IC ₅₀ (µg mL ⁻¹)
<u>Positive controls:</u>	
➤ Ascorbic acid (Vitamin C)	5
➤ Kaempferol	7
<u>Crude extracts:</u>	
➤ Dichloromethane	41
➤ Ethyl acetate	45
<u>Isolated compounds:</u>	
➤ [2 <i>E</i> ,6 <i>E</i> ,10 <i>E</i>]-(+)-4β-hydroxy-3-methyl-5β-(3,7,11,15-tetramethyl-2,6,10,14-hexadecatetraenyl)-2-cyclohexen-1-one [52]	>300
➤ α-Mangostin [53]	>300
➤ Rubraxanthone [54]	195
➤ 1,3,7-Trihydroxy-2,4-bis(3-methylbut-2-enyl)xanthone [55]	189
➤ Stigmasterol [56]	>300

The crude extracts and isolated compounds were evaluated for their antioxidant potential via DPPH assay. From the assay's result in Table 4.6, it revealed that the dichloromethane and ethyl acetate extracts showed a moderate antioxidant activity, with IC₅₀ values of 41 and 45 µg mL⁻¹, respectively. The antioxidant activity of both extracts appeared to be much weaker as compared to those of the positive controls, ascorbic acid (5 µg mL⁻¹) and kaempferol (7 µg mL⁻¹). It was because both the extracts contained not only phenolic compounds but also non-phenolic constituents, such as hydrocarbons and terpene derivatives which are poor antioxidants.

Among the isolated compounds, only rubraxanthone [54] and 1,3,7-trihydroxy-2,4-bis(3-methylbut-2-enyl)xanthone [55] were found to give significant antioxidant activity with IC₅₀ values of 195 and 189 µg mL⁻¹, respectively, but their antioxidant effects were reported to be much weaker than those of the positive controls. Meanwhile, the remaining compounds were found to be inactive towards DPPH radicals showing an IC₅₀ value of more than 300 µg mL⁻¹.

The significant antioxidant activity of compound 54 and 55 was due to the presence of two hydroxyl groups bonded to aromatic rings, except for the chelated hydroxyl group, 1-OH because the hydrogen is being hydrogen bonded to the carbonyl group. These compounds are able to scavenge the DPPH radicals by donating their hydrogen radicals from the hydroxyl group; as a result, another radical is formed at oxygen atom and is resonance-stabilized as shown in Figures 4.45 and 4.46. On the other hand, compound 53 also contained two hydroxyl groups but it gave a much weaker DPPH scavenging. In fact, there are many factors which govern the antioxidant capacity of a compound, including the number of hydroxyl group available, the stability of the compound after release of hydrogen radicals and the rate of releasing the hydrogen radicals (Weng and Huang, 2014). Hence, the cause for its poor antioxidant activity is only known by performing structure-antioxidant activity study on this compound. In the meantime, compound 52 and 56 gave a negative result in the DPPH assay due to the absence of phenolic moiety, which is important for delocalization of the radicals formed after the release of hydrogen radicals.

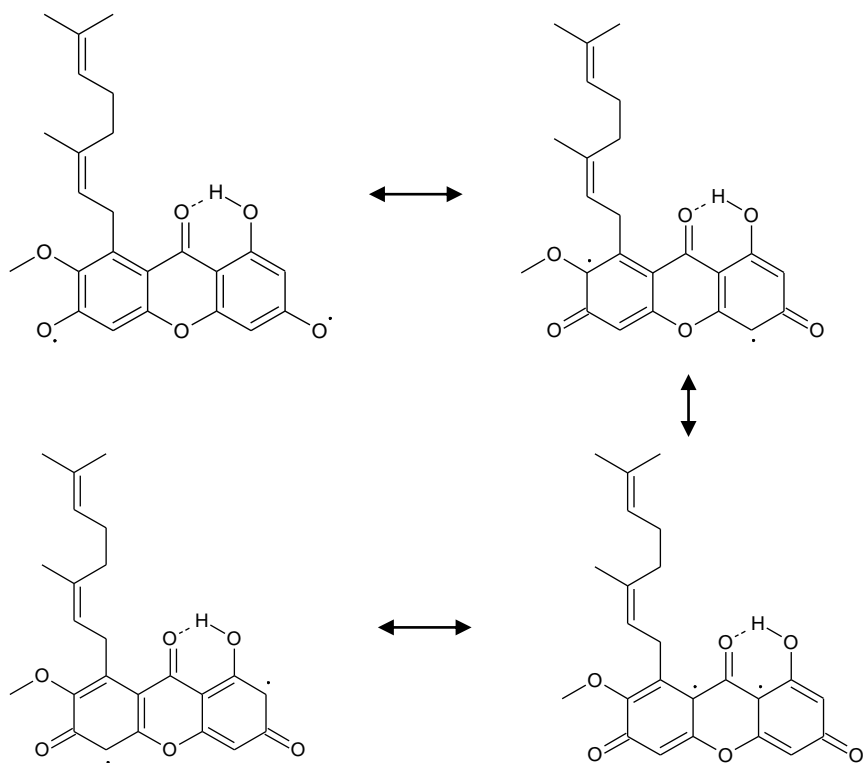


Figure 4.45: Resonance-stabilized of free radicals formed in compound 54

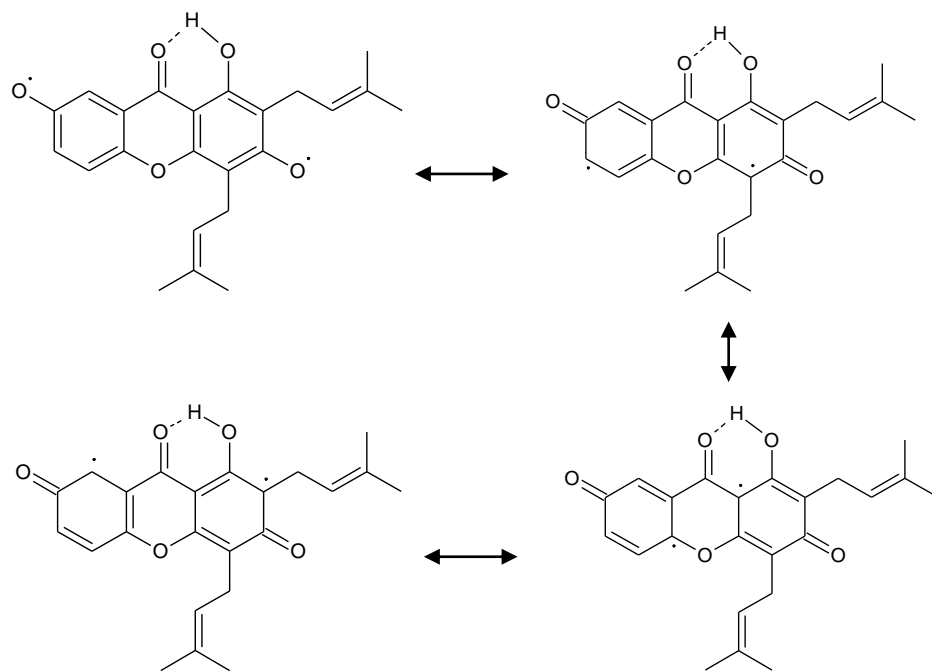


Figure 4.46: Resonance-stabilized of free radicals formed in compound 55

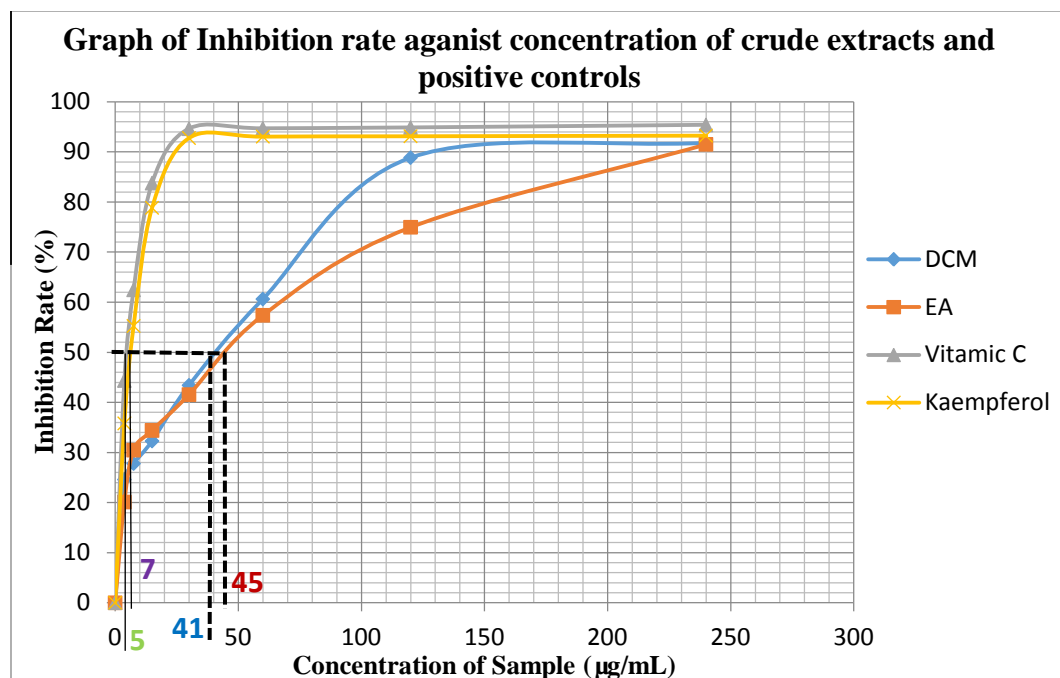


Figure 4.47: Graph of inhibition rate against concentration of crude extracts and positive controls

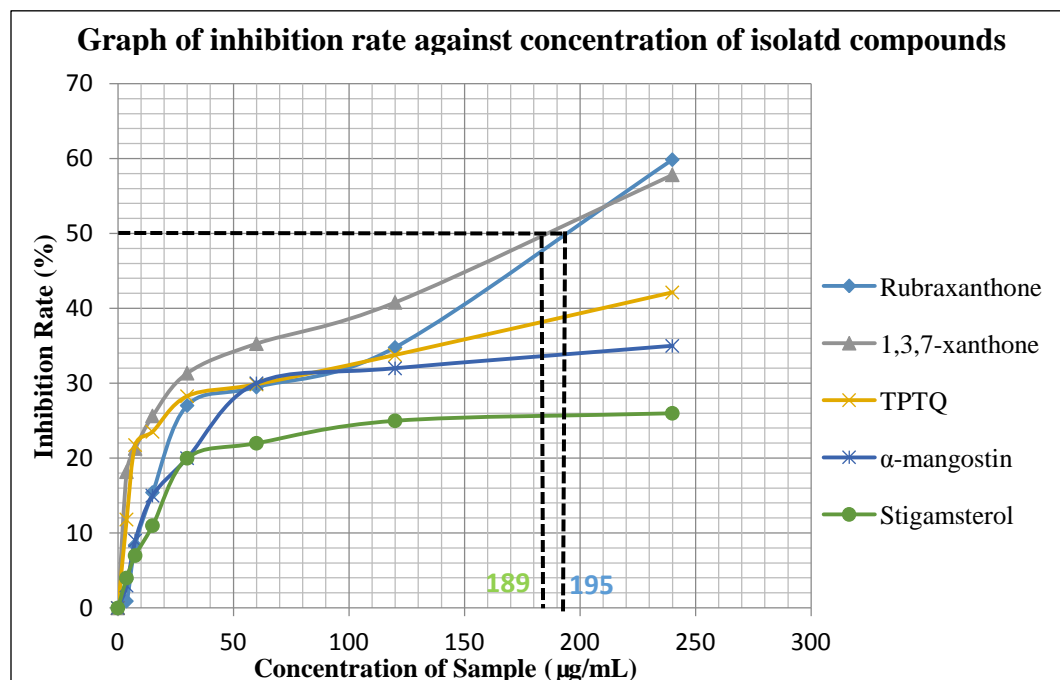


Figure 4.48: Graph of inhibition rate against concentration of isolated compounds

CHAPTER 5

CONCLUSIONS

5.1 Conclusion

This study has successfully yielded a total of five chemical compounds, namely [2*E*,6*E*,10*E*]-(+)-4 β -hydroxy-3-methyl-5 β -(3,7,11,15-tetramethyl-2,6,10,14-hexadecatetraenyl)-2-cyclohexen-1-one [52], α -mangostin [53], rubraxanthone [54], 1,3,7-trihydroxy-2,4-*bis*(3-methylbut-2-enyl)xanthone [55] and stigmasterol [56] from the stem bark of *Garcinia parvifolia*. The structures of all these compounds were elucidated on the basis of spectroscopic methods including NMR, UV/Vis, FT-IR spectroscopy and LC-MS.

All the crude extracts and isolated compounds were examined for their antioxidant potential via DPPH assay. The dichloromethane and ethyl acetate extracts displayed moderate DPPH scavenging activity with IC₅₀ values of 41 and 45 $\mu\text{g mL}^{-1}$, respectively. Among the isolated compounds, only compounds 54 and 55 were found to be active towards DPPH radicals with IC₅₀ values of 195 and 189 $\mu\text{g mL}^{-1}$, respectively. On the other hand, compounds 52, 53 and 56 gave insignificant antioxidant activity showing IC₅₀ values of more than 300 $\mu\text{g mL}^{-1}$.

5.2 Future Studies

In future study, modern separation techniques, such as High Performance Liquid Chromatography (HPLC), Ultra Performance Liquid Chromatography (UPLC) and centrifugal chromatography, are suggested to be utilized in place of gravity column chromatography for isolation of minor active compounds from the plant species. Besides, the five isolated compounds which showed a poor antioxidant activity should be studied for their other biological potentials such as antiplasmodial, antimicrobial and anticancer activities. Next, the isolated compounds should be further studied for their potential derivatives via organic synthesis. It is aimed to synthesize the chemical derivatives with improved biological effects and lower toxicity.

REFERENCES

- Ahmad, M., Yamin, B. M. and Lazim, A. M., 2013. A Study on Dispersion and Characterization of α -Mangostin Loaded pH Sensitive Microgel Systems. *Chemistry Central Journal*, 7(85), pp. 1-6.
- Aukkanimart, R., Boonmars, T., Sriraj, P., Songsri, J., Laummaunwai, P., Waraasawapati, S., Boonyarat, C., Rattanasuwan, P. and Boonjaraspinyo, S., 2015. Anthelmintic, Anti-inflammatory and Antioxidant Effects of *Garcinia mangostana* Extract in Hamster *Opisthorchiasis*. *Experimental Parasitology*, 154, pp. 5-13.
- Auranwiwat, C., Trisuwan, K., Saiai, A., Pyne, S. G. and Ritthiwigrom, T., 2014. Antibacterial Tetraoxygenated Xanthenes from the Immature Fruits of *Garcinia cowa*. *Fitoterapia*, 98, pp. 179-183.
- Baliga, M. S., Bhat, H. P., Prai, R. J., Bloor, R. and Palatty, P. L., 2011. The Chemistry and Medicinal Uses of the Underutilized Indian Fruit Tree *Garcinia indica* Choisy (Kokum): A Review. *Food Research International*, 44, pp. 1790-1799.
- Bui, D. A., Vu, M. K., Nguyen, H. D., Nguyen, L.-T. T., Dang, S. V. and Nguyen, L.-H. D., 2014. A Protostane and Two Lanostanes from the Bark of *Garcinia ferrea*. *Phytochemistry Letters*, 10, pp. 123-126.
- Butler, M. S., 2004. The Role of Natural Product Chemistry in Drug Discovery. *Journal of Natural Product*, 67, pp. 2141-2153.
- Chen, Y., He, S., Tang, C., Li, J. and Yang, G., 2015. Caged Polyprenylated Xanthenes from the Resin of *Garcinia hanburyi*. *Fitoterapia*, 109, pp. 106-112.
- Chien, S.-C., Chyu, C.-F., Chang, I.-S., Chiu, H.-L. and Kuo, Y.-H., 2008. A Novel Polyprenylated Phloroglucinol, Garcinialone, from the Roots of *Garcinia multiflora*. *Tetrahedron Letters*, 49, pp. 5276-5278.
- Cooper, R. and Nicola, G., 2014. *Natural Product Chemistry*. United State: Taylor & Francis Group.
- Cragg, G. M. and Newman D. J., 2013. Natural Products: A Continuing Source of Novel Drug Leads. *Biochimica et Biophysica Acta*, pp. 3670-3695.

- Crozier, A., Clifford, M. N. and Ashihara, H., 2006. *Plant Secondary Metabolites*. United Kingdom: Blackwell Publishing Ltd.
- Deng, Y.-X., Guo, T., Shao, Z.-Y., Xie, H. and Pan, S.-L., 2013. Three New Xanthenes from the Resins of *Garcinia hanburyi*. *Planta Medica*, 79(9), pp. 792-796.
- Dhawale, P. G., 2013. Phytochemical Analysis of Eight Medicinal Plants from Amravati District (MS) India. *International Journal of Scientific and Research Publications*, 3(1), pp. 1-3.
- Dias, D. A., Urban, S. and Roessner, U., 2012. A Historical Overview of Natural Products in Drug Discovery. *Metabolites*, 2, pp. 303-336.
- Dyary, H. O., Arifah, A. K., Sharma, R. S. K., Rasedee, A., Aspollah, M. S. M., Zakaria, Z. A., Zuraini, A. and Somchit, M. N., 2015. In Vivo Antitrypanosomal Activity of *Garcinia hombroniana* Aqueous Extract. *Research in Veterinary Science*, 100, pp. 226-231.
- Ee, G. C. L., Lim, C. K. and Rahmat, A., 2005. Structure-Activity Relationship of Xanthenes from *Mesua daphnifolia* and *Garcinia nitida* Towards Human Estrogen Receptor Negative Breast Cancer Cell Line. *Natural Product Sciences*, 11(4), pp. 220-224.
- Elfita, E., Muharni, M., Latief, M., Darwati, D., Widiyantoro, A., Supriyatna, S., Bahti, H. H., Dachriyanus, D., Cos, P., Maes, L., Foubert, K., Apers, S. and Pieters, L., 2009. Antiplamodial and other constituents from four Indonesian *Garcinia* spp. *Phytochemistry*, 70, pp. 907-912.
- Elya, B., He, H. P., Kosela, S., Hanafi, M. and Hao, X. J., 2008. A New Cytotoxic Xanthone from *Garcinia rigida*. *Fitoterapia*, 79, pp. 182-184.
- Fu, M., Feng, H.-J., Chen, Y., Wang, D.-B. and Yang, G.-Z., 2012. Antioxidant Activity of *Garcinia xanthochymus* Leaf, Root and Fruit Extracts In Vitro. *Chinese Journal of Natural Medicines*, 10(2), pp. 129-134.
- Gao, X.-M., Yu, T., Lai, F. S. F., Pu, J.-X., Qiao, C.-F., Zhou, Y., Liu, X., Song, J.-Z., Luo, K. Q. and Xu, H.-X., 2010. Novel Polyprenylated Benzophenone Derivatives from *Garcinia paucinervis*. *Tetrahedron Letters*, 51, pp. 2442-2446.

- Gerten, D., Salma, I., Shafie, M. S. M., Shariah, U., Brooke, P., Wong, W. W. W. and Norhayati, M. H., 2015. Traditional Knowledge and Practices Related to Genus Citrus, Garcinia, Mangifera and Nephelium in Malaysia. *Open Access Library Journal*, 2, pp. 1-11.
- Gontijo, V. S., Souza, T. C. D., Rosa, I. A., Soares, M. G., Silva, M. A. D., Vilegas, W., Júnior, C. V. and Santos, M. H. D., 2012. Isolation and Evaluation of the Antioxidant Activity of Phenolic Constituents of the Garcinia brasiliensis Epicarp. *Food Chemistry*, 132, pp. 1230-1235.
- Halbwirth, H., 2010. The Creation and Physiological Relevance of Divergent Hydroxylation Patterns in the Flavonoid Pathway. *International Journal of Molecular Sciences*, 11, pp. 595-621.
- Hassan, S. H. A., Fry, J. R. and Bakar, M. F. A., 2013. Phytochemicals Content, Antioxidant Activity and Acetylcholinesterase Inhibition Properties of Indigenous Garcinia Parvifolia Fruit. *Biomed Research International*, pp. 1-7.
- Hay, A.-E., Hdesbeux, J.-J., Duval, O., Labaëd, M., Grellier, P. and Richomme, P., 2004. Antimalarial Xanthenes from Calophyllum caledonicum and Garcinia vieillardii. *Life Sciences*, 75, pp. 3077-3085.
- Hay, A.-E., Merza, J., Landreau, A., Litaudon, M., Pagniez, F., Pape, P. P. and Richomme, P., 2008. Antileishmanial Polyphenols from Garcinia vieillardii. *Fitoterapia*, 79, pp. 42-46.
- Hussain, S., Fareed, S., Ansari, S. and Khan M. S., 2012. Marine Natural Products: A Lead for Anti-cancer. *Indian Journal of Geo-Marine Sciences*, 41(1), pp. 27-39.
- Ibrahim, M. Y., Hashim, N. M., Mariod, A. A., Mohan, S., Abdulla, M. A., Abdelwahab, S. I. and Arbab, I. A., 2014. α -Mangostin from Garcinia mangostana Linn: An Updated Review of Its Pharmacological Properties. *Arabian Journal of Chemistry*, pp. 1-13.
- Ilnuma, M., Tosa, H., Tanaka, T. and Riswan, S., 1996. Three New Xanthenes from the Bark of Garcinia dioica. *Chemical and Pharmaceutical Bulletin*, 44(1), pp. 232-234.

- Jamila, N., Khairuddean, M., Yaacob, N. S., Kamal, N. N. S. N. M., Osman, H., Khan, S. N. and Khan, N., 2014. Cytotoxic Benzophenone and Triterpene from *Garcinia hombroniana*. *Bioorganic Chemistry*, 54, pp. 60-67.
- Jantan, I., Pizar, M. M., Idris, M. S., Taher, M. and Ali, R. M., 2002. In Vitro Inhibitory Effect of Rubraxanthone Isolated from *Garcinia parvifolia* on Platelet-Activating Factor Receptor Binding. *Planta Medica*, 68, pp. 1133-1134.
- Kaennakam, S., Siripong, P. and Tip-pyang, S., 2015. Kaennacowanols A-C, Three New Xanthenes and Their Cytotoxicity from the Roots of *Garcinia cowa*. *Fitoterapia*, 102, pp. 171-176.
- Kardono, L. B. S., Hanafi, M., Sherley, G., Kosela, S. and Harrison, L. J., 2006. Bioactive Constituents of *Garcinia porrecta* and *G. parvifolia* Grown in Indonesia. *Pakistan Journal of Biological Science*, 9(3), pp. 483-486.
- Klaiklay, S., Sukpondma, Y., Rukachaisirikul, V. and Phongpaichit, S., 2012. Friedolanostanes and Xanthenes from the Twigs of *Garcinia hombroniana*. *Phytochemistry*, 85, pp. 161-166.
- Komguem, J., Meli, A. L., Manfouo, R. N., Lontsi, D., Ngounou, F. N., Kuete, V., Kamdem, H. W., Tane, P. and Ngadjui, B. T., 2005. Xanthenes from *Garcinia smeathmannii* (Oliver) and Their Antimicrobial Activity. *Phytochemistry*, 66, pp. 1713-1717.
- Konziase, B., 2015. Protective Activity of Biflavonoids from *Garcinia kola* Against Plasmodium Infection. *Journal of Ethnopharmacology*, 172, pp. 214-218.
- Kourkoutas, Y., Karatzas, K. A. G., Valdramidis, V. P. and Chorianopoulos, N., 2014. Bioactive Natural Products: Facts, Applications, and Challenges. *BioMed Research International*, pp. 1-3.
- Kuete, V., Komguem, J., Beng, V. P., Meli, A. L., Tangmouo, J. G., Etoa, F.-X. and Lontsi, D., 2007. Antimicrobial Components of the Methanolic Extract from the Stem Bark of *Garcinia smeathmannii* Oliver (Clusiaceae). *Journal of Botany*, 73(3), pp. 347-354.
- Kumar, S. and Pandey, A. K., 2013. Chemistry and Biological Activities of Flavonoids: An Overview. *The Scientific World Journal*, pp. 1-16.

- Lannang, A. M., Komguem, J., Ngninzeko, F. N., Tangmouo, J. G., Lontsi, D., Ajaz, A., Choudhary, M. I., Ranjit, R., Devkota, K. P. and Sondengam, B. L., 2005. Banganxanthone A and B, Two Xanthenes from the Stem Bark of *Garcinia polyantha* Oliv. *Phytochemistry*, 66, pp. 2351-2355.
- Latifah, U. Z., Rahim, R. A., Sudrajat, H. and Khairi, S., 2009. Antiplasmodial Activity of Alkaloids from *Garcinia parvifolia* Miq. Stem Bark. *Journal of Iranian Chemical Research*, 3, pp. 59-63.
- Lauvaud, A., Richomme, P., Gatto, J., Aumond, M.-C., Poullain, C., Litaudon, M., Andriantsitohaina, R. and Guilet, D., 2015. A tocotrienol Series With An Oxidative Terminal Prenyl Unit from *Garcinia amplexicaulis*. *Phytochemistry*, 109, pp. 103-110.
- Lee, D.-S., Cho, Y.-S. and Je, J.-Y., 2013. Antioxidant and Antibacterial Activities of Chitosan-Phloroglucinol Conjugate. *Canadian Journal of Fisheries and Aquatic Sciences*, 16(4), pp. 229-235.
- Lee, L.-T., Tsai, H.-P., Wang, C.-C., Chang, C.-N., Liu, W.-C., Hsu, H.-C., Hsieh, C.-T., Chen, Y.-C., Tseng, H.-W., Gau, R.-J., Liu, S.-H., Chen, I.-S. and Iinuma, M., 2012. Guttiferone F from the Fruit of *Garcinia multiflora* and Its Anti-hepatocellular Carcinoma Activity. *Biomedicine & Preventive Nutrition*, 3, pp. 247-252.
- Lemke, T. L. and Williams, D. A., 2013. FOYE's Principles of Medicinal Chemistry. 7th edition. China: Lippincott Williams & Wilkins.
- Li, Y., Wang, Z., Wu, X., Yang, Y., Qin, Y., Xia, C., Meng, Y., Li, M., Gao, X.-M. and Hu, Q., 2015. Biphenyl Derivatives from the Twigs of *Garcinia bracteata* and Their Biological Activities. *Phytochemistry Letters*, 11, pp. 24-27.
- Lim, T. K., 2012. *Garcinia parvifolia*. Edible Medicinal and Non-Medicinal Plants. 2, pp. 115-119.
- Lin, K.-W., Huang, A.-M., Yang, S.-C., Weng, J.-R., Hour, T.-C., Pu, Y.-S. and Lin, C.-N., 2012. Cytotoxic and Antioxidant Constituents from *Garcinia subelliptica*. *Food Chemistry*, 135, pp. 851-859.

- Louh, G. N., Lannang, A. M., Mbazona, C. D., Tangmouo, J. G., Komguem, J., Castilho, P., Ngninzeko, F. N., Qamar, N., Lontsi, D., Choudhary, M. I. and Sondengam, B. L., 2007. Polyanxanthone A, B and C, Three Xanthenes from the Wood Trunk of *Garcinia polyantha* Oliv. *Phytochemistry*, 69, pp. 1013-1017.
- Lukitaningsih, E., 2012. Phytosterol Content in Bengkoang (*Pachyrhizus erosus*). *Journal of Pharmacon*, 13(2), pp.47-54.
- Luo, L., Qin, J.-K., Dai, Z.-K. and Gao, S.-H., 2013. Synthesis and Biological Evaluation of Novel Benzo[b]xanthone Derivatives As Potential Antitumor Agents. *Journal of the Serbian Chemical Society*, 78(9), pp. 1301-1308.
- Magadula, J. J., 2010. A Bioactive Isoprenylated Xanthenes and Other Constituents of *Garcinia edulis*. *Fitoterapia*, 81, pp. 420-423.
- Magadula, J. J., Kapingu, M. C., Bezabih, M. and Abegaz, B. M., 2008. Polyisoprenylated Benzophenones from *Garcinia semseii* (Clusiaceae). *Phytochemistry Letters*, 1, pp. 215-218.
- Mahabusarakam, W., Chairerk, P. and Taylor, W. C., 2005. Xanthenes from *Garcinia cowa* Roxb. *Latex. Phytochemistry*, 66, pp. 1148-1153.
- Mahamodo, S., Riviere, C., Neut, C., Abedini, A., Ranarivelo, H., Duhai, N., Roumy, V., Hennebelle, T., Sahpaz, S. S., Lemoine, A., Razafimahefa, D., Razanamahefa, B., Bailleul, F. and Andriamihaja, B., 2014. Antimicrobial prenylated benzoylphloroglucinol derivatives and xanthenes from the leaves of *Garcinia goudotiana*. *Phytochemistry*, 102, pp., 162-168.
- Mawa, S. and Said, I. M., 2012. Chemical Constituents of *Garcinia prainiana*. *Sains Malaysiana*, 41(5), pp. 585-590.
- Mohamed, G. A. and Ibrahim, S. R. M., 2007. Eucalyptone G, A New Phloroglucinol Derivatives and Other Constituents from *Eucalyptus globules* Labill. *General Papers*, pp. 281-291.
- Mohammed, H., 2009. Natural and Synthetic Flavonoid Derivatives with Potential Antioxidant and Anticancer Activities. Germany: Universität des Saarlandes.

- Mulholland, D. A., Mwangi, E. M., Dlova, N. C., Plant, N., Crouch., N. R. and Coombes, P. H., 2013. Non-toxic Melanin Production Inhibitors from *Garcinia livingstonei* (Clusiaceae). *Journal of Ethnopharmacology*, 149, pp. 570-575.
- Ngo, L. T., Okogun, J. I. and Folk, W. R., 2013. 21st Century Natural Product Research and Drug Development and Traditional Medicines. *Natural Product Reports*, 30(4), pp. 584-592.
- Ngoupayo, J., Tabopda, T. K. and Ali, M. S., 2009. Antimicrobial and Immunomodulatory Properties of Prenylated Xanthenes from Twigs of *Garcinia staudtii*. *Bioorganic and Medicinal Chemistry*, 17(15), pp. 5688-5695.
- Nguyen, H. D., Trinh, B. T. D. and Nguyen, L.-H. D., 2011a. Guttiferones Q-S, Cytotoxic Polyisoprenylated Benzophenones from the Pericarp of *Garcinia cochinchinensis*. *Phytochemistry Letters*, 4, pp. 129-133.
- Nguyen, H. D., Trinh, B. T. D., Tran, Q. N., Nguyen, H. D., Pham, H. D., Hansen, P. E., Duus, F., Connolly, J. D. and Nguyen, L.-H. D., 2011b. Friedolanostane, Friedocycloartane and Benzophenone Constituents of the Bark and Leaves of *Garcinia benthami*. *Phytochemistry*, 72, pp. 290-295.
- Nguyen, L.-H. D., Vo, H. T., Pham, H. D., Connolly, J. D. and Harrison, L. J., 2002. Xanthenes from the bark of *Garcinia merguensis*. *Phytochemistry*, 63, pp. 467-470.
- Nilar, Nguyen, L.-H. D., Venkatraman, G., Sim, K.-Y. and Harrison, L. J., 2005. Xanthenes and benzophenones from *Garcinia griffithii* and *Garcinia mangostana*. *Phytochemistry*, 66, pp. 1718-1723.
- Niu, S.-L., Li, Z.-L., Ji, F., Liu, G.-Y., Zhao, N., Liu, X.-Q. and Jing, Y.-K., 2012. Xanthenes from the stem bark of *Garcinia bracteata* with growth inhibitory effects against HL-60 cells. *Phytochemistry*, 77, pp. 280-286
- Panthong, K., Pongcharoen, W., Phongpaichit, S. and Taylor, W. C., 2006. Tetraoxygenated xanthenes from the fruits of *Garcinia cowa*. *Phytochemistry*, pp. 999-1004.
- Pattalung, P. N., Wiriyaichitra, P. and Ongsakul, M., 1988. The Antimicrobial Activities of Rubraxanthone Isolated from *Garcinia parvifolia* Miq. *Journal of the Science Society of Thailand*, 14, pp. 67-71.

- Pierre, L. L. and Moses, M. N., 2015. Isolation and Characterization of Stigmasterol and β -Sitosterol from *Odontonema Strictum* (Acanthaceae). *Journal of Innovations in Pharmaceuticals and Biological Sciences*, 2(1), 88-95.
- Pinto, M. M. M., Sousa, M. E. and Nascimento, M. S. J., 2005. Xanthone Derivatives: New Insights in Biological Activities. *Current Medicinal Chemistry*, 12, pp. 2517-2538.
- Ritthiwigrom, T., Laphookhieo, S. and Pyne, S. G., 2013. Chemical constituents and biological activities of *Garcinia cowa* Roxb. *Maejo International Journal of Science and Technology*, 7(2), pp. 212-231.
- Rukachaisirikul, V., Naklue, W., Phongpaichit, S., Towatana, N. H. and Maneenoon, K., 2006. Phloroglucinols, depsidones and xanthenes from the twigs of *Garcinia parvifolia*. *Tetrahedron*, pp. 8578-8585.
- Rukachaisirikul, V., Ritthiwigrom, T., Pinsa, A., Sawangchote, P. and Taylor, W. C., 2003. Xanthenes from the Stem Bark of *Garcinia nigrolineata*. *Phytochemistry*, 64, pp. 1149-1156.
- Rukachaisirikul, V., Trisuwan, K., Sukpondma, Y. and Phongpaichit, S., 2008. A New Benzoquinone Derivatives from the Leaves of *Garcinia parvifolia*. *Archives of Pharmacal Research*, 31(1), pp. 17-20.
- Ryu, H. W., Cho, J. K., Curtis-Long, M. J., Yuk, H. J., Kim, Y. S., Jung, S., Kim, Y. S., Lee, B. W. and Park, K. H., 2011. α -Glucosidase Inhibition and Antihyperglycemic Activity of Prenylated Xanthenes from *Garcinia mangostana*. *Phytochemistry*, 72, pp. 2148-2154.
- Salim, A. A., Chin Y.-W. and Kinghorn, A. D., 2008. *Drug Discovery from Plants*. pp. 1-24.
- Sangsuwon, C. and Jiratchariyakul, W., 2015. Antiproliferative Effect of Lung Cancer Cell Lines and Antioxidant of Macluraxanthone from *Garcinia speciosa* Wall. *Procedia-Social and Behavioral Sciences*, 197, pp. 1422-1427.
- Santa-Cecilia, F. V., Freitas, L. A. S., Vilela, F. C., Veloso, C. D. C., Rocha, C. Q. D., Moreira, M. E. C., Dias, D. F., Giusti-Paiva, A. and Santos, M. H. D., 2011. Antinociceptive and Anti-inflammatory Properties of 7-

Epiclusianone, A Prenylated Benzophenone from *Garcinia brasiliensis*. *European Journal of Pharmacology*, 670, pp. 280-285.

- Saxena, M., Saxena, J., Nema, R., Singh, D. and Gupta, A., 2013. Phytochemistry of Medicinal Plants. *Journal of Pharmacognosy and Phytochemistry*, 1(6), pp. 168-182.
- Semwal, R. B., Semwal, D. K., Vermaak, I. and Viljoen, A., 2015. A Comprehensive Scientific Overview of *Garcinia cambogia*. *Fitoterapia*, 102, pp. 134-148.
- Sindhi, V., Gupta, V., Sharma, K., Bhatnagar, S., Kumari, R. and Dhaka, N., 2013. Potential applications of antioxidants-A review. *Journal of Pharmacy Research*, 7, pp. 828-835.
- Singh, I. P. and Bharate, S. B., 2008. Phloroglucinol Compounds of Natural Origin. *Royal Society of Chemistry*, 23, pp. 558-591.
- Siong, K. H., 2003. Indigenous Fruits of Sarawak. Japan: International Tropical Timber Organization and Malaysia: Sarawak Forest Department.
- Siridechakorn, I., Phakhodee, W., Ritthiwigrom, T., Promgool, T., Deachathai, S., Cheenpracha, S., Prawat, U. and Laphookhieo, S., 2012. Antibacterial Dihydrobenzopyran and Xanthone Derivatives from *Garcinia cowa* Stem Barks. *Fitoterapia*, 83, pp. 1430-1434
- Sukandar, E. R., Ersam, T., Fatmawati, S., Siripong, P., Aree, T. and Tip-pyang, S., 2016. Cylindroxanthenes A-C, Three New Xanthenes and Their Cytotoxicity from the Stem Bark of *Garcinia cylindrocarpa*. *Fitoterapia*, 108, pp. 62-65.
- Syamsudin, Kumala, S. and Sutaryo, B., 2007a. Screening of Some Extracts from *Garcinia parvifolia* Miq. (Guttiferae) for Antiplasmodial, Antioxidant, Cytotoxic and Antibacterial Activities. *Asian Journal of Plant Sciences*, 6(6), pp. 972-976.
- Syamsudin, Tjokrosanto, S., Wahyuono, S., Darmono and Mustofa, 2007b. In Vitro and In Vivo Antiplasmodial Activities of Stem Bark Extracts of *Garcinia parvifolia* Miq (Guttiferae). *International Journal of Tropical Medicine*, 2(2), pp. 41-44.
- Taher, M., Susanti, D., Rezali, M. F., Zohri, F. S. A., Ichwan, S. J. A., Alkhamaiseh, S. I. and Ahmad, F., 2012. Apoptosis, Antimicrobial and

Antioxidant Activities of Phytochemicals from *Garcinia malaccensis* Hk.f. *Asian Pacific Journal of Tropical Medicine*, pp. 136-141.

- Tan, S. Y., Koh, C. Y., Siow, H. J. M., Li, T., Wong, H. F., Heyzer, A. and Tan, H. T. W., 2013. 100 Common Vascular Plants of the Nee Soon Swamp Forest, Singapore. Singapore: Raffles Museum of Biodiversity Research.
- Tan, W.-N., Khairuddean, M., Wong, K.-C., Khaw, K.-Y. and Vikneswaran, M., 2014. New Cholinesterase Inhibitors from *Garcinia atroviridis*. *Fitoterapia*, 97, pp. 261-267.
- Tang, Z.-Y., Xia, Z.-X., Qiao, S.-P., Jiang, C., Shen, G.-R., Cai, M.-X. and Tang, X.-Y., 2015. Four New Cytotoxic Xanthenes from *Garcinia nuijiangensis*. *Fitoterapia*, 102, pp. 109-114.
- Tesso, H., 2005. Isolation and Structure Elucidation of Natural Products from Plants. Hamburg: University of Hamburg.
- Thoison, O., Cuong, D. D., Gramain, A., Chiaroni, A., Hung, N. V. and S évenet, 2005. Further Rearranged Prenylxanthenes and Benzophenones from *Garcinia bracteata*. *Tetrahedron*, 61, 8529-8535.
- Thong, N. M., Quang, D. T., Bui, N. H. T., Dao, D. Q. and Nam, P. C., 2015. Antioxidant Properties of Xanthenes Extracted from the Pericarp of *Garcinia mangostana* (Mangosteen): A theoretical Study. *Chemical Physics Letters*, 625, pp. 30-35.
- Trinh, B. T. D., Nguyen, N.-T. T., Ngo, N. T. N., Tran, P. T., Nguyen, L.-T. T. and Nguyen, L.-H. D., 2013. Polyisoprenylated Benzophenone and Xanthone Constituents of the Bark of *Garcinia cochinchinensis*. *Phytochemistry Letters*, pp. 224-227.
- Trisuwan, K., Boonyaketguson, S., Rukachaisirikul, V. and Phongpaichit, S., 2014. Oxygenated Xanthenes and Biflavanoids from the Twigs of *Garcinia xanthochymus*. *Tetrahedron Letters*, 55, pp. 3600-3602.
- Trisuwan, K., Rukachaisirikul, V., Phongpaichit, S., And Hutadilok-Towatana, N., 2013. Tetraoxygenated Xanthenes and Biflavanoids from the Twigs of *Garcinia merguensis*. *Phytochemistry Letters*, 6, pp. 511-513.

- Velíšek, J., Dav ílek, J. and Cejpek, K., 2007. Biosynthesis of Food Constituents: Natural Pigments. Part 1 – A Review. *Czech Journal of Food Sciences*, 25(6), pp. 291–315.
- Vo, H. T., Nguyen, N.-T. T., Maas, G., Werz, U. R., Pham H. D. and Nguyen L.-H. D., 2012a. Xanthoness from the bark of *Garcinia pedunculata*. *Phytochemistry Letters*, pp. 766-769.
- Vo, H. T., Nguyen, N.-T. T., Nguyen, H. T., Do, K. Q., Connolly, J. D., Maas, G., Heilmann J., Werz, U. R., Pham, H. D. and Nguyen, L.-H. D., 2012b. Cytotoxic Tetraoxygenated Xanthoness from the Bark of *Garcinia schomburgkiana*. *Phytochemistry Letters*, 5, pp. 553-557.
- Wahyuni, F. S., Stanslas, J., Lajis, N. H. and Dachriyanus, 2015. Cytotoxicity Studies of Tetraprenyltoluquinone, A Prenilated Hydroquinone from *Garcinia cowa* Roxb on H-460, MCF-7 and DU-145. *International Journal of Pharmacy and Pharmaceutical Sciences*, 7(3), pp. 60-63.
- Weng, X. C. and Huang, Y., 2014. Relationship Structure-Antioxidant Activity of Hindered Phenolic Compounds. *Grasas Aceites*, 65(4), pp. 1-8.
- Wittenauer, J., Falk, S., Schweiggert-Weisz, U. and Carle, R., 2012. Characterization and Quantification of Xanthoness from the Aril and Pericarp of Mangosteens (*Garcinia mongostana* L.) and a Mangosteen Containing Functional Beverage by HPLC-DAD-MSⁿ. *Food Chemistry*, 134, pp. 445-452.
- Wu, Y.-P., Zhao, W., Xia, Z.-Y., Kong, G.-H., Lu, X.-P., Hu, Q.-F. and Gao, X.-M., 2013. Three New Xanthoness from the Stems of *Garcinia oligantha* and Their Anti-TMV Activity. *Phytochemistry*, 6, 629-632.
- Xu, Y.-J., Chiang, P.-Y., Lai, Y.-H., Vittal, J. J., Wu, X.-H., Tan, B. K. H., Imiyabir, Z. and Goh, S.-H., 2000. Cytotoxic Prenylated Depsidones from *Garcinia parvifolia*. *Journal of Natural Products*, 63, pp. 1361-1363.
- Xu, Y.-J., Lai, Y.-H., Imiyabir, Z. and Goh, S.-H., 2001. Xanthoness from *Garcinia parvifolia*. *Journal of Natural Products*, 64, pp. 1191-1195.
- Yoswathana, N. and Eshtiaghi, M., 2015. Optimization of Subcritical Ethanol Extraction for Xanthone from Mangosteen Pericarp. *International Journal of Chemical Engineering and Application*, 6(2), pp. 115-119.